

Politecnico di Torino

Master's Degree in Energy and Nuclear Engineering  
A.Y. 2023/2024



**Politecnico  
di Torino**

Master's Degree Thesis

**Cost-optimal investment decision for the  
natural gas infrastructure of Piedmont  
with biomethane distributed sources**

Supervisors:

Prof. Pierluigi Leone  
Prof. Marco Cavana

Candidate:

Diego MORETTO

March 2024



## Abstract

The aim of this study is to identify the different evolution paths of the gas infrastructure in Piedmont region considering, on the one hand, the perspective decrease of natural gas consumptions (according to European and national decarbonization targets for 2030 and 2050) and, on the other hand, the development of the biomethane sector as a distributed source of renewable gas.

An optimization model is used to determine the most cost-effective decision that the Transmission System Operator should take about decommissioning or replacement of existing pipelines in the regional gas network.

The Piedmontese network has been first represented on GIS software from open-source data. Then, a preliminary fluid dynamic analysis has been performed using MATLAB for the determination of pipelines capacities. Input data, such as the current network configuration, gas demands at the nodes, gas sources, pipeline capacities, and investment costs, are provided to the Python optimization model. This model is available in literature and has been modified to consider the perspective connections of the biomethane plants, that have been estimated according to the evolution of the revamping of existing biogas power plants following the new incentive schemes on biomethane production.

The primary outputs of the model consist of network configuration, including divestments and new pipeline diameters, as well as gas dispatch, gas demand, and the costs' Present Value in 2050.

Two main evolution scenarios are considered: one without renewable gas penetration and one with the injection of biomethane from domestic production.

All scenarios have shown partial refurbishment and partial decommissioning of the infrastructure, with smaller diameter pipelines to be needed in the future. A scenario with variable injection of biomethane have been considered, resulting in reduced costs with respect to the base scenario, favoring the injection of part of the available biomethane sources. Furthermore, it has been observed that including all potential sources of biomethane reduces the share of decommissioned infrastructure, resulting in higher costs.

## Table of contents

Abstract .....	i
List of figures .....	iv
List of tables .....	vi
1. Introduction .....	1
1.1 Future scenarios of European energy system .....	1
1.2 Italian energy system scenarios .....	7
2. Case study: Piedmont gas network.....	16
2.1 Description of the current network.....	16
2.2 Network model in QGIS .....	18
3. Optimization model.....	23
3.1 Description of the model .....	23
3.2 Mathematical formulation .....	24
4. Base scenario input data .....	38
4.1 Network topology.....	38
4.2 Gas demand .....	38
4.3 Gas source .....	46
4.4 Pipeline capacity .....	48
4.5 Year of decommissioning/refurbishment .....	63
4.6 Unit investment and O&M costs .....	64
5. Biomethane scenario input data .....	68
5.1 What is biomethane? .....	69
5.2 Plants producibility .....	70
5.3 Updated network topology .....	79
5.4 Year of plants connection.....	80
5.5 Connection pipeline costs.....	81

5.6	Year of connection decision.....	82
6.	Results.....	83
6.1	Base scenario.....	83
6.2	Biomethane scenario.....	88
6.3	Results comparison.....	97
7.	Conclusions.....	99
8.	Bibliography.....	101

## List of figures

<b>Figure 1.1</b> - “Distributed Energy” and “Global Ambition” scenarios description [6] .....	3
<b>Figure 1.2</b> - Energy demand per carrier for EU27 [6].....	4
<b>Figure 1.3</b> - Energy demand per sector for EU27 [6].....	4
<b>Figure 1.4</b> - Share of energy supply per carrier for EU27 [6] .....	5
<b>Figure 1.5</b> - Methane demand per sector for EU27 [6] .....	6
<b>Figure 1.6</b> – Annual gas production per scenario for EU27 [6] .....	6
<b>Figure 1.7</b> – Methane supply for EU27 [6] .....	7
<b>Figure 1.8</b> - Imports and production of natural gas in Italy, by country of origin [11].....	10
<b>Figure 1.9</b> - Snam gas transmission network scheme [12].....	11
<b>Figure 2.1</b> - Snam gas network mapping details, box 01 October 2015 [14].....	16
<b>Figure 2.2</b> - Snam gas network mapping details, box 03 October 2015 [14].....	16
<b>Figure 2.3</b> - Legend of Snam Gas Transmission Network scheme [14] .....	18
<b>Figure 2.4</b> – QGIS reference layer .....	19
<b>Figure 2.5</b> – QGIS gas network layer.....	19
<b>Figure 2.6</b> – QGIS model scheme of Piedmont’s Gas Network .....	20
<b>Figure 3.1</b> – Overview of the optimization method .....	23
<b>Figure 3.2</b> – Example scheme of reverse flow from regional to national network.....	35
<b>Figure 4.1</b> – Particular end nodes of the network model.....	40
<b>Figure 4.2</b> – National scenarios in 2030 and 2040 [7] .....	43
<b>Figure 4.3</b> – Gas demand evolution per sector, 2025-2050, DE scenario.....	44
<b>Figure 4.4</b> - Gas demand evolution per sector, 2025-2050, GA scenario .....	45
<b>Figure 4.5</b> - Gas demand evolution per sector, 2025-2050, LT scenario .....	46
<b>Figure 4.6</b> – Nodes of gas source of the network model.....	47
<b>Figure 4.7</b> – Scheme of conservation of momentum for 1D flow, applied to a pipeline’s control volume.....	49
<b>Figure 4.8</b> – Conservation of mass and conservation of momentum equations scheme.....	52
<b>Figure 4.9</b> – QGIS representation of reduction valves (in yellow) .....	55
<b>Figure 4.10</b> – Pipelines’ capacities per diameter.....	61
<b>Figure 4.11</b> – Extrapolated correlation curve of capacities and diameters .....	62
<b>Figure 4.12</b> – Pipelines construction year distribution.....	63
<b>Figure 4.13</b> – Average unit investment costs per diameter ranges.....	66

<b>Figure 5.1</b> – Schematic overview of inputs and outputs of the biogases production process [40]	69
<b>Figure 5.2</b> – Locations of existing biogas plants in Piedmont, in Atlaimpanti [42]	71
<b>Figure 5.3</b> – Biogas plants in Piedmont per province, GSE database	72
<b>Figure 5.4</b> – N° of biogas plants in Piedmont, per installed capacity, GSE database	72
<b>Figure 5.5</b> - Locations of existing biogas plants in Piedmont, in Arpa Piemonte geoportal [43]	73
<b>Figure 5.6</b> - Biogas plants in Piedmont per province, Arpa Piemonte database	74
<b>Figure 5.7</b> - N° of biogas plants in Piedmont, per installed capacity, Arpa Piemonte database	74
<b>Figure 5.8</b> – N° of biogas plants per incentive type	76
<b>Figure 5.9</b> – Electrical efficiency curve	77
<b>Figure 5.10</b> - QGIS scheme of Piedmont’s Gas Network, with biomethane connections	79
<b>Figure 5.11</b> – N° of possible biomethane connections per year	80
<b>Figure 6.1</b> – Network configuration in 2050, GA scenario, base case	84
<b>Figure 6.2</b> - Network configuration in 2050, DE scenario, base case	84
<b>Figure 6.3</b> - Network configuration in 2050, LT scenario, base case	85
<b>Figure 6.4</b> – Diameter distribution per demand evolution scenario, base case	85
<b>Figure 6.5</b> – Gas demand evolution per scenario	86
<b>Figure 6.6</b> – Gas dispatch in 2050, per demand scenario, base case	87
<b>Figure 6.7</b> – Network configuration in 2050, GA scenario, fixed injection case	88
<b>Figure 6.8</b> - Network configuration in 2050, DE scenario, fixed injection case	89
<b>Figure 6.9</b> - Network configuration in 2050, LT scenario, fixed injection case	89
<b>Figure 6.10</b> – Gas dispatch in 2050, per demand scenario, fixed injection case	90
<b>Figure 6.11</b> – Network configuration in 2050, GA scenario, variable injection case	91
<b>Figure 6.12</b> - Network configuration in 2050, DE scenario, variable injection case	92
<b>Figure 6.13</b> - Network configuration in 2050, LT scenario, variable injection case	92
<b>Figure 6.14</b> - Gas dispatch in 2050, per demand scenario, variable injection case	93
<b>Figure 6.15</b> – Biomethane injection evolution 2025-2050, per scenario	94
<b>Figure 6.16</b> – Diameter distribution in 2050, per case study, GA scenario	95
<b>Figure 6.17</b> - Diameter distribution in 2050, per case study, DE scenario	96
<b>Figure 6.18</b> – Diameter distribution in 2050, per case study, LT scenario	96

## List of tables

<b>Table 1.1</b> - Italy gas demand, 2017 – 2021 [5].....	9
<b>Table 1.2</b> - Italy gas demand in 2030, per type of gas [5].....	12
<b>Table 1.3</b> - Italy gas demand in 2040, per type of gas [5].....	12
<b>Table 2.1</b> - Comparison between model and MASE data .....	21
<b>Table 2.2</b> – Attributes of high-pressure pipelines.....	22
<b>Table 2.3</b> – Attributes of transmission pipelines .....	22
<b>Table 3.1</b> – Definition of parameters and variables of the model, base scenario .....	25
<b>Table 3.2</b> – Additional parameters of the model, fixed biomethane injection scenario .....	32
<b>Table 3.3</b> – Additional variables and parameters for the model, variable biomethane injection scenario.....	36
<b>Table 4.1</b> – Monthly consumption fractions, for variable profile A and constant profile B ...	39
<b>Table 4.2</b> – Comparison between modelled demand and MASE demand data per region, with scale factors for correction .....	42
<b>Table 4.3</b> – Input data of initial annual demand, monthly profile, and type of demand per node .....	42
<b>Table 4.4</b> – Annual demand reduction percentages per sector and range of years, DE scenario .....	44
<b>Table 4.5</b> - Annual demand reduction percentages per sector and range of years, GA scenario .....	44
<b>Table 4.6</b> - Annual demand reduction percentages per sector and range of years, LT scenario .....	45
<b>Table 4.7</b> – Input data of available annual gas source per node .....	48
<b>Table 4.8</b> – SIMPLE algorithm input data for high-pressure nodes.....	56
<b>Table 4.9</b> - SIMPLE algorithm input data for high-pressure pipelines .....	57
<b>Table 4.10</b> - SIMPLE algorithm input data for transmission nodes.....	58
<b>Table 4.11</b> - SIMPLE algorithm input data for transmission pipelines.....	59
<b>Table 4.12</b> – Results of fluid dynamic simulation, mass flowrates in pipelines .....	59
<b>Table 4.13</b> - Results of fluid dynamic simulation, absolute pressures at nodes .....	60
<b>Table 4.14</b> – Values of capacity per pipeline diameter .....	62
<b>Table 4.15</b> – Pipelines’ technical parameters input data .....	64



<b>Table 4.16</b> – Nominal Unit investment cost of transmission pipelines per year (average values, median) [34] .....	65
<b>Table 4.17</b> – Pipelines count per diameter range.....	66
<b>Table 4.18</b> – Input unit costs per network level .....	67
<b>Table 5.1</b> – Biogas plants database comparison .....	76
<b>Table 5.2</b> – Biomethane connections input data.....	82
<b>Table 5.3</b> – Year of connection decision per biomethane plant .....	82
<b>Table 6.1</b> – Objective function value per demand evolution scenario, base case .....	83
<b>Table 6.2</b> - Objective function value per demand evolution scenario, fixed injection case ....	90
<b>Table 6.3</b> - Objective function value per demand evolution scenario, variable injection case	91
<b>Table 6.4</b> – N° of plants connection per demand scenario, variable biomethane injection case .....	93



# 1. Introduction

The European Union and its member states are committed to the fight against climate change through the adoption of EU and national policies and measures for the decarbonisation process. With the 2015 Paris Agreement, UNFCCC<sup>1</sup> member states set the goal of keeping the global average temperature increase below 2°C, trying, if possible, to stay below 1,5°C [1]. Subsequently, the European “Green Deal” was set. It consists of policy initiatives proposed by the European Commission with the overall goal of achieving climate neutrality in Europe by 2050. The set of initiatives also includes the 'Fit for 55%' package, which aims to achieve a 55% reduction in CO<sub>2</sub> emissions by 2030, compared to 1990 levels.

These legally binding targets have been incorporated into EU Regulation 2021/1119, the so-called 'European Climate Regulation', which was adopted on 30 June 2021 [2] [3].

These agreements have been recently updated after the outbreak of the energy crisis caused by the war in Ukraine. The European Commission adopted the REPowerEU plan [4], where the target for biomethane production has been raised from 17 bcm to 35 bcm by 2030, and hydrogen production and imports from 5,6 to 20 million tonnes [5].

## 1.1 Future scenarios of European energy system

Future scenarios on energy system are developed to support the European plans for energy infrastructure and achieve the climate objectives, particularly in this period of global energy crisis. The analysis is limited to infrastructure development scenarios.

### 1.1.1 TYNDP 2022

At European level, ENTSO<sup>2</sup>-E and ENTSO<sup>3</sup>G have published the TYNDP (Ten Year Network Development Plan) 2022 scenarios, which are fully compliant with the Paris Agreement and with the European ambitions for achieving climate neutrality by 2050 [6].

---

<sup>1</sup> United Nations Framework Convention on Climate Change

<sup>2</sup> European Network of Transmission System Operators for electricity sector

<sup>3</sup> European Network of Transmission System Operators for gas sector

The scenarios aim to provide a quantitative basis for infrastructure investment planning and information about the evolution of integrated energy system perspectives, while remaining both technology and energy-carrier neutral. They provide a view of the possible energy system of the future, focusing on the role of the electricity and gaseous carriers, in response to the changes of the supply and the demand. To determine the different scenarios, ENTSO-E and ENTSOG firstly have defined the main drivers of the scenarios:

1. *Green transition*, related to the European targets for GHG emissions.
2. *Societal decisions*, which affects the centralisation/decentralisation and the autonomy of the future energy system, impacting on the infrastructure, with possible increase of localised self-production (prosumers).
3. *Energy intensity*, considers both consumer behaviour and technological innovation, leading to increased user participation, with the possibility of reducing demand while having an increase in demand due to new technologies.
4. *Technological process*, related for example to the increase in size of existing technologies for energy production, which already reached maturity, or having technologies used for driving other energy processes (like electrolysis for hydrogen production).

In this document, three main scenarios have been analysed, according to their time scale and future energy system:

- *National Trends* (NT), aligned with national policies which are derived from European objectives, whose duration is until 2040, they include only gas and electricity as energy carriers.
- *Distributed Energy* (DE), it satisfies the targets of reducing 55% of the emissions by 2030 and reaching carbon neutrality by 2050. It is a scenario driven by the distributed generation of energy, with strong penetration of renewables and citizen's action, reducing energy imports.
- *Global Ambition* (GA) remains in line with the previous scenario on the goals to be achieved, it is instead driven by mainly centralised production and global energy trades to accelerate towards decarbonization.

The latter two are compliant with the COP21<sup>4</sup>, they include all energy carriers and sector and are developed until 2050 at European level. In the figure below are reported the main assumptions for each of the long-term scenarios:



	 <b>Distributed Energy</b> Higher European autonomy with renewable and decentralised focus	 <b>Global Ambition</b> Global economy with centralised low carbon and RES options
<b>Green Transition</b>	At least a 55 % reduction in 2030, climate neutral in 2050	
<b>Driving force of the energy transition</b>	Transition initiated at a local/national level (prosumers) Aims for EU energy autonomy through maximisation of RES and smart sector integration (P2G/L)	Transition initiated at a European/international level High EU RES development supplemented with low carbon energy and imports
<b>Energy intensity</b>	Reduced energy demand through circularity and better energy consumption behaviour Digitalisation driven by prosumer and variable RES management	Energy demand also declines, but priority is given to decarbonisation of energy supply Digitalisation and automation reinforce competitiveness of EU business
<b>Technologies</b>	Focus of decentralised technologies (PV, batteries, etc.) and smart charging	Focus on large scale technologies (offshore wind, large storage)
	Focus on electric heat pumps and district heating	Focus on hybrid heating technology
	Higher share of EV, with e-liquids and biofuels supplementing for heavy transport	Wide range of technologies across mobility sectors (electricity, hydrogen and biofuels)
	Minimal CCS and nuclear	Integration of nuclear and CCS

Figure 1.1 - “Distributed Energy” and “Global Ambition” scenarios description [6]

In both COP21-related scenarios, the total final energy demand will decrease thanks to more efficient technologies and conscious use of energy. The share of electricity demand will increase, thanks to a high penetration of renewables, which are in good combination with electricity storage (such as batteries or in form of hydrogen) when demand is lower than production. In the DE scenario, electricity demand in 2050 accounts for 52% of the total demand, while hydrogen reaches 17% (including non-energy use, e.g. need for steel industry). In the GA the shares are respectively 43% and 21%. For all sectors the energy demand shows a substantial decrease in both scenarios, due to:

- Increased insulation of buildings, which require less heating.
- Active participation of consumers, which are less restrictive on modifying the heating and cooling setpoints and tends to use more public transport.
- Use of more efficient technologies

<sup>4</sup> The 21<sup>st</sup> meeting of the Conference of the Parties (Cop 21) to the Convention on Climate Change held in Paris in 2015.

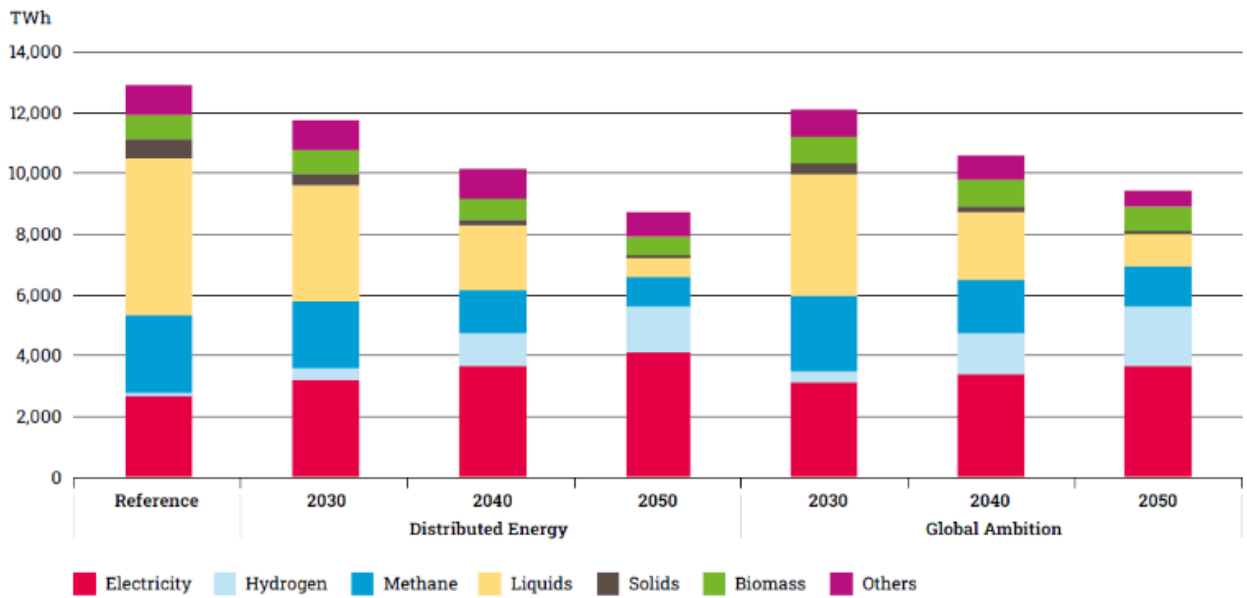


Figure 1.2 - Energy demand per carrier for EU27 [6]

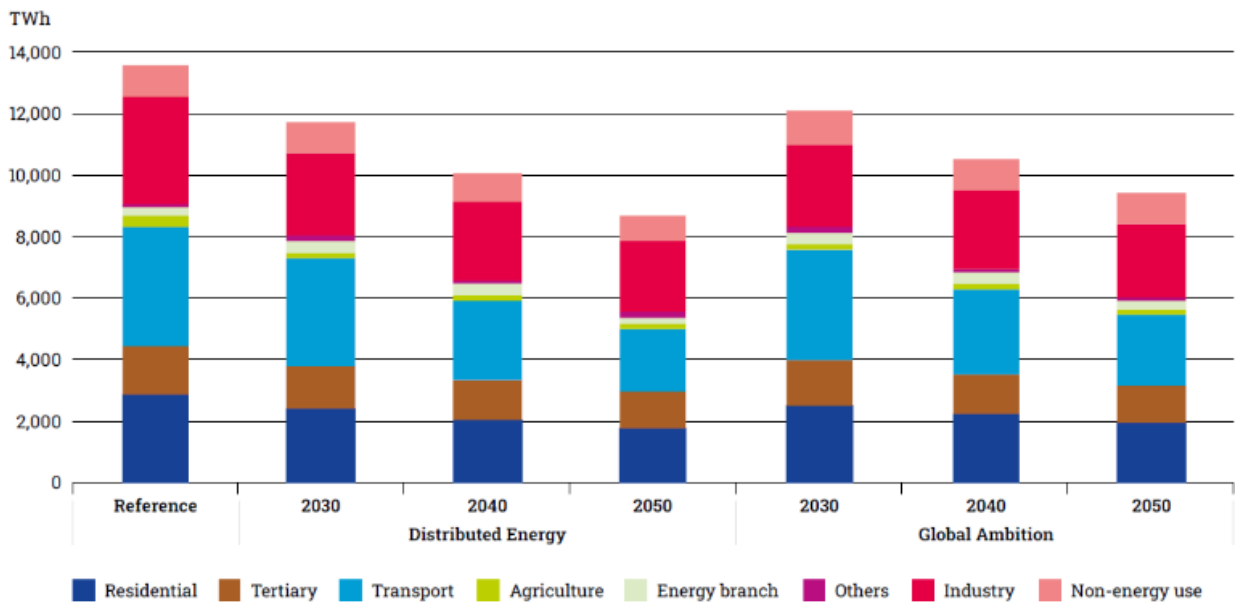


Figure 1.3 - Energy demand per sector for EU27 [6]

Regarding the primary energy supply, the share of renewables increases, especially for PV and wind generation, reaching 80% in GA, and 95% in DE by 2050. In DE higher shares of biomass are shown, while GA shows stronger contribution of nuclear and hydrogen.

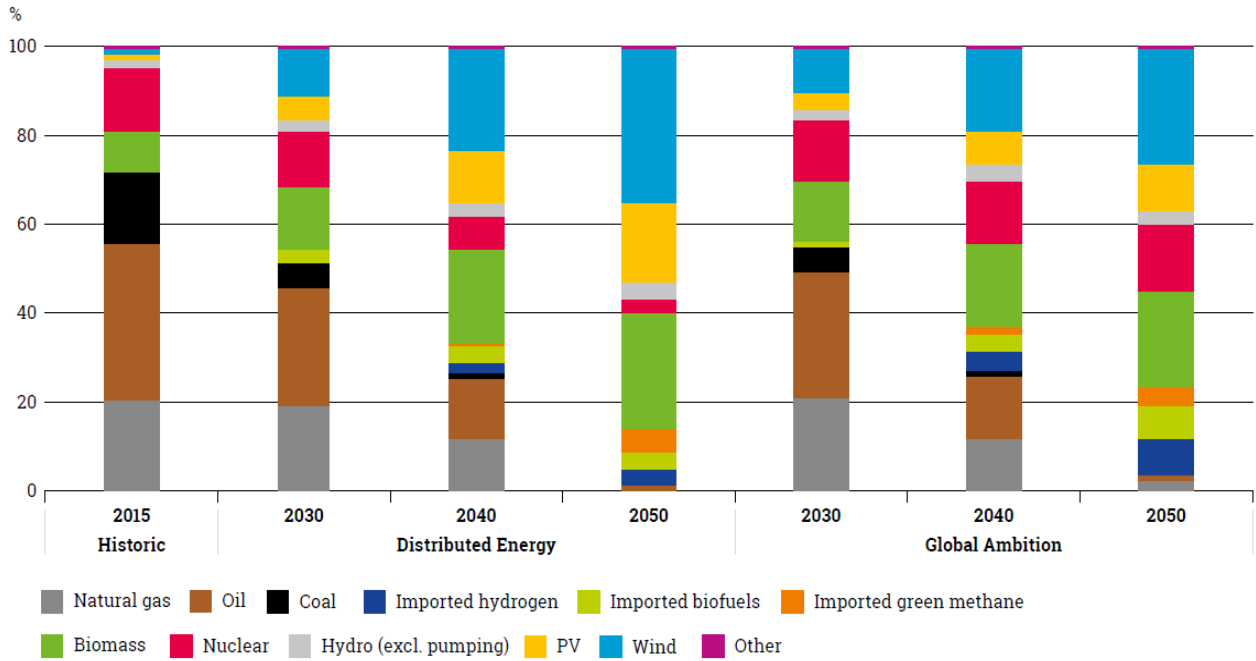


Figure 1.4 - Share of energy supply per carrier for EU27 [6]

#### 1.1.1.1 The role of natural gas

For what concern specifically the natural gas, its role has been challenged by the recent decarbonization policies and may be seen as not a valid candidate for the future of the energy system. However, since it is a low polluting fuel with respect to coal and oil, it will cover an important role as bridging fuel for the energy transition, as well as its infrastructure which could be exploited to transport green gases like hydrogen and biomethane.

The figures below show the methane demand, supply, and the whole gas production for all scenarios.

In the NT scenario, methane demand covers a relevant and stable role until 2030, after which biomethane and hydrogen productions start to kick in. By 2040 the import from other countries is still high.

In DE and GA, the methane demand decreases, however still present up to 2050, mainly for its indirect use in hydrogen production (through steam reforming), that is quite high in 2040 already. In 2050, the imports of natural gas are close to zero in GA and strongly reduced in DE.

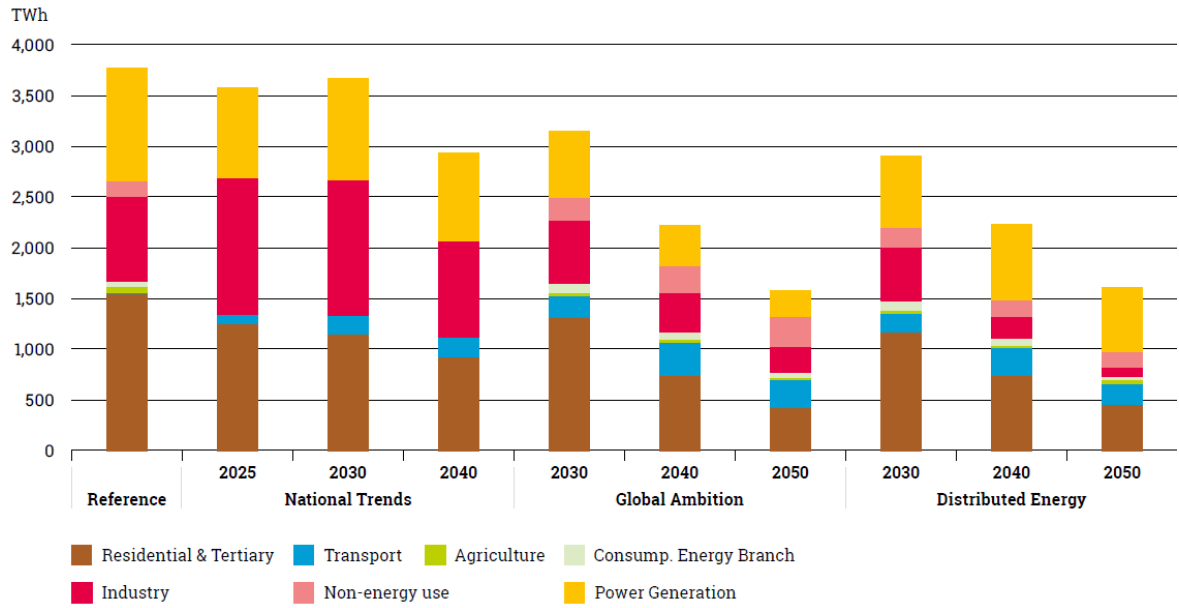


Figure 1.5 - Methane demand per sector for EU27 [6]

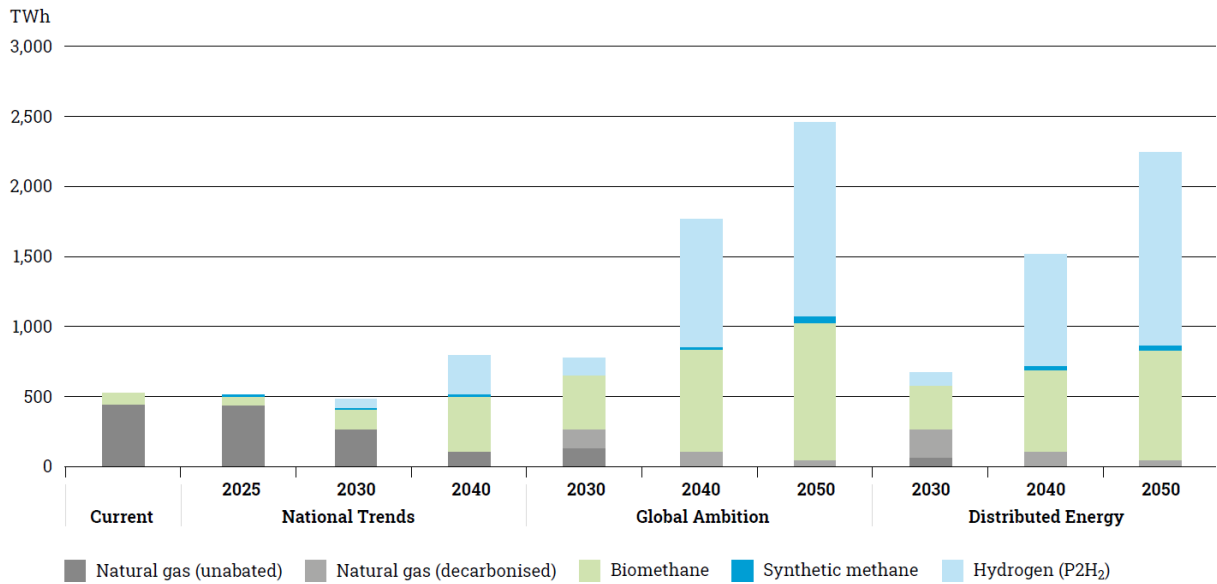


Figure 1.6 – Annual gas production per scenario for EU27 [6]



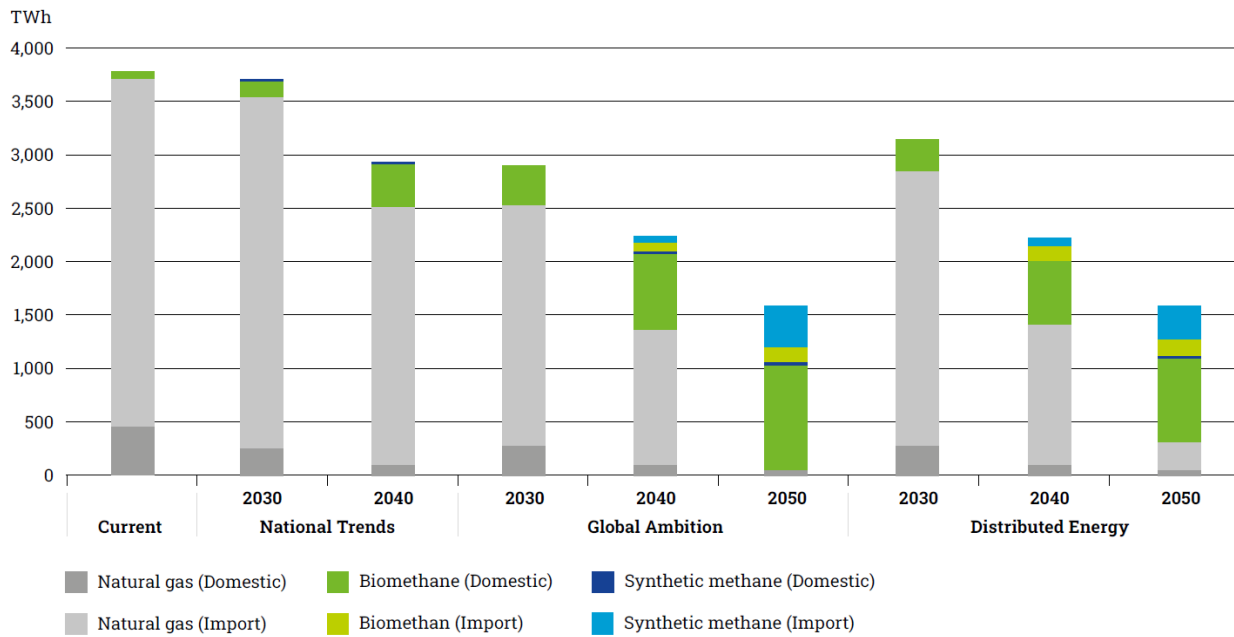


Figure 1.7 – Methane supply for EU27 [6]

Biomethane, coupled with hydrogen, represent the main candidate for the decarbonization process of natural gas, with a later incoming of synthetic methane (produced through methanation).

## 1.2 Italian energy system scenarios

A similar study has been carried out at national level, thanks to the collaboration between Snam and Terna, the Italian TSOs for gas and electricity networks. They published the “*Documento di Descrizione degli Scenari*” (DDS) in 2022, which presents a vision of probable future developments of the Italian energy system [7].

These scenarios have been developed in a context of both evolution and uncertainty: through the “*Piano Nazionale di Ripresa e Resilienza*” (PNRR) about 55 billion have been earmarked for the ecological transition, to increase energy efficiency with a high penetration of renewables and green gases [8]. At the same time, the energy crisis has been exposed to geopolitical developments related to the war in Ukraine.

The scenarios presented in the document are the following:

- *Fit-for-55*, a policy scenario to 2030, with 2019 as starting year. It targets the European objective of reaching -55% of the GHGs emissions by 2030 thanks to high spread of renewables and green gases, with the exploitation of CCS/U<sup>5</sup> technology too.
- *Distributed Energy*, up to 2040, with Fit-for-55 as starting point. It defines the intermediate and not binding objectives at 2040, to satisfy the NZE<sup>6</sup> by 2050.
- *Global Ambition*, up to 2040, with Fit-for-55 as starting point. It defines the intermediate and not binding objectives at 2040, to satisfy the NZE by 2050.
- *Late Transition*, contrasting with policies. It is a scenario in which the targets on emissions are reached with a delay of 5-10 years. It refers to the “*National Trend Italia*” published in 2021 by Terna, which is aligned with the “*Piano Nazionale Integrato per l’Energia e il Clima*” 2019 (PNIEC) targets. The recent geo-political events and the European initiatives are not considered in this scenario.

The DE and GA scenarios are lined up with the corresponding ENTSOs’ scenarios. The document also considers the energy strategies of the other European countries, which can influence the Italian energy system.

### 1.2.1 Current Italian gas system

In Italy, natural gas covers a crucial role since it accounts for almost half of the electricity generation [9]. It will still play a central role in power generation for the coming decade, and its consumption is unlikely to drastically fall. Reducing dependence on Russian gas imports is a key objective in the future, achieving a more diversified range of gas supply source, as demonstrated by the objectives of the REPower EU plan.

In 2021, after covid pandemic, Italy experienced an economic rebound, at the same time having an increase on gas consumption of about 7,2%, due to a colder climate and a recovery of the tertiary sector [7].

---

<sup>5</sup> Carbon Capture Storage and Utilization

<sup>6</sup> Net Zero Emissions

In the table below is reported the evolution of the annual consumptions of gas (methane and biomethane), up to 2021:

*Table 1.1 - Italy gas demand, 2017 – 2021 [7]*

Miliardi di m <sup>3</sup>	2017	2018	2019	2020	2021
Civile	29,1	29,0	28,3	27,6	30,2
Industria	10,8	10,6	10,4	9,9	10,8
Trasporti	1,3	1,3	1,4	1,2	1,4
Altri usi**	3,1	3,2	3,2	3,0	2,9
Generazione elettrica e calore	30,8	28,6	31,1	29,6	31,3
<b>Domanda di Gas Naturale e Biometano</b>	<b>75,2</b>	<b>72,7</b>	<b>74,5</b>	<b>71,3</b>	<b>76,6</b>
di cui biometano	0	0,03	0,05	0,10	0,16

The total annual demand of gas is about 76,6 billion of m<sup>3</sup>, almost totally imported.

The total imports in 2021 accounted for 96% of the gas supplied, and the remanent 4% from the national production. National production of biomethane passed from 99 million of m<sup>3</sup> in 2020, to 159 million of m<sup>3</sup> in 2021, as also stated in the PNIEC 2023 [10].

In the graph below are reported the shares of gas imports, for the different entry points, which corresponds to different country suppliers. Comparing the 2021 situation with the later 2022, due to Ukraine war began in February 2022, the shares of import from each supplier changed, with new agreements stipulated. The most evident cut comes from Russian imports. In the 1<sup>st</sup> semester of 2021, the import from Russia was about 14 bcm, which dropped to 4,7 bcm in the last semester of 2022. Algeria became the main importer providing 12 bcm in last semester. Imports from Northen Europe (mainly from Norway and the Netherlands) nearly doubled, as well as the ones from Azerbaijan [11].

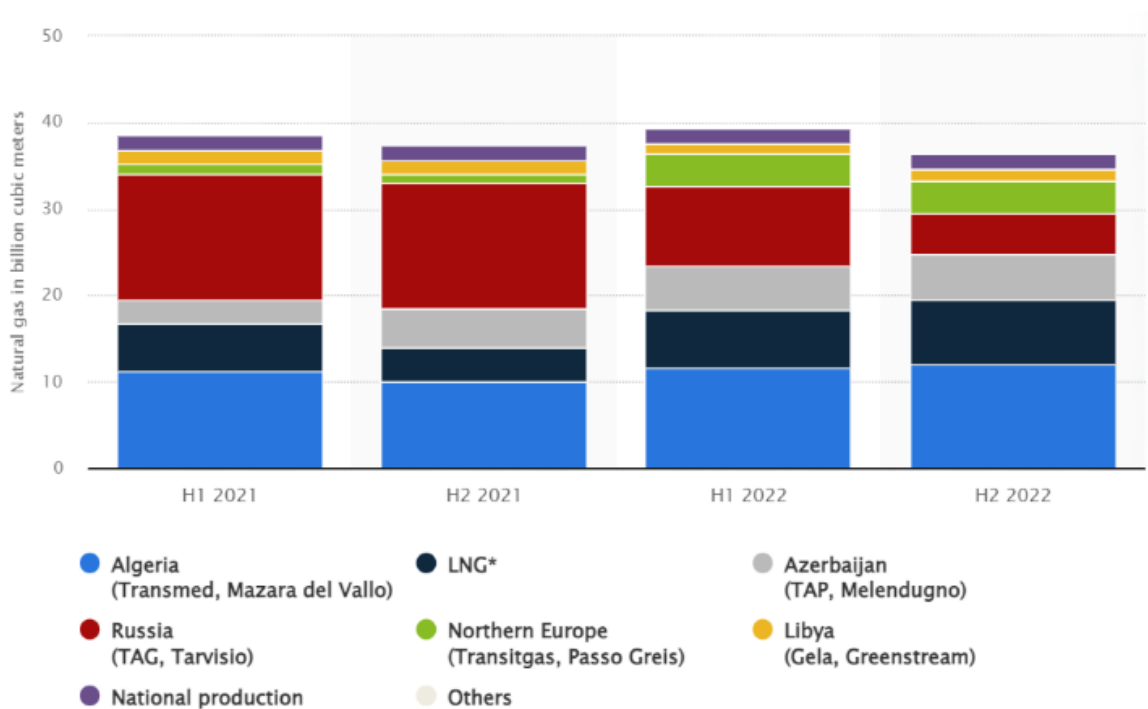


*Figure 1.8 - Imports and production of natural gas in Italy, by country of origin [11]*

For what concern the gas infrastructure, the transmission network in Italy is managed mostly by Snam<sup>7</sup> and SGI<sup>8</sup>, and it is characterized by 9 entry points for the import of gas. Once gas is imported, produced or regasified from LNG, it is transported to the regional redelivery points. Snam is the main TSO in Italy. It controls 13 compression station points, to guarantee the continuous transport of gas, with a dispatch centre to monitor and control the delivery. The total volume of gas transported accounts for 75,4 bcm, in a network of more than 38000 km of length [12].

<sup>7</sup> Main TSO for gas system in Italy

<sup>8</sup> “Società Gas Italiana”, TSO in centre of Italy



*Figure 1.9 - Snam gas transmission network scheme [12]*

### 1.2.2 2030 projection

The DDS predicts that gas demand will reach 66,2 bcm by 2030, encompassing natural gas, biomethane, and hydrogen in the *Fit-for-55* scenario. This scenario relies on energy efficiency, electric renewables, and the development of biomethane and green hydrogen. Carbon capture technologies are necessary to reduce emissions from certain industrial production processes. Biomethane demand is equally distributed among the civil, industry, and transport sectors. Hydrogen will be used for industrial, transportation, and other purposes, such as biofuel or fertilizer production, and desulphurization processes.

In the alternative scenario of a late transition to 2030, gas demand would amount to 61,7 bcm, including natural gas, biomethane, and hydrogen. Compared with the previous scenario, the total gas demand is lower, but the amount of natural gas is higher, with lower demand for renewable gases, as shown in Table 1.2. The decarbonization objective in this scenario is to achieve a -40% reduction in CO<sub>2</sub> emissions by 2030, which is a less ambitious target.

This is why biomethane has not yet been fully integrated into the energy system and the use of hydrogen has been postponed, as well as the implementation of carbon capture. Furthermore, the demand for biomethane and hydrogen is solely intended for the transportation sector.

*Table 1.2 - Italy gas demand in 2030, per type of gas [7]*

SCENARIO	2030 LT		2030F55	
	Gm <sup>3</sup>	TWh	Gm <sup>3</sup>	TWh
GAS NATURALE	60,6	641	58,6	620
BIOMETANO	1,0	11	5,4	57
IDROGENO (Gm <sup>3</sup> met eq)	0,1	1	2,2	23
<b>TOTALE</b>	<b>61,7</b>	<b>653</b>	<b>66,2</b>	<b>700</b>

### 1.2.3 2040 projection

By 2040, the DE and GA scenarios aim to bridge the gap between the -55% emissions reduction target in 2030 and achieving *Net Zero Emissions* by 2050. The total gas demand is projected to reach 53 bcm and 59.4 bcm for the two scenarios respectively.

In the DE scenario, due to higher electricity penetration, natural gas is less necessary in the civil sector compared to the GA trend.

The LT follows the trend set by the PNIEC 2019, until 2040. The scenario shows higher demand for natural gas in the civil and industrial sectors due to low electrification and lower efficiency. Additionally, natural gas is more commonly used in the transport sector due to the lower presence of electric vehicles.

Biomethane is primarily used for the civil sector to satisfy the heating demand simultaneously with heat pumps, in all scenarios.

The demand for hydrogen is distributed differently comparing all scenarios:

- DE, hydrogen is required in all sectors, apart from the civil sector that will be highly electrified.
- GA has the highest demand for H<sub>2</sub> at 12 bcm, with significant use in the civil sector as a possible substitute for heat pumps.
- In LT, hydrogen is primarily used in the transport and industrial sectors.

*Table 1.3 - Italy gas demand in 2040, per type of gas [7]*

SCENARIO	2040 LT		2040 DE-IT		2040 GA-IT	
	Gm <sup>3</sup>	TWh	Gm <sup>3</sup>	TWh	Gm <sup>3</sup>	TWh
GAS NATURALE	56,6	599	35,4	375	37,1	393
BIOMETANO	7,0	74	10,3	109	10,3	109
IDROGENO (Gm <sup>3</sup> met eq)	3,9	41	7,3	77	12,0	127
<b>TOTALE</b>	<b>67,5</b>	<b>714</b>	<b>53,0</b>	<b>561</b>	<b>59,4</b>	<b>629</b>

#### 1.2.4 Future gas supply

In terms of future Italian gas supply, gas demand will continue to be met by imports, with domestic production decreasing year by year. Imports from the south will increase, as will the use of LNG. Exports from Italy are maximised where greater diversification from Russian gas is considered, resulting in increased flows from the south transiting Italy.

Imports are higher in the LT scenario than in DE and GA, due to the higher demand for natural gas and the lower penetration of biomethane in the energy system.

Biomethane supply is assumed to come entirely from national production, reaching 10,3 bcm in 2040 in both DE and GA.

Hydrogen production will be driven by electrolysis processes, with the possibility to supply blue hydrogen produced by SMR<sup>9</sup> and coupled with CCS. Due to its high demand in 2040 (12 bcm in GA and 7,3 bcm in DE), some imports may be necessary by pipeline or in liquefied form. Italy could take advantage of its proximity to North Africa to import by pipeline hydrogen efficiently produced from the abundant natural resources available (solar and wind) and thus at a lower cost [7].

Hydrogen is also seen as an element in the decarbonisation of the gas network, blended with natural gas and biomethane. Within the technological and regulatory constraints of the transport infrastructure, the carrier will make a significant contribution to reducing emissions from conventional natural gas technologies.

#### 1.2.5 The coming role of biomethane

The reference context in which the PNIEC 2019 has been developed, has changed dramatically. The objectives set by the plan are still a long way off, both because they are ambitious in terms of investment and timeframe, and because of some slowdowns due to recent events (pandemic, war in Ukraine, rising energy prices).

The update of the plan considers recent events that have highlighted the country's low security of supply. The aim is to make Italy a country with a central role in the Mediterranean and Europe, becoming a real hub for energy production and transit. The reference year for the construction of the new plan is 2021, from which a trend scenario up to 2030 has been

---

<sup>9</sup> Steam Methane Reforming

constructed. The plan emphasises the need to accelerate renewable electricity, renewable gas production (biomethane and hydrogen) and other biofuels, CCS, electric car use and heat pumps.

For what concern biomethane, the measures to achieve the objectives set by the draft PNIEC 2023 include:

- the reduction of the costs of connecting biomethane to the gas distribution and transmission networks.
- promoting the use of biomethane and other advanced biofuels in the transport sector, according to Ministerial Decree 2/03/18 [10].
- the achievement of 2,3 billion m<sup>3</sup> of biomethane production by June 2026, according to Ministerial Decree 15/09/22 [10].

D.M. 15/09/22 aims to promote biomethane injected into the natural gas network through capital support (equal to a maximum of 40% of the expenses incurred) and an energy account incentive (incentive tariff applied to the net production of biomethane).

Newly built biomethane production plants, whether agricultural or waste-based, and interventions for the conversion (total or partial) of existing agricultural electricity production plants fuelled by biogas to biomethane are eligible for the incentives provided for in the Ministerial Decree [13].

The scenarios presented in the PNIEC 2023 also considers the resources allocated to achieve the ecological transition, through PNRR and the REPowerEU plan [4].

PNRR includes an allocation of dedicated funds for the development of biomethane, totalling 1,92 billion euros, to achieve the objectives of national production described above, through the following lines of action [8]:

- Converting existing agricultural biogas plants to produce biomethane for industry, transport, and heating.
- Providing financial support for the construction of new plants (from scratch).
- Disseminating environmentally friendly practices in the biogas production phase (minimum tillage sites, innovative low-emission systems for digestate distribution) to



reduce the use of synthetic fertilisers and increase the supply of organic matter in the soil.

- Promote the replacement of at least 300 inefficient and obsolete tractors with methane/biomethane powered vehicles equipped with precision farming tools.

When injected into the gas grid, biomethane can strongly contribute to greenhouse gas savings, and thus its development represents an important component in achieving the European decarbonisation targets.

## 2. Case study: Piedmont gas network

### 2.1 Description of the current network

The master's thesis will focus on the regional gas network in Piedmont. A geographical and schematic representation of the pipelines of the entire transport network regulated by Snam, can be accessed from the TSO's website [14]. The part of the network related to Piedmont is shown below, divided into two boxes (North and South):

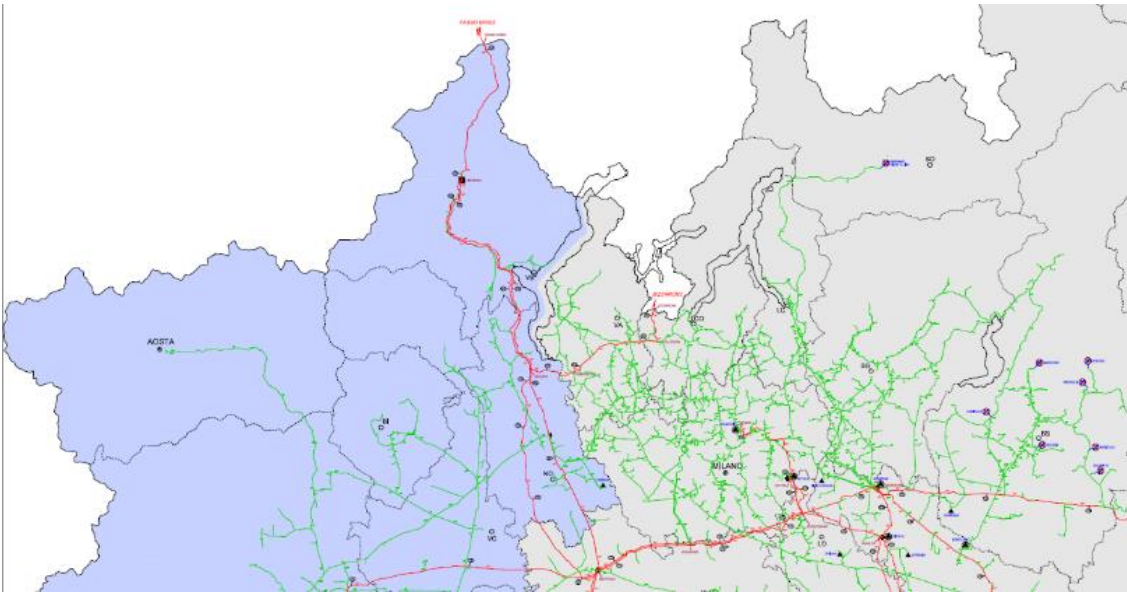


Figure 2.1 - Snam gas network mapping details, box 01 October 2015 [14]

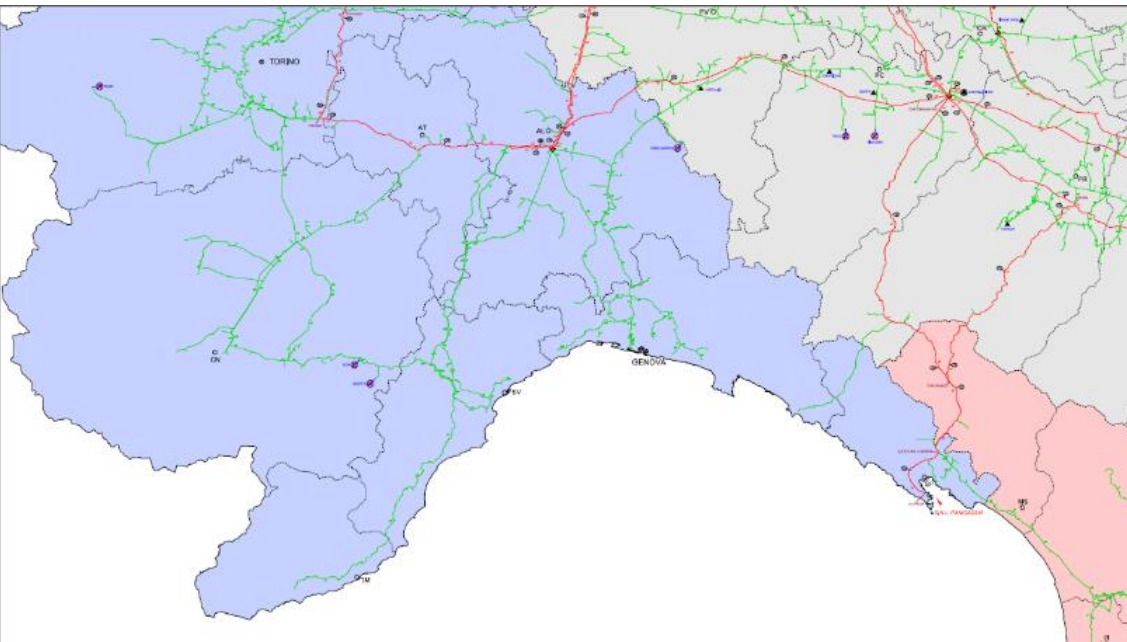


Figure 2.2 - Snam gas network mapping details, box 03 October 2015 [14]

Through the figures, two network layers can be distinguished, one in red and one in green, representing the national and regional network, respectively. The Snam network code indicates that the difference between the two networks is due to the different level of working pressure, with gas moving from the main network backbone until branching off and reaching the redelivery points (e.g. ReMi<sup>10</sup> substations, industries, thermal power stations), with decreasing pressures and pipeline diameters.

In particular, the national network operates at higher working pressures (up to 75 bar), while the regional network typically works at pressures lower than 24 bar [15].

In general, most of the pipelines exercised by the transporter are part of the 1<sup>st</sup>, 2<sup>nd</sup>, and 3<sup>rd</sup> species, according to the classification of transport piping in Ministerial Decree 17<sup>th</sup> of April 2008, in relation to the maximum working pressure [16].

The Piedmontese network is characterized by one main entry point for gas import/export, namely the “Passo del Gries”, which is one of the 9 entry points of the entire Italian gas transmission network. However, Piedmont is not an isolated region, instead it is interconnected with others (Lombardy, Liguria, Emilia-Romagna, Aosta Valley), so there are several pipelines that cross Piedmont and other regions too.

For the case study, those pipelines are virtually interrupted at the Piedmont borders, by considering the end points as gas import/export nodes or simply as redelivery points.

Other peculiar nodes can be seen in the network. As per the legend, in the schematic of the network can be identified:

- One compression station, located in Masera.
- Two domestic production points.
- Three interconnection points with other TSOs, located in Roure, Ceva, and Nucetto.
- Two sorting nodes.

---

<sup>10</sup> Gas Pressure Reducing Station, ReMi stands for “Regolazione e Misura”, where the gas flow is measured, reduced in pressure, and odorized.

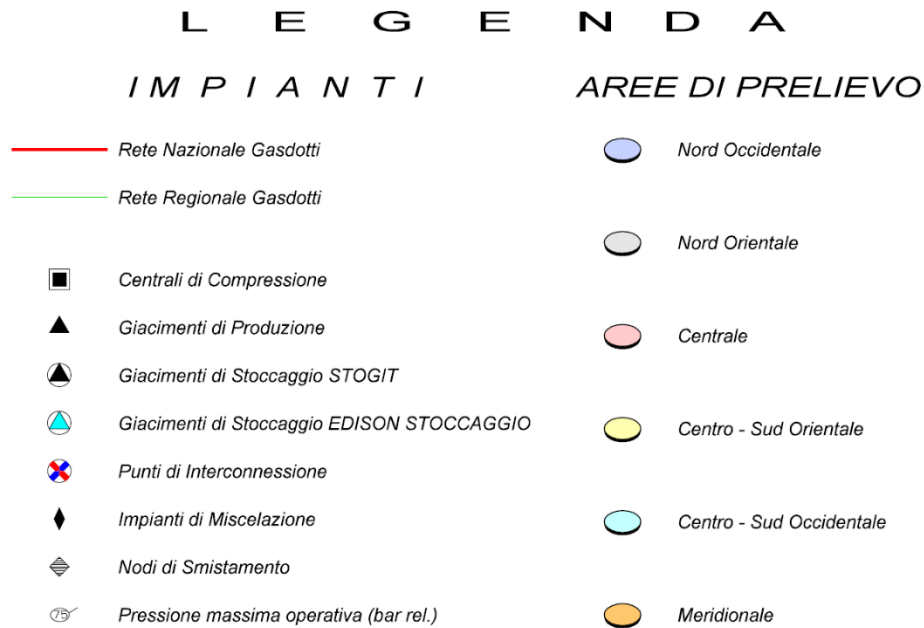


*Figure 2.3 - Legend of Snam Gas Transmission Network scheme [14]*

## 2.2 Network model in QGIS

The following step consists of exploiting the available schemes of the network in form of pdf files and build an interactive graphical model which provides the characteristics of each pipeline, necessary for the next phases of the study.

By using a free and open-source geographic information system, QGIS, it is possible to import the two pdf files (one for the north part of Piedmont, the other for the south part) in the software, in the form of a Raster file.

Then the Raster files are georeferenced, so that they can geographically coincide with the Google Satellite layer, to have an acceptable match between the reality and the schematic of the network. Below is shown the reference layer on which the network model is then built:



*Figure 2.4 – QGIS reference layer*

The adopted coordinate system is the WGS<sup>11</sup> 84 / Pseudo-Mercator. Once the drawing base is set, the transmission (red) and the high-pressure (green) network layers are created, by drawing linear elements following the lines of the scheme.

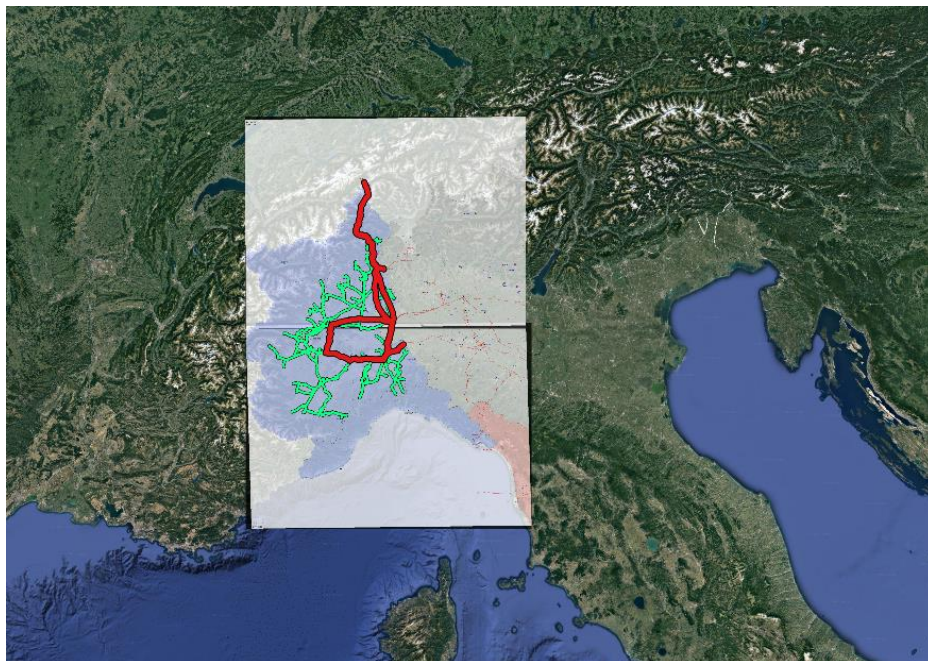


*Figure 2.5 – QGIS gas network layer*

---

<sup>11</sup> World Geodetic System, a standard used in cartography, geodesy, and satellite navigation.

Regarding the layer containing the pipelines, four attribute fields necessary for the optimization model are defined:

- *Type*, indicating the category of the line, either transmission or high-pressure.
- *Start*, indicating the start node of the line. This field is a string to which is assigned the name of the municipality surrounding the drawn node, or a fictitious name as input.
- *End*, that is the end node of the line. The field is a string, with the name of the nearest municipality to the node, especially for the lines that terminate within a reduction substation.
- *Length*, of the pipeline, measured in km, calculated by the software using a function.
- *Diameter*, of the pipeline, measured in inches. The values of diameter are taken from the schemes in Figure 2.1 and Figure 2.2 , for lines on which it is shown. If the diameter is not indicated, it is assumed to be equal to that of one of the adjacent lines, typically the smallest.

The final configuration is represented in the figure below. The modelled network consists of 580 nodes and 616 pipelines, for a total extension of 2387 km, divided into national network (38 pipelines and 604 km) and regional network (578 pipelines and 1784 km).

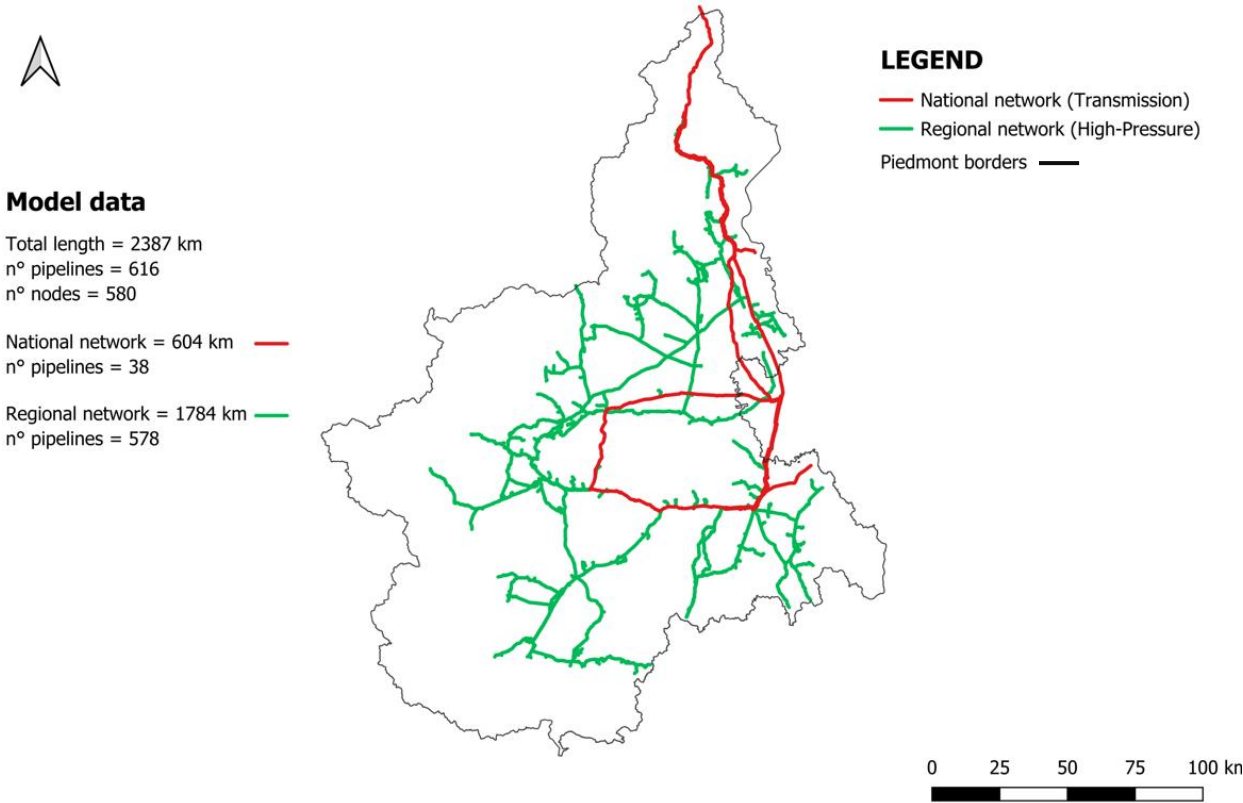


Figure 2.6 – QGIS model scheme of Piedmont’s Gas Network

To assess the accuracy of the model, a comparison is made with real data. As specific data on the length and number of lines in Piedmont alone is not available, they are estimated using an updated list of the network's pipelines as of January 2023, published by MASE<sup>12</sup> with the director's decree of May 25 [17].

The list includes both existing pipelines, new planned connections, and lines with commissioning years beyond 2015. The latter two are not included in the comparison.

Table 2.1 reports the characteristics of the regional network for the model and the MASE's list. The model's accuracy in terms of network length is about 91.8%, while in terms of the number of pipelines, it reaches 72.9%.

It can be noted that several lines have not been included, but their length is not too significant. The difference in length is primarily related to the quality of the PDF imported into the GIS, which makes some pipelines difficult to be seen.

*Table 2.1 - Comparison between model and MASE data*

	<b>High-Pressure network</b>	
	<b>Model</b>	<b>MASE</b>
<b>Length</b>	1784 km	1943 km
<b>N° of pipelines</b>	578	793

For what concern the transmission level, all the pipelines shown in the scheme are drawn up to Piedmont’s borders, with a part of network that crosses Lombardy too.

The tables below resume the attributes of the pipelines, for both transmission and high-pressure networks. In chapter 4, it is explained how gas demand is evaluated for specific end nodes that connect Piedmont with other regions or connect Snam with other TSOs.

The attribute fields of the QGIS model will serve as input for the Python code, which is discussed in the next chapter and used for network optimization.

---

<sup>12</sup> Italian ministry of environment and energy security, “Ministero dell’Ambiente e della Sicurezza Energetica”

*Table 2.2 – Attributes of high-pressure pipelines*

id	Type	Length [km]	Start	End	D (")
1	High-Pressure	0,3	Gravellona Toce	Riduzione1	12
2	High-Pressure	0,4	Briona	Riduzione5	30
3	High-Pressure	15,0	Castellazzo Novarese	Intermezzo23	26
4	High-Pressure	21,8	Intermezzo23	Peschiera	20
5	High-Pressure	5,3	Intermezzo23	Intermezzo21	26
6	High-Pressure	5,2	Busignetto	Mandria	26
7	High-Pressure	5,2	Castellazzo Novarese	Sologno	26
8	High-Pressure	0,1	Intermezzo3	Riduzione50	16
9	High-Pressure	0,0	Intermezzo3	Riduzione7	16
.....					
559	High-Pressure	0,6	Riduzione43	Campone	12
560	High-Pressure	4,0	Campone	Tanchello	8
561	High-Pressure	0,1	Tanchello	Casale Corte Cerro	8
562	High-Pressure	0,9	Tanchello	Gattugno	8
563	High-Pressure	0,1	Gattugno	Omegna_1	8
564	High-Pressure	0,5	Gattugno	Germagno	8
565	High-Pressure	0,1	Germagno	Omegna_2	8
566	High-Pressure	0,9	Germagno	Intermezzo124	8
567	High-Pressure	3,3	Campone	Ornavasso	8
568	High-Pressure	2,2	Intermezzo124	Omegna_4	8
569	High-Pressure	0,3	Intermezzo124	Omegna_3	8
570	High-Pressure	7,2	Intermezzo125	Isella	8
571	High-Pressure	0,0	Intermezzo125	Mergozzo	8
572	High-Pressure	0,2	Intermezzo129	Riduzione44	12
573	High-Pressure	0,6	Riduzione44	Intermezzo130	12
574	High-Pressure	0,2	Intermezzo130	Villadossola_2	8
575	High-Pressure	0,2	Intermezzo130	Villadossola_1	8
576	High-Pressure	5,0	Riduzione44	Intermezzo131	12
577	High-Pressure	1,1	Intermezzo131	Domodossola_2	8
578	High-Pressure	0,2	Intermezzo131	Domodossola_1	8

*Table 2.3 – Attributes of transmission pipelines*

id	Type	Length [km]	Start	End	D (")
1	Transmission	42,3	Passo Gries	Masera	48
2	Transmission	34,7	Masera	Gravellona Toce	48
3	Transmission	26,7	Gravellona Toce	Mescia	48
4	Transmission	12,3	Gattico-Veruno	Cascina Monferrona	48
5	Transmission	2,6	Margattino	Intermezzo3	34
6	Transmission	8,8	Cascina Monferrona	Briona	48
7	Transmission	38,0	Briona	Castello d'Agogna	48
8	Transmission	48,5	Mortara	Smistamento	30
9	Transmission	27,2	Mortara	Gasperini	24
10	Transmission	8,9	Gasperini	Castelceriolo	24
.....					
30	Transmission	21,1	Lucedio	Neirole	42
31	Transmission	7,1	Oviglio	Masio	22
32	Transmission	4,3	Masio	Cerro Tanaro	22
33	Transmission	6,8	Cerro Tanaro	Moglia	22
34	Transmission	1,2	Intermezzo60	Intermezzo61	22
35	Transmission	8,9	Intermezzo40	Oviglio	22
36	Transmission	22,5	Revigliasco d'Asti	Intermezzo60	22
37	Transmission	7,4	Oviglia	Poirino_1	26
38	Transmission	47,0	Intermezzo129	Colazza	34



### 3. Optimization model

#### 3.1 Description of the model

As stated in the abstract, the objective of this master thesis is to find the optimal gas network configuration of Piedmont with the aim of minimizing the total investment and operational costs for the network TSO between 2025 and 2050.

Pyomo, an open-source Python-based software package for modelling and solving optimization problems, is utilized for this purpose [18]. The diagram below provides an overview of the optimization method:

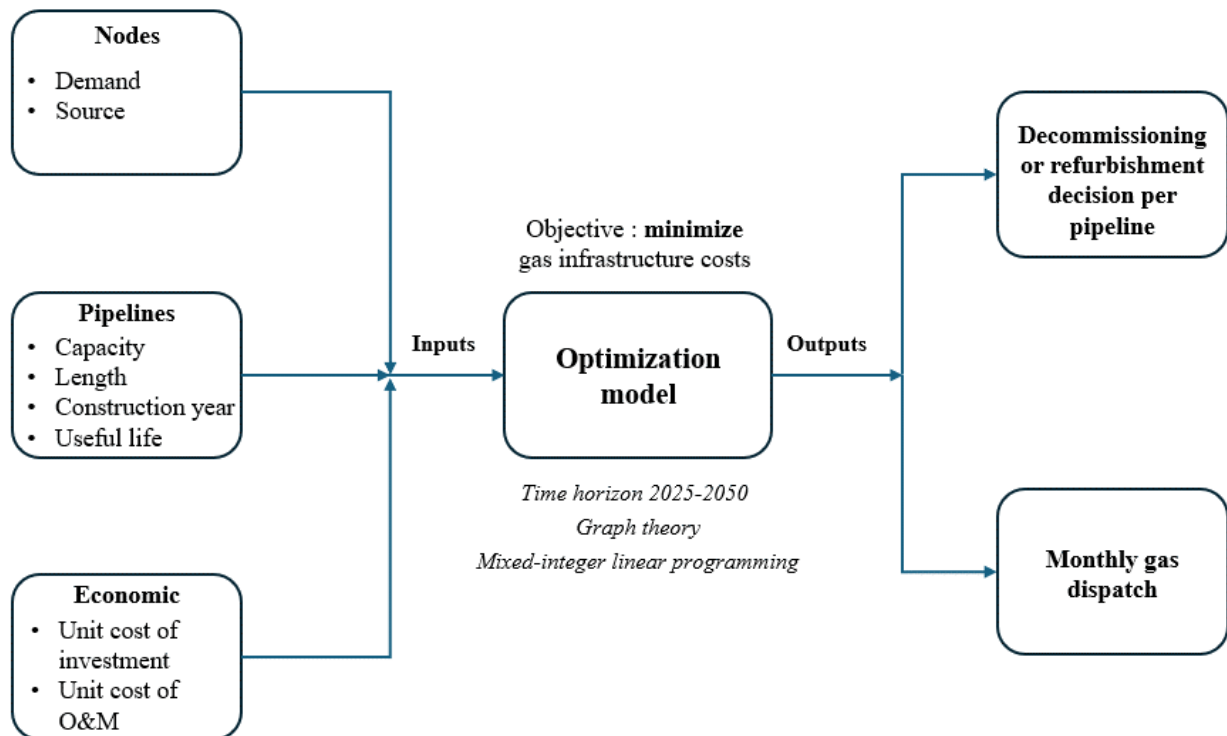


*Figure 3.1 – Overview of the optimization method*

Pyomo is used to define the parameters (input data), variables, constraints, and objective function. The main decision variables are the decommissioning and/or refurbishment of a pipeline after its service life, and the gas dispatch to the end-users along the whole planning horizon. The main outputs are the decommissioning and refurbishment decisions per pipeline, the utilization of pipelines (dispatch of the gas) and the total costs for the considered period.

The optimization model is based on graph theory and mixed-integer linear programming (MILP). In linear programming, the objective function and all constraints are linear functions. The term 'mixed integer' refers to the fact that some decision variables in the problem are forced to assume fixed integer values, as reported in the following section.

The reference Pyomo code is taken from the GitHub<sup>13</sup> platform, in Sebastian Zwickl-Bernhard's repository [19]. The publisher has carried an application of the model on an Austrian federal state [20]. The reference code is then modified to be applied to this case study, to permit the injection of biomethane.

In the next section are defined the main constraints of the model for the base case, followed by additional constraints for the case with biomethane injection.

## 3.2 Mathematical formulation

### 3.2.1 Base scenario

This section presents the primary mathematical formulations that comprise the model, including the definition of the objective function and constraints.

As stated in the previous section, the primary decision variables are the new capacity to be installed for each line at the end of its useful life and the distribution of gas in the network, specifically the amount of gas transported in each pipeline. The model takes decisions to minimize the total infrastructure costs over the analysis period.

Economic variables and parameters are evaluated on an annual basis. Gas distribution variables and parameters, such as demand and resources, are instead evaluated monthly.

The set of variables and parameters that appear in the equations of the mathematical model are listed below, together with their units of measurement and a brief definition.

---

<sup>13</sup> GitHub is an AI-powered developer platform used to host open-source software development projects.

Table 3.1 – Definition of parameters and variables of the model, base scenario

<b>Indexes</b>	<b>Definition</b>	
y	Year	
m	Month	
l	Gas network level (transmission or high-pressure)	
p	Pipeline of the network	
n	Node of the network	
<b>Parameters</b>	<b>Definition</b>	<b>Unit of Measurement</b>
i	Interest rate	-
$\omega$	Weighted average cost of capital	-
$c_l^{inv}$	Unit investment costs at level $l$	€/MW/km
$c_l^{fix}$	Unit fixed costs at level $l$	€/MW/km
$\pi_{y,l,p}^{pre}$	Book value of pre-existing pipeline $p$ , at $l$ in $y$	€
$\gamma_{l,p,y}^{pre}$	Capacity of pre-existing pipeline $p$ , at $l$ in $y$	MW
$L_{l,p}$	Length of pipeline $p$ , at level $l$	km
$q_{n,l,y,m}^{dem,loc}$	Local gas demand at node $n$ , level $l$ , in $y$ and $m$	MWh
$q_{n,y}^{max,source,loc}$	Available annual local source at node $n$ , in $y$	MWh
$y_{l,p}^{inv}$	Year of investment decision (end of life) per pipeline $p$ , at $l$	-
$f_{l,p,y}^{ref}$	Depreciation factor per pipeline $p$ , at $l$ in $y$	-
<b>Variables</b>	<b>Definition</b>	<b>Unit of Measurement</b>
Capex	Total capital expenditures	€
Opex	Total operational expenditures	€
$\pi_{y,l,p}$	Book value of pipeline $p$ in $y$ at $l$	€
$\gamma_{l,p,y}$	Capacity of pipeline $p$ in $y$ at $l$	MW
$\pi_{(y_{l,p}^{inv},l,p)}^{ref}$	Book value of refurbished pipeline $p$ , at $l$ , in the investment decision year	€
$\gamma_{l,p,y}^{ref}$	Refurbished capacity of pipeline $p$ , at $l$ , in $y$	MW

$\gamma_{1,p,y}^{\text{ref}}$	Refurbished capacity of pipeline $p$ , at $l$ , in the investment decision year	MW
$q_{p,l,y,m}$	Gas transported in pipeline $p$ , at $l$ , in $y$ and $m$	MW
$q_{n,l',y,m}^{\text{dem,del}}$	Quantity of gas delivered from level $l$ to level $l'$ , through node $n$ , in $y$ and $m$	MWh

The constraints are represented by linear equations that correlate the variables and input parameters.

The first step is to define the objective function to be minimised, which is the total infrastructure costs over the period of analysis:

$$f(x) = \text{Capex} + \text{Opex} \quad (1)$$

where  $x$  are all the decision variables of the model,

Capex is the total capital expenditure,

Opex represents the operation and maintenance expenditures,

both evaluated throughout the investment period within 2025-2050.

Analysing each term of equation 1, Capex is defined as:

$$\text{Capex} = \sum_{y=y_0}^{y_{\text{end}}-1} \alpha_y \cdot \omega \cdot \pi_y + \alpha_{y_{\text{end}}} \cdot \pi_{y_{\text{end}}} \quad (2)$$

where  $y$  represents the year,

$\pi_y$  is the total yearly book value of the pipelines, expressed in €,

$\omega$  is the Weighted Average Cost of Capital, assumed equal to 5% [20],

$\alpha_y$  is the discount factor.

The discount factor in each year is calculated through the following equation:

$$\alpha_y = \frac{1}{(1+i)^{y-2025}} \quad (3)$$

where  $i$  represents the interest rate, assumed equal to 2,5% [20].

The calculation of Capex is done according to the declining-balance depreciation method.

Depreciation is an accounting practice used to spread the cost of a tangible or

physical asset over its useful life. It represents how much of the asset's value has been used up in any given period [21]. The depreciation rate is assumed equal to the WACC.

The yearly book value of the pipelines  $\pi_y$  derives from the sum of the book values of each pipeline, at each network level (transmission and high-pressure):

$$\pi_y = \sum_l \sum_p \pi_{y,l,p} \quad (4)$$

The single pipeline book value is evaluated as it follows:

$$\pi_{y,l,p} = \pi_{y,l,p}^{pre} + f_{l,p,y}^{ref} \cdot \pi_{(y_{l,p}^{inv},l,p)}^{ref} \quad (5)$$

$\pi_{y,l,p}^{pre}$  is the book value of the pre-existing pipeline, assumed equal to 0 for the whole period (null asset value is considered for already existing pipelines).

$\pi_{(y_{l,p}^{inv},l,p)}^{ref}$  is the book value of the refurbished pipeline, calculated in the year of investment decision.

$f_{l,p,y}^{ref}$  is the depreciation factor, that varies each year. Before the year of investment decision  $y_{l,p}^{inv}$ , it is equal to 0, then it decreases as the depreciation of the asset increases. It is calculated as follows:

$$f_{(l,p,y)}^{ref} = \begin{cases} 1 - \frac{1}{20} \cdot (y - y_{l,p}^{inv}) & : \forall y \geq y_{l,p}^{inv} \\ 0 & : \forall y < y_{l,p}^{inv} \end{cases} \quad (6)$$

The book value of the refurbished pipeline is evaluated through eq. 7:

$$\pi_{(y_{l,p}^{inv},l,p)}^{ref} = c_l^{inv} \cdot \gamma_{l,p,y_{l,p}^{inv}}^{ref} \cdot L_{l,p} \quad (7)$$

$\gamma_{l,p,y_{l,p}^{inv}}^{ref}$  is the capacity expressed in MW of the refurbished pipeline in the year of investment decision.

$c_l^{inv}$  is the unit investment cost, expressed in €/MW/km, and it varies per network level.

$L_{l,p}$  is the length of the pipeline, in km.

The refurbished capacity per pipeline, at each pressure level, in year  $y$  different from the investment decision one, is evaluated:

$$\gamma_{l,p,y}^{ref} = \begin{cases} 0 & : \forall y < y_{l,p}^{inv} \\ \gamma_{l,p,y-1}^{ref} & : \forall y > y_{l,p}^{inv} \end{cases} \quad (8)$$

Eq. 8 imposes that, after the year of refurbishment/decommissioning decision, the renewed capacity cannot be changed.

The overall capacity of a pipeline  $\gamma_{l,p,y}$ , at each network level and in each year, depends on the pre-existing capacity (before the refurbishment/decommissioning decision) and the newly installed capacity:

$$\gamma_{l,p,y} = \gamma_{l,p,y}^{pre} + \gamma_{l,p,y}^{ref} \quad (9)$$

$\gamma_{l,p,y}^{pre}$  is the capacity, expressed in MW, of the pre-existing pipeline. It is set to 0 after the year of investment decision, as the refurbished pipeline capacity  $\gamma_{l,p,y}^{ref}$  is considered instead.

For what concern the Opex, it is calculated in equation 10:

$$Opex = \sum_{y=y_0}^{y_{end}} a_y \cdot \lambda_y \quad (10)$$

where  $\lambda_y$  is the yearly fixed cost of operation and maintenance, expressed in €.

Its calculation is done through the following equation:

$$\lambda_y = \sum_l c_l^{fix} \cdot \sum_p \gamma_{l,p,y} \cdot L_{l,p} \quad (11)$$

$c_l^{fix}$  is the unit fixed cost, expressed in €/MW/km, and it varies per network level.

Once economic constraints have been established, mass balances are set for the nodes of the network. Firstly, the monthly mass balance constraint at the generic node n is defined. No storage reservoirs of gas are present in Piedmont, so they are not considered in the equation:

$$q_{n,l,y,m}^{source} - q_{n,l,y,m}^{demand} - k_{peak} \cdot (q_{n,l,y,m}^{export} + q_{n,l,y,m}^{import}) = 0 \quad (12)$$

$q_{n,l,y,m}^{source}$  is the source of gas at node n, at each network level, in each year and month, expressed in MWh.

$q_{n,l,y,m}^{demand}$  is the demand of gas at node n, at each network level, in each year and month, expressed in MWh.

$k_{peak}$  is the peak factor, assumed equal to 730 h.

$q_{n,l,y,m}^{export}$  is the gas export from the node n, expressed in MW.

$q_{n,l,y,m}^{import}$  stands for the gas import to the node n, expressed in MW.

Each term of eq. 12 can be additionally split. The nodal monthly demand is divided in two terms, the local demand of the node  $q_{n,l,y,m}^{dem,loc}$  (e.g. the demand of an industry) and the delivered gas  $q_{n,l',y,m}^{del}$  between the transmission and the high-pressure network levels:

$$q_{n,l,y,m}^{demand} = q_{n,l,y,m}^{dem,loc} + q_{n,l',y,m}^{dem,del} \quad (13)$$

The same reasoning is done on the nodal monthly source. It consists of the local source of the node  $q_{n,l,y,m}^{source,loc}$  (e.g. national production of gas) and the received gas  $q_{n,l',y,m}^{dem,del}$  from the upper network levels (in this case the gas coming from the transmission network).

$$q_{n,l,y,m}^{source} = q_{n,l,y,m}^{source,loc} + q_{n,l',y,m}^{dem,del} \quad (14)$$

Therefore, the term  $q_{n,l',y,m}^{dem,del}$  only appears for nodes that belong to both the transmission and high-pressure networks. When balancing on the transmission side, the term  $q_{n,l',y,m}^{dem,del}$  appears in  $q_{n,l,y,m}^{demand}$ , while for the high-pressure side it appears in  $q_{n,l,y,m}^{source}$ . In this case study  $q_{n,l',y,m}^{dem,del}$  is imposed to be  $\geq 0$ , meaning that no reverse flow of gas from the high-pressure network to the transmission network is possible.

The annual local source is limited to the available max annual source at the considered node:

$$\sum_m q_{n,l,y,m}^{source,loc} \leq q_{n,y}^{max,source,loc} \quad (15)$$

Regarding the quantity of gas exports and imports from node  $n$  at  $l$ , it can be split between the amount of gas transported by each pipeline connected to the node, according to equations 16 and 17:

$$q_{n,l,y,m}^{export} = \sum_{p \in P_{n,l}^{export}} q_{p,l,y,m} \quad (16)$$

$$q_{n,l,y,m}^{import} = \sum_{p \in P_{n,l}^{import}} q_{p,l,y,m} \quad (17)$$

where  $q_{p,l,y,m}$  is the variable amount of gas, expressed in MW, transported by  $p$  at  $l$ .

$P_{n,l}^{export}$  represents the set of pipelines, at  $l$ , connected to  $n$ , that can export gas from the node.

$P_{n,l}^{import}$  represents the set of pipelines, at  $l$ , connected to  $n$ , that can import gas to the node.

As gas in the pipelines have a direction, the amount transported can be either negative or positive. If gas flows in the opposite direction with respect to the one assumed,  $q_{p,l,y,m}$  results to be negative (the end node defined in the attribute fields of the pipelines will act as a starting node, and vice versa).

The amount of gas transported, in MW, is limited to the pipeline capacity:

$$q_{p,l,y,m} \leq \gamma_{p,l,y} \cdot 1,1 \quad (18)$$

$$-q_{p,l,y,m} \leq \gamma_{p,l,y} \cdot 1,1 \quad (19)$$

The use of a minus sign in equation 19 is necessary when the amount of gas being transported is negative. A tolerance of 10% on the pipeline capacity limits is considered.

The equations above show that exports and imports are hourly variables. This is because the transport capacity of a line refers to the maximum flow rate that can pass through it.



The capacity of a pipeline, in MW, can be defined as:

$$\gamma = \dot{m}_{max} \cdot HHV \quad (20)$$

where  $\dot{m}_{max}$  stands for the maximum hourly flowrate [kg/h] acceptable in the pipeline, while HHV is the higher heating value [MWh/kg] of the gas.

The mass balances at the nodes are calculated monthly. Therefore, the hourly exports and imports are adjusted to monthly values using a peak factor of 730 hours, resulting in a constant mass flow rate for all hours of the month.

The model is limited in terms of fluid dynamics and temporal resolution. The first limitation is since no fluid dynamic analysis is performed during optimization, so the way gas is distributed does not consider the pressures at the nodes (hence any excessive pressure drops) and the velocities in the pipelines. The second limitation is that the mass balances are calculated on a monthly rather than an hourly basis. However, considering an hourly time resolution would result in too many constraints and thus computational difficulties.

The only fluid-dynamic limit is imposed on the amount of gas transported in the pipeline  $q_{p,l,y,m}$  (hence the maximum flow rate), through the capacity. The pipeline capacity  $\gamma_{l,p,y}$ , and thus the maximum acceptable flow rate, is correlated to the pipeline diameter for both existing and refurbished/decommissioned pipes. In fact, the decision variable on the capacity of new pipelines  $\gamma_{l,p,y}^{ref}$  is limited to a list of integer values, hence the term mixed integer in MILP.

The set of capacities and diameters is later shown in chapter 4, as well as its construction.

### 3.2.2 Biomethane injection scenario

This section presents the additional constraints for the case where biomethane injection into the grid is introduced. A distinction is done between the case with non-variable biomethane (all production plants connected to the grid and all biomethane is accepted) and the case with variable biomethane (the decision to connect is taken by the TSO, as is the amount of biomethane withdrawn and injected into the grid). In chapter 5 is explained how the input parameters for both scenarios have been derived.

#### 3.2.2.1 Fixed injection of biomethane

For the case where the entire distributed biomethane resource is accepted, new parameters are introduced, and some of the constraints defined above are modified. Part of the additional parameters are listed in the following table:

*Table 3.2 – Additional parameters of the model, fixed biomethane injection scenario*

<b>Indexes</b>	<b>Definition</b>	
$b$	Plant of biomethane	
<b>Parameters</b>	<b>Definition</b>	<b>Unit of Measurement</b>
$p_{b,n,y,l}^{bio}$	Available biomethane source, per biomethane plant $b$ , connected to node $n$ , at $l$ , in $y$	MWh
$L_b^{bio}$	Length of connection pipeline, per biomethane plant $b$	km
$Capex_{bio}$	Total capital expenditures for the connections of biomethane plants	€
$Opex_{bio}$	Total operational expenditures for the connections of biomethane plants	€

$\pi_{y,l,b}^{bio,con}$	Book value of connection pipeline per $b$ and $l$ , in the year of connection $y_{l,b}^{con}$	€
$\gamma_{l,b,y_{l,b}^{con}}^{bio}$	Capacity of connection pipeline per $b$ and $l$ , in the year of connection $y_{l,b}^{con}$	MW
$y_{l,b}^{con}$	Year of connection per biomethane plant $b$ , at $l$	-
$f_{l,b,y}^{bio}$	Depreciation factor of connection pipeline per $b$ , at $l$ in $y$	-

Starting with the objective function, the investment and operational costs for biomethane plant connections are added. These costs are fixed (hence parameters) as the scenario involves the connection of all plants:

$$f(x) = Capex + Opex + Capex_{bio} + Opex_{bio} \quad (21)$$

The investment in biomethane is calculated as follows:

$$Capex_{bio} = \sum_{y=y_0}^{y_{end}-1} a_y \cdot \omega \cdot \pi_y^{bio} + a_{y_{end}} \cdot \pi_{y_{end}}^{bio} \quad (22)$$

$\pi_y^{bio}$  is the total yearly book value of the biomethane connection pipelines, expressed in €. It is calculated through eq. 23:

$$\pi_y^{bio} = \sum_l \sum_b \pi_{y,l,b}^{bio} \quad (23)$$

The book value of each biomethane plant connection pipeline, at  $l$  in  $y$  is defined as:

$$\pi_{y,l,b}^{bio} = f_{l,b,y}^{bio} \cdot \pi_{y_{l,b}^{con},l,b}^{bio,con} \quad (24)$$

$\pi_{y_{l,b}^{con},l,b}^{bio,con}$  represents the book value of the connection pipeline in the year of connection of the biomethane plant, expressed in €, and it is calculated through eq. 25.

$$\pi_{y_{l,b}^{con},l,b}^{bio,con} = \gamma_{l,b,y_{l,b}^{con}}^{bio} \cdot c_l^{inv} \cdot L_b^{bio} \quad (25)$$

The depreciation factor  $f_{l,b,y}^{bio}$  is defined below:

$$f_{l,b,y}^{bio} = \begin{cases} 1 - \frac{1}{20} \cdot (y - y_{l,b}^{con}) & : \forall y \geq y_{l,b}^{con} \\ 0 & : \forall y < y_{l,b}^{con} \end{cases} \quad (26)$$

As consequence, before the year of connection, the book value of the connection pipeline  $\pi_{y,l,b}^{bio}$  is 0 (since no connection has been realized yet), then it decreases as the depreciation of the asset increases.

For what concern the Opex related to biomethane, it is calculated as follows:

$$Opex_{bio} = \sum_{y=y_0}^{y_{end}} \alpha_y \cdot \lambda_y^{bio} \quad (27)$$

where  $\lambda_y^{bio}$  is the yearly fixed cost of operation and maintenance, expressed in €.

Its calculation is done through the following equation:

$$\lambda_y^{bio} = \sum_l c_l^{fix} \cdot \sum_b \gamma_{l,b,y}^{bio} \cdot L_b^{bio} \quad (28)$$

$\gamma_{l,b,y}^{bio}$  represents the capacity of the connecting pipeline, per biomethane plant  $b$ , at  $l$  in  $y$ . The capacity is set to 0 before the connection of the biomethane plant:

$$\gamma_{l,b,y}^{bio} = \begin{cases} \gamma_{l,b,y-1}^{bio} & : \forall y \geq y_{l,b}^{con} \\ 0 & : \forall y < y_{l,b}^{con} \end{cases} \quad (29)$$

In terms of mass balances, equation 12 is modified to inject the available source of biomethane at each node  $n$ :

$$q_{n,l,y,m}^{source} - q_{n,l,y,m}^{demand} - k_{peak} \cdot (q_{n,l,y,m}^{export} + q_{n,l,y,m}^{import}) + \frac{q_{n,y,l}^{bio}}{12} = 0 \quad (30)$$

$q_{n,y,l}^{bio}$  represents the annual available source of biomethane (hence the producibility of the plants connected to node n), and it is divided equally in each month, assuming a constant biomethane production throughout the year. It derives from the sum of the producibility of biomethane plants connected to the node:

$$q_{n,y,l}^{bio} = \sum_b p_{b,n,y,l}^{bio} \quad (31)$$

In this scenario,  $q_{n,l',y,m}^{dem,del}$  is imposed to be  $\geq 0$  except for a few nodes, where reverse flow from the regional network to the national network is possible, assuming the presence of a compressor in parallel with the reduction cabin. This is related to the fact that in two of the gas demand evolution scenarios, fixed biomethane production exceeds gas demand in isolated parts of the regional grid, as in the example below.

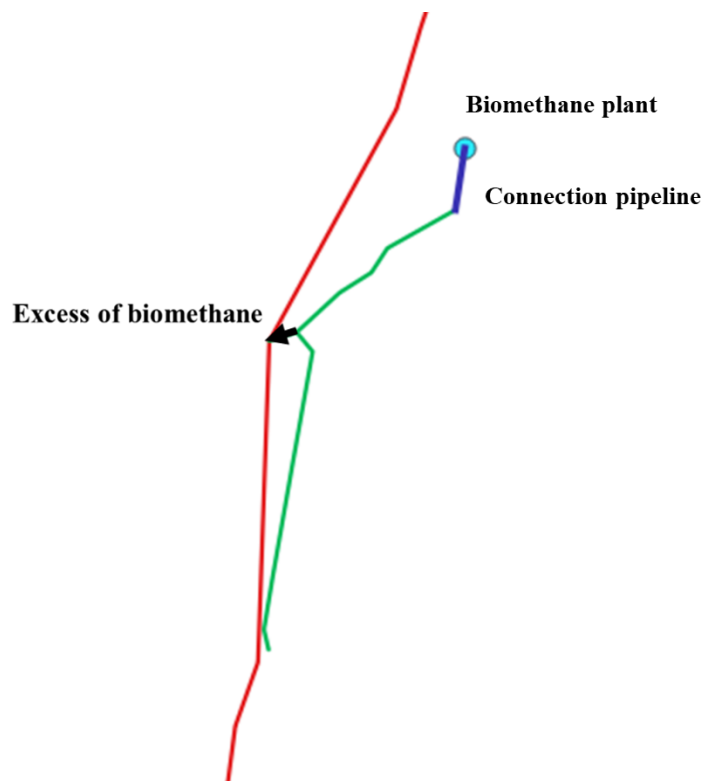


*Figure 3.2 – Example scheme of reverse flow from regional to national network*

Having to accept all biomethane production, it is therefore assumed that there is a possibility of using the national grid to handle the excess production.

### 3.2.2.2 Variable injection of biomethane

In the scenario involving variable biomethane injection, the TSO has the possibility to decide whether to connect biomethane plants to the grid and inject the desired amount of biomethane, within the limits of the plants' production.

The decision to connect is made on the individual plant, in the year of possible connection, i.e. the year of the biogas incentive expiry. The following is a list of the needed additional variables and parameters.

*Table 3.3 – Additional variables and parameters for the model, variable biomethane injection scenario.*

<b>Variables</b>	<b>Definition</b>	<b>Unit of Measurement</b>
$v_{b,n,y,l,m}^{bio}$	Variable injected biomethane source per $b$ , at node $n$ , at $l$ , in $y$ and $m$	MWh
$dec_{b,y,l}$	Binary decision variable per biomethane plant $b$ , at $l$ in $y$	-
<b>Parameters</b>	<b>Definition</b>	<b>Unit of Measurement</b>
$\gamma_{l,b}^{dec,con}$	Year of biomethane plant connection decision, per $b$ , at $l$	-

Eq. 23 is modified, to consider the variable decision to connect or not the biomethane plant, with the aim of minimizing the infrastructure total costs:

$$\pi_y^{bio} = \sum_l \sum_b \pi_{y,l,b}^{bio} \cdot dec_{b,y,l} \quad (32)$$

$dec_{b,y,l}$  is the binary decision variable, on the connection of the biomethane plant  $b$ , at  $l$  in  $y$ . Once the decision has been made, it cannot be changed, as imposed by the following constraint:

$$dec_{b,y,l} = \begin{cases} dec_{b,y-1,l} & : \forall y \geq y_{l,b}^{dec,con} \\ 0 & : \forall y < y_{l,b}^{dec,con} \end{cases} \quad (33)$$

Before the biomethane plant connection decision year  $y_{l,b}^{dec,con}$ , the variable is set to 0.

Focusing on Opex, the calculation of  $\lambda_y^{bio}$  in equation 28 is modified as follows:

$$\lambda_y^{bio} = \sum_l c_l^{fix} \cdot \sum_b dec_{b,l,y} \cdot \gamma_{l,b,y}^{bio} \cdot L_b^{bio} \quad (34)$$

In this way, the decision variable acts both on investments and operational costs related to the connections to realize.

The mass balance equation is modified to consider the variable injection of biomethane. The variability of the source is related to the decision to connect or not the biomethane plant and to the possibility of regulating the amount of green gas to inject, as reported in equation 35 and equation 36:

$$q_{n,l,y,m}^{source} - q_{n,l,y,m}^{demand} - k_{peak} \cdot (q_{n,l,y,m}^{export} + q_{n,l,y,m}^{import}) + \sum_b v_{b,n,y,l,m}^{bio} = 0 \quad (35)$$

The variable monthly injection of biomethane, per plant  $b$  and node  $n$ , is limited by the available biomethane source  $\frac{p_{b,n,y,l}^{bio}}{12}$ . If it is decided not to connect the hub to that node, the variable injection must be null. This is imposed through the decision variable:

$$v_{b,n,y,l,m}^{bio} \leq dec_{b,y,l} \cdot \frac{p_{b,n,y,l}^{bio}}{12} \quad (36)$$

In this scenario it is considered the possibility of having reverse flow of excess biomethane too.

## 4. Base scenario input data

This chapter outlines the input data for the base case, which does not involve any injection of biomethane into the grid. As per the equations defined in section 3.2.1, the base scenario includes the decision to decommission or replace pipelines at the end of their useful life, and how to distribute gas in the network, considering a decreasing gas demand until 2050. The objective is to minimize the overall investment and operational costs throughout the entire period.

The input data includes:

- Network topology (nodes and pipelines),
- Monthly gas demand per node and year,
- Available annual gas source per node,
- Pipeline technical data (transport capacities, year of installation, pipeline's useful life),
- Unit investment and operational costs of the gas infrastructure.

### 4.1 Network topology

The network topology is constructed by transferring the list of attributes from QGIS to Pyomo. The network configuration is created using the names of the start and end nodes of the pipelines. Sets of nodes and pipelines are then created, differentiated by network type (transmission or high-pressure), as well as export and import pipelines for each node. Additional information is recorded, such as the diameter of the pipeline in inches and the length of the pipeline in km.

### 4.2 Gas demand

For gas demand, it is necessary to define the monthly demand for each node of the network throughout the period 2025-2050. First, the demand in 2025 is constructed, and then an annual demand reduction is applied, for each scenario of the DDS discussed in the first chapter.



#### 4.2.1 Initial gas demand

The reference demand data are obtained from the Snam website. The website provides transport capacities and booked capacities for each redelivery point of the regional network (ReMi cabins, industries, thermoelectric plants, etc.), per thermal year [22]. To each node of the network, is assigned a value of booked capacity, expressed in kWh/day, by matching the name of the node assigned in QGIS and the name of the redelivery point.

The booked capacity is the maximum daily quantity of gas that each consumer can inject or withdraw from the network, expressed in kWh/day or in Sm<sup>3</sup>/day [23]. Along with the capacity, the type of redelivery point is assigned, which can be:

- Distribution (civil)
- Thermoelectric
- Industry
- Transport

Two monthly consumption profiles have been constructed, as shown in the table below, one constant (profile B) and one variable (profile A). Profile B is constant, while Profile A is variable and based on the monthly average of gas consumption in Italy from 2019 to 2022 [24]. The fractions are obtained dividing the monthly consumption by the total consumption. Profile A has been chosen for civil demand, while for the other redelivery sites a constant consumption is assumed throughout the year.

*Table 4.1 – Split of annual consumptions into monthly consumptions*

A [%]	B [%]	Month
13,53%	8,33%	january
10,42%	8,33%	february
9,88%	8,33%	march
7,17%	8,33%	april
5,82%	8,33%	may
5,68%	8,33%	june
6,50%	8,33%	july
5,55%	8,33%	august
6,50%	8,33%	september
7,31%	8,33%	october
9,61%	8,33%	november
12,04%	8,33%	december

The booked capacity is assumed to be the maximum daily consumption required by the node during the year. Since mass balances are calculated monthly in the code, the booked capacity is taken as the average daily consumption of the month of January, which is the month with the highest consumption during the year, for redelivery points with civil demand.

This is done to avoid having an average daily consumption equal to the booked capacity for each month and considering that civil demand is strongly dependent on the seasonality. For what concern the other types of consumption, the daily consumption is instead considered constant for each month of the year and equal to the booked capacity.

After establishing the daily consumption, the annual gas demand for each node is derived.

However, certain nodes in the network are unique: they serve as end points for pipelines connecting Piedmont with other regions, or as redelivery points for other TSOs, or as national entry/exit points. The figure below highlights these nodes:

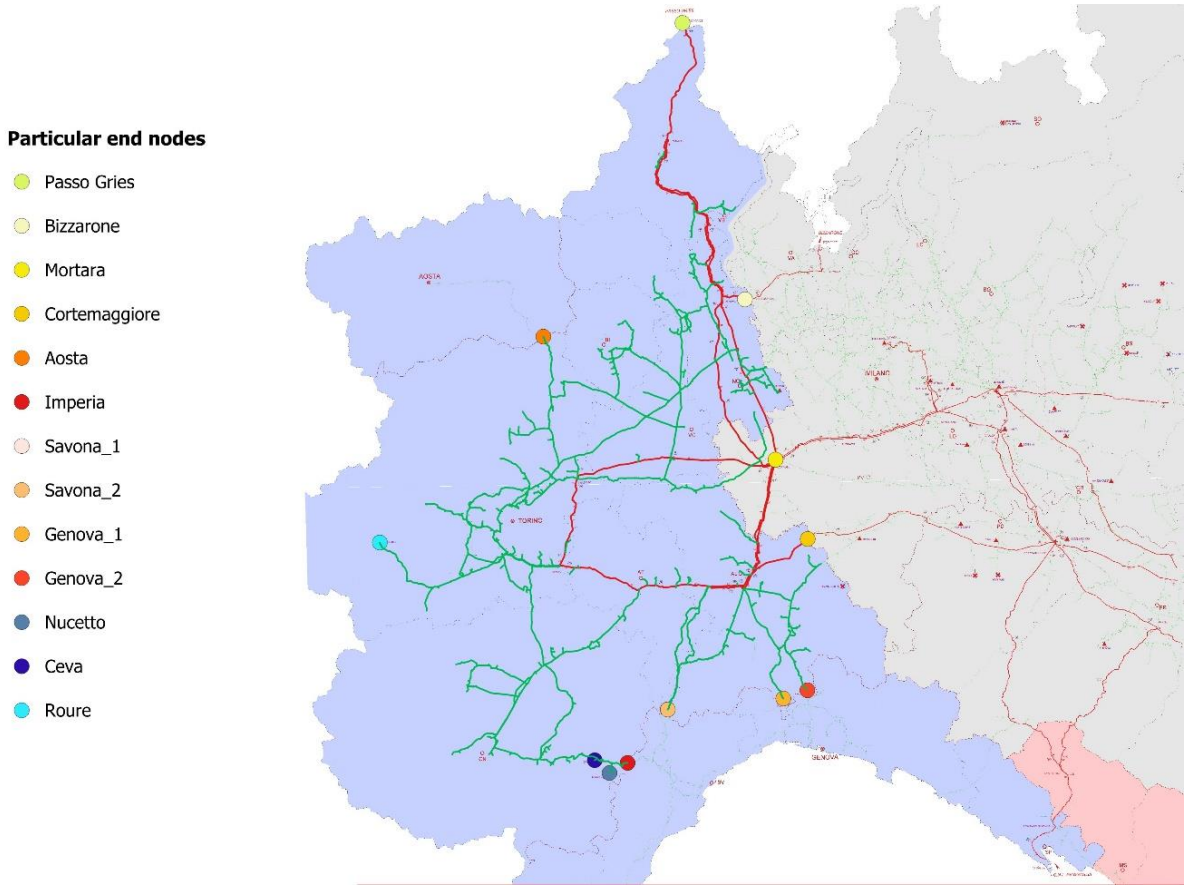


Figure 4.1 – Particular end nodes of the network model

Starting with the nodes highlighted in yellow, the demand of Passo Gries has not been considered, so it is assumed that the node will only act as a national entry point. This assumption neglects the presence of the compressor located in Masera.

Regarding Bizzarone, to the node is assigned the booked capacity of the national exit point of Bizzarone, which is interconnected with foreign countries [25].

Mortara is considered just as sorting node connected to other Italian regions, with no demand assigned for simplicity.

For Cortemaggiore node, the booked capacity of all its redelivery points is assigned, as if the red pipeline went all the way to the city and distributed gas to all redelivery points, neglecting any other redelivery points in Lombardy and Emilia Romagna served by the considered transmission pipeline.

The orange-highlighted nodes in the Piedmont regional network are interconnection points with Liguria and Aosta Valley. The southern hubs serve Liguria's demand. The booked capacity of all the redelivery points in the main cities, namely Imperia, Savona, and Genoa, is allocated accordingly. The same is done for the northern node, which serves Aosta Valley.

Finally, the blue nodes are interconnection points with other TSOs that operate the gas transport network in Piedmont, namely Energie Rete Gas and Metanodotto Alpino. In the TSOs websites are published the transportation capacities and booked capacities in  $\text{Sm}^3/\text{day}$  for each redelivery point, by thermal year. To Ceva and Nucetto nodes is assigned the sum of the booked capacities of all the regional redelivery points operated by Energie Rete Gas, for the thermal year 21/22, as of September 2022 [26]. To Roure is assigned the sum of the booked capacities of all regional redelivery points managed by Metanodotto Alpino for the thermal year 21/22 [27].

Since these nodes serve several redelivery points, a monthly demand profile of type A is assumed for simplicity, as if the demand is all civil. Thus, from the booked capacities in  $\text{kWh}/\text{day}$ , the monthly demand in January is obtained and from the A profile, the annual demand for the node is derived.

After constructing the annual demand for each node, the total annual demands by region are obtained. For the sake of simplicity, the demand of the Bizzarone and Cortemaggiore nodes is considered as part of the demand of Piedmont. To verify the appropriateness of the demand obtained based on the booked capacity, a comparison has been made with the data provided by MASE on the annual gas demand by region [28].

Specifically, the annual regional demand has been averaged for the years 2018 to 2022, obtaining the following values for Piedmont, Liguria, and Aosta Valley:

*Table 4.2 – Comparison between modelled demand and MASE demand data per region, with scale factors for correction*

Region	Model demand [TWh/y]	MASE demand [TWh/y]	Scale factor
Piedmont	139,5	83,7	1,67
Aosta Valley	1,1	1,1	1
Liguria	15,7	16	0,98

The table shows that the demand of Piedmont has been overestimated compared to the average of the last years, while for Liguria it has been underestimated. The annual demand of each node is then corrected using the scaling factors shown in Table 4.2. Through this procedure, the annual demand in 2025 for all nodes of the modelled network has been estimated.

The table below shows the input data to provide to the code. It contains the name of the node, the type of node, the yearly demand, the monthly profile (A or B type) and the type of redelivery point. The monthly demand is calculated by multiplying the annual demand with one of the indexes shown in Table 4.1, depending on the month of interest. The parameter  $q_{n,l,y,m}^{dem,loc}$  is then determined for 2025.

*Table 4.3 – Input data of initial annual demand, monthly profile, and type of demand per node*

Node	Type	Yr.-dem. [MWh/y]	Time-res.	Composition
Passo Gries	Transmission	0	A	Absent
Masera	Transmission	72920	A	Distribution
Gravellona Toce	Transmission	68484	A	Distribution
Gattico-Veruno	Transmission	205709	A	Distribution
Margattino	Transmission	0	A	Absent
Cascina Monferrona	Transmission	0	A	Absent
Briona	Transmission	0	A	Absent
Mortara	Transmission	0	A	Absent
.....				
Omegna_4	High-Pressure	147684	A	Distribution
Omegna_3	High-Pressure	8993	B	Industry
Mergozzo	High-Pressure	13009	A	Distribution
Villadossola_2	High-Pressure	50672	A	Distribution
Villadossola_1	High-Pressure	71001	B	Industry
Domodossola_2	High-Pressure	159338	A	Distribution
Domodossola_1	High-Pressure	21300	B	Industry
Riduzione50	High-Pressure	0	A	Absent
Intermezzo188	High-Pressure	0	A	Absent
Intermezzo184	High-Pressure	0	A	Absent
Intermezzo185	High-Pressure	0	A	Absent

#### 4.2.2 Gas demand evolution

For each node of the network, it is necessary to establish the evolution of gas demand between 2025 and 2050. The expected Italian gas demand in 2030 and 2040 has been estimated in the DDS, starting with the gas demand in 2021. This has been carried out for 2 scenarios at 2030 and 3 scenarios at 2040, i.e. the national scenarios discussed in chapter 1:

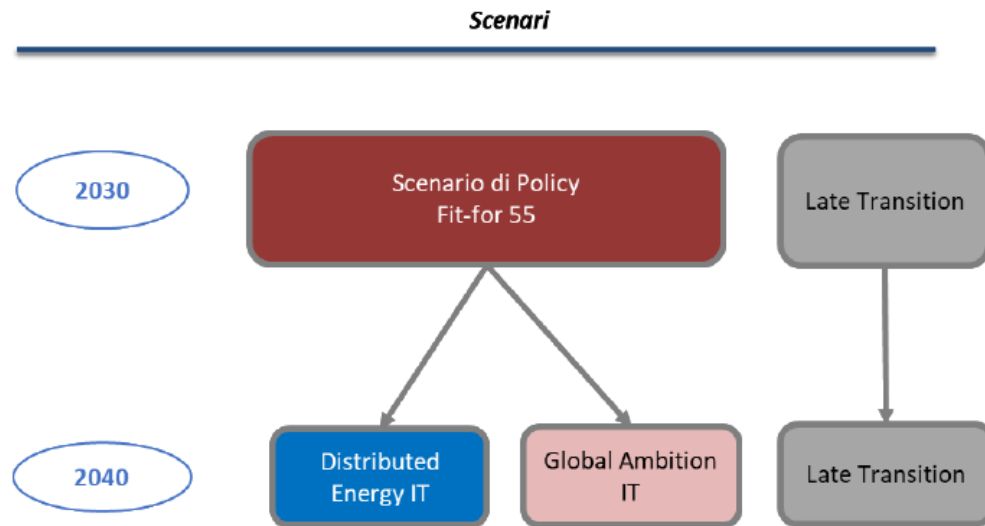


*Figure 4.2 – National scenarios in 2030 and 2040 [7]*

The same demand evolution is applied to the model created, starting in 2025. With the data provided in Table 1.1, Table 1.2, and Table 1.3, the annual demand reduction percentages per sector and per scenario are derived. It is assumed that the 2021 data in Table 1.1 are relative to 2025, as the initial demand calculated for 2025 considers the average of the last few years, where gas demand has not faced a constant decrease, also due to the pandemic. It is therefore consistent to expect that annual gas demand will not vary much between 2021 and 2025.

##### 4.2.2.1 DE scenario

The *Distributed Energy* scenario in 2040, is characterized by the intermediate scenario *Fit-for 55* in 2030. Therefore, a first reduction profile is adopted between 2025-2030, and a second reduction profile between 2030-2050, assuming a decrease in demand between 2040-2050 in line with the previous decade. The calculated annual demand reduction percentages with respect to the initial demand, divided per sector, are shown in the table below.

*Table 4.4 – Annual demand reduction percentages per sector and range of years, DE scenario*

	Distribution	Industry	Transport	Thermoelectric
<b>FF55 2025-2030</b>	6,0%	1,7%	-35,7%	7,0%
<b>DE 2030-2040</b>	4,7%	3,9%	5,9%	3,1%
<b>DE 2040-2050</b>	4,7%	3,9%	5,9%	3,1%

The annual gas demand evolution per sector is obtained for the period 2025-2050:

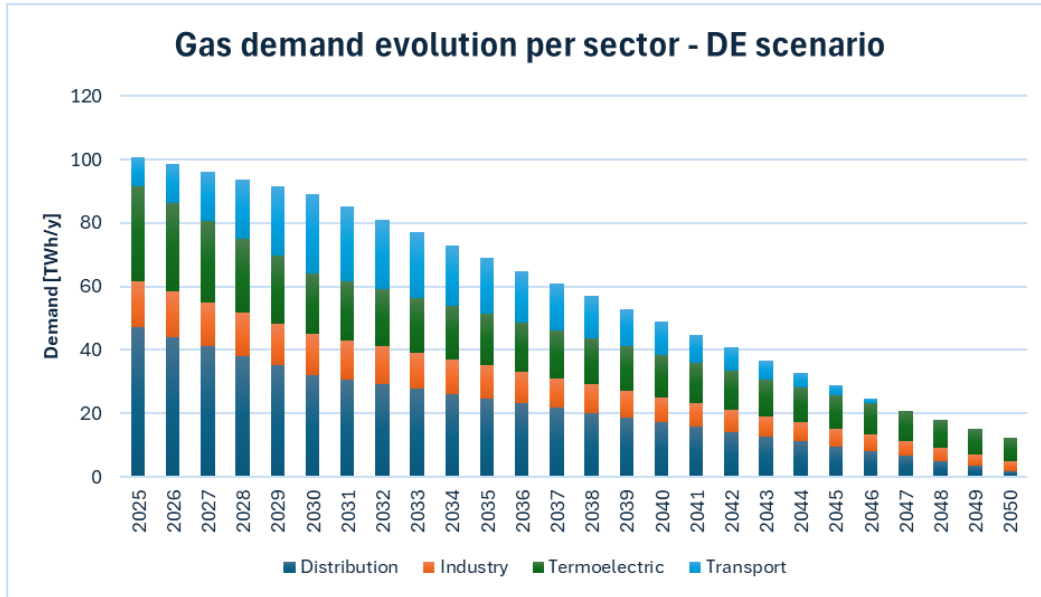


*Figure 4.3 – Gas demand evolution per sector, 2025-2050, DE scenario*

#### 4.2.2.2 GA scenario

The *Global Ambition* scenario in 2040, is characterized by the intermediate scenario *Fit-for 55* in 2030. Therefore, a first reduction profile is adopted between 2025-2030, and a second reduction profile between 2030-2050, assuming a decrease in demand between 2040-2050 in line with that of the previous decade. The calculated annual demand reduction percentages with respect to the initial demand, divided per sector, are shown in the table below.

*Table 4.5 - Annual demand reduction percentages per sector and range of years, GA scenario*

	Distribution	Industry	Transport	Thermoelectric
<b>FF55 2025-2030</b>	6,0%	1,7%	-35,7%	7,0%
<b>GA 2030-2040</b>	4,2%	4,3%	5,9%	2,7%
<b>GA 2030-2040</b>	4,2%	4,3%	5,9%	2,7%

The annual gas demand evolution per sector obtained for the period 2025-2050, is shown in the figure:

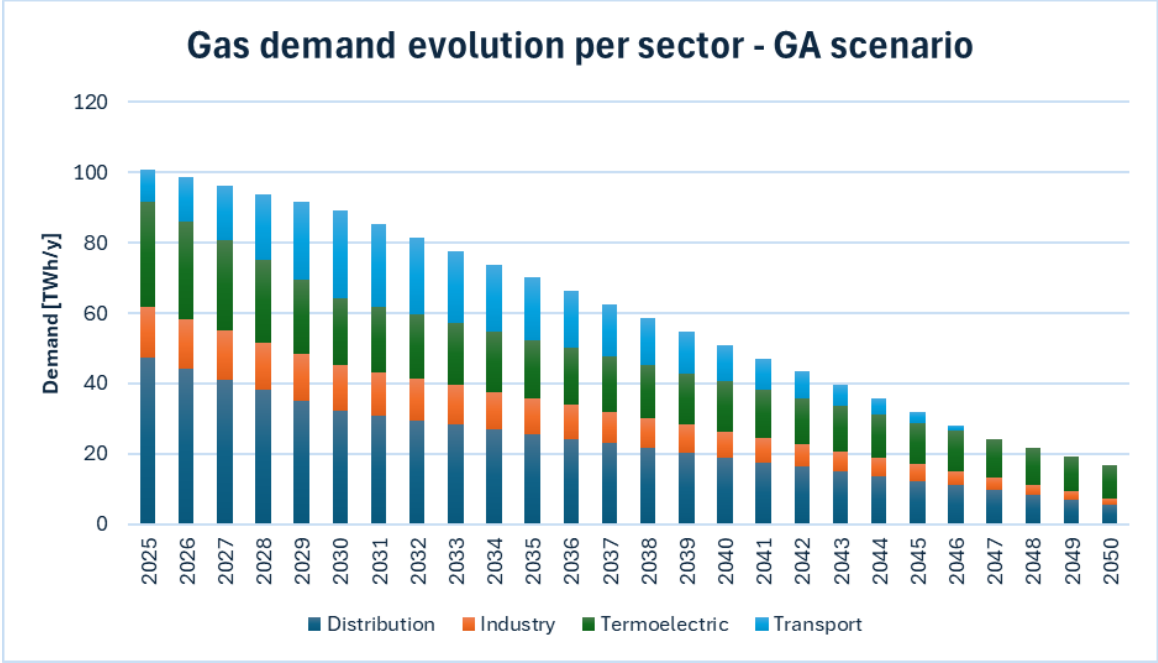


Figure 4.4 - Gas demand evolution per sector, 2025-2050, GA scenario

4.2.2.3 LT scenario

The *Late Transition* scenario in 2040, is characterized by the intermediate scenario *Late Transition* in 2030. Therefore, a first reduction profile is adopted between 2025-2030, and a second reduction profile between 2030-2050, assuming a decrease in demand between 2040-2050 in line with that of the previous decade. The calculated annual demand reduction percentages with respect to the initial demand, divided per sector, are shown in the table below.

Table 4.6 - Annual demand reduction percentages per sector and range of years, LT scenario

	Distribution	Industry	Transport	Thermoelectric
LT 2025-2030	6,0%	2,6%	-38,6%	5,3%
LT 2030-2040	1,6%	0,6%	3,9%	-0,5%
LT 2040-2050	1,6%	0,6%	3,9%	-0,5%

The annual gas demand evolution per sector obtained for the period 2025-2050, is shown in the figure:

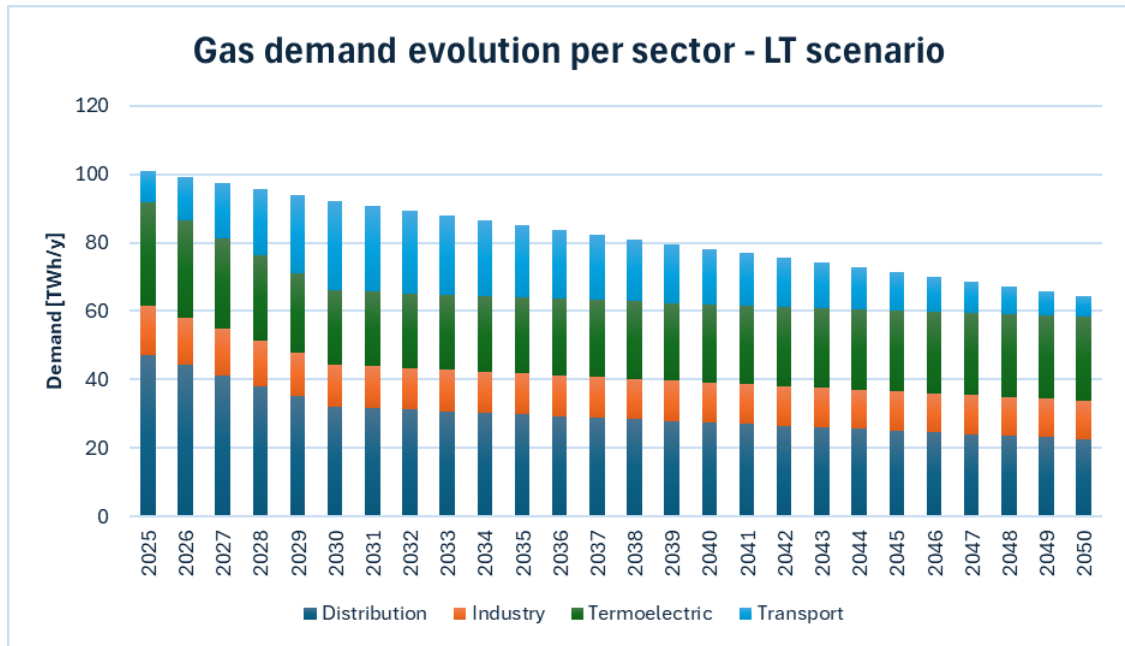


Figure 4.5 - Gas demand evolution per sector, 2025-2050, LT scenario

For each scenario the parameter  $q_{n,l,y,m}^{dem,loc}$  is finally determined for each year of the period of analysis, as the reduction rates are applied to the initial gas demands shown in Table 4.3.

### 4.3 Gas source

Once the nodal gas demand has been established, it is necessary to determine which nodes in the network will supply the gas. From the Snam network diagram, in Figure 2.1 and Figure 2.2, it can be seen that gas in Piedmont can generally be supplied from Passo Gries as well as from other national entry points such as Panigaglia, Tarvisio, Gorizia, etc.

This is due to the fact that the national network connects several Italian regions.

It is assumed that gas can be supplied from Passo Gries and Panigaglia only. This excludes gas coming from the north-eastern or southern national entry points.

Therefore, the Cortemaggiore hub is virtually considered as the entry point for gas from Panigaglia, where regasification of LNG occurs. Mortara is treated only as a hub, without



knowing whether gas can arrive as a resource from the east of Italy or go out to serve Lombardy's gas demands.

The other gas resource point is a national production node in the regional network (high-pressure), namely Trecate.

In the figure below are highlighted the nodes that are sources of gas, with the amount of available annual source indicated:

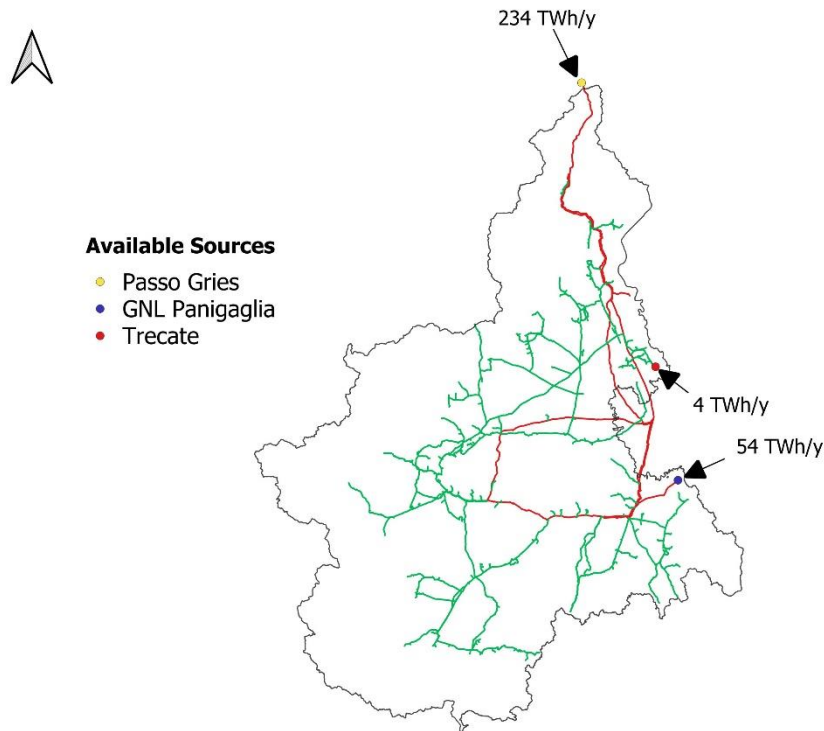


*Figure 4.6 – Nodes of gas source of the network model*

To assess the annual gas resources available from entry points, the Snam document on the transport capacities of entry and exit points interconnected with the national network is used as a reference [25]. In fact, as reported in the network code, the transport capacity at the entry points interconnected with foreign countries is the maximum capacity that can be made available to the users for the transportation service, either continuous or interruptible, and for entry points from domestic natural gas production it is the daily gas flow rate that the transportation system can receive and transport up to the redelivery points, according to the technical checks carried out by the transporter [16].

The transport capacity allocated to the entry point in kWh/day is converted to MWh/year. The table below shows the input data for the gas sources:

*Table 4.7 – Input data of available annual gas source per node*

Node	Type	Source [MWh/y]	Comment
Passo Gries	Transmission	233776165	value per year
Cortemaggiore	Transmission	53515715	value per year
Trecate	High-Pressure	3916450	value per year

The available annual source per node is assumed constant throughout the analysis period. The parameter  $q_{n,y}^{\max,source,loc}$  is finally determined.

#### 4.4 Pipeline capacity

As explained in the previous chapter, it is necessary to provide the pipeline capacity  $\gamma_{l,p,y}$  as input data. To get a value of the capacity, the maximum flowrate per pipeline needs to be evaluated. To do so, a fluid dynamics analysis of the network is carried out, with the purpose of checking the correctness of the model created in QGIS too (e.g. to check that none of the nodes is isolated, due to possible mistakes on assigning the correct name to a node). Nevertheless, the network contains loops, so the flowrates can't be determined without iterative methods.

##### 4.4.1 Fluid dynamics analysis

MATLAB is used to carry the fluid dynamic analysis of the network. The developed algorithm exploits the conservation of mass and a simplified version of Newton's Second Law of Motion [29].

The conservation of mass for 1D flow is defined:

$$\frac{\partial \rho}{\partial t} + \frac{\partial(\rho \cdot v)}{\partial x} = 0 \quad (37)$$

The same is done for the conservation of momentum for 1D flow:

$$\frac{\partial(\rho \cdot v)}{\partial t} + \frac{\partial(\rho \cdot v^2)}{\partial x} + \frac{\partial p}{\partial x} + \frac{\lambda \cdot \rho \cdot v \cdot |v|}{2 \cdot D} + \rho \cdot g \cdot \sin \alpha = 0 \quad (38)$$

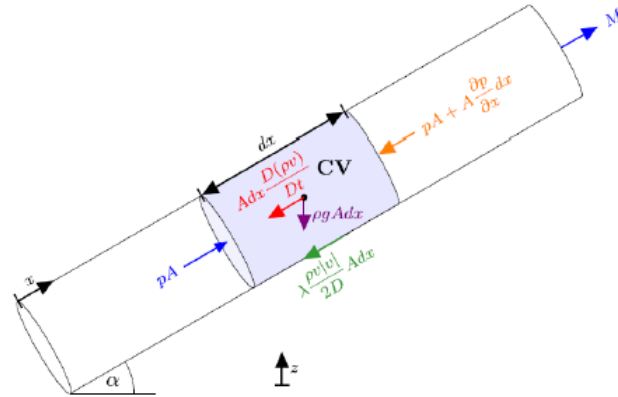


*Figure 4.7 – Scheme of conservation of momentum for 1D flow, applied to a pipeline’s control volume*

where  $\rho$  represents the gas density [kg/m<sup>3</sup>],

$v$  is the gas velocity [m/s],

$p$  the gas pressure [Pa],

$\lambda$  is the friction factor [-],

$\alpha$  is the generic angle of inclination of the pipeline,

$D$  is the diameter of the pipeline [m],

$g$  is the gravity acceleration [m/s<sup>2</sup>].

$\lambda$  can be evaluated according to the type of flow, which can be laminar or turbulent. In the first case:

$$\lambda = \frac{Re}{64} \quad (39)$$

where  $Re$  is the Reynolds number:

$$Re = \rho \cdot v \cdot \frac{D}{\mu} \quad (40)$$

$\mu$  is the dynamic viscosity [ $Pa \cdot s$ ]. In case the flow is turbulent, the friction factor can be derived from the Colebrook White Equation:

$$\frac{1}{\lambda^{0,5}} = -2 \cdot \log_{10} \left( \frac{2,51}{Re \cdot \lambda^{0,5}} + \frac{R}{3,71 \cdot D} \right) \quad (41)$$

where R is the internal pipeline roughness measured in mm.

Some simplifications are performed on eq. 38, with the following hypothesis:

- Compressible gas, which means that  $\rho = f(p, T)$
- Isothermal flow, with the isothermal speed of sound  $c^2 = \frac{p}{\rho}$ .
- Creeping motion, with low speed of gas in the pipeline ( $v \leq 25$  m/s), so the convective term (2<sup>nd</sup> in eq. 38) is not considered.
- Slow changes at boundary conditions, so the inertia term (1<sup>st</sup> in eq. 38) can be neglected (steady state conditions).

The momentum equation become the following:

$$\frac{\partial p}{\partial x} + \frac{\lambda \cdot \rho \cdot v \cdot |v|}{2 \cdot D} + \rho \cdot g \cdot \sin \alpha = 0 \quad (42)$$

By substituting  $v = \frac{\dot{m}}{\rho \cdot A}$ ,  $\rho = \frac{p}{c^2}$  and multiplying all the terms by p:

$$\frac{\partial p^2}{\partial x} + 2 \cdot g \cdot \sin \alpha \cdot \frac{p^2}{c^2} = - \frac{\lambda \cdot c^2 \cdot \dot{m} \cdot |\dot{m}|}{A^2 \cdot D} \quad (43)$$

Next passage consists of substituting  $p^2 = P$  and to integer over the length L of the pipeline.

First, a further simplification is to consider horizontal pipes, so that gravity term is overlooked, obtaining the final pressure drop equation in a pipeline, also known as Fergusson Equation:

$$P_1 - P_2 = \lambda \cdot c^2 \cdot \frac{L}{A^2 \cdot D} \cdot \dot{m} \cdot |\dot{m}| \quad (44)$$

The expression can be modified through the definition of the pressure drop coefficient  $R_{fc}$ :

$$R_{fc} = R_{fc}(\dot{m}) = \lambda \cdot L \cdot D \cdot \frac{c^2}{A^2} \cdot |\dot{m}| \quad (45)$$

so that equation 44 becomes:

$$P_1 - P_2 = R_{fc}(\dot{m}) \cdot \dot{m} \quad (46)$$

Regarding the conservation of mass shown in equation 37, applying all the hypothesis it becomes:

$$\frac{1}{A} \cdot \frac{\partial \dot{m}}{\partial x} = 0 \quad (47)$$

Equations 47 and 46 can be rewritten in matrix form:

$$XM = -M_{ext} \quad (48)$$

$$X^t P = R_{fc}(M) \cdot M \quad (49)$$

where the first equation is the flowrates balance applied to each node,

X represents the incidence matrix,

M is the vector of flowrates in the pipelines,

$M_{ext}$  is the vector of nodal demands.

The second equation is the simplified momentum conservation equation, where  $X^t$  is the incidence matrix transposed, while P is the vector of nodal pressures squared.

The characteristics of the system of equations are summarized in the scheme below, where  $b$  is the number of branches (pipelines) and  $n$  is the number of nodes:

$$\begin{array}{l}
 \text{Compressible} \\
 \left\{ \begin{array}{l}
 \begin{array}{l}
 n \times b \quad b \times 1 \quad n \times 1 \\
 \mathbf{X} \cdot \mathbf{M} + \mathbf{M}_{\text{ext}} = 0
 \end{array} \\
 \text{Continuity equation} \\
 \text{conservation of mass}
 \end{array} \right. \begin{array}{l}
 n \text{ equations} \\
 b \text{ unknowns} \\
 \text{Pipeline mass flows}
 \end{array} \\
 \\
 \left\{ \begin{array}{l}
 b \times n \quad n \times 1 \quad b \times b \quad b \times 1 \\
 \mathbf{X}^t \cdot \mathcal{P} = \mathbf{R}_{f_c}(\mathbf{M}) \cdot \mathbf{M}
 \end{array} \right. \begin{array}{l}
 b \text{ equations} \\
 n \text{ unknowns} \\
 \text{Nodal pressures}
 \end{array} \\
 \hline
 \begin{array}{l}
 n + b \text{ equations} \\
 b + n \text{ unknowns}
 \end{array}
 \end{array}$$

Figure 4.8 – Conservation of mass and conservation of momentum equations scheme

The momentum equation can be rewritten in a more explicit form, by multiplying both terms by the inverse of the pressure drop coefficient matrix  $R_{f_c}$ :

$$Y_{f_c}(M) = \text{inv}(R_{f_c}(M)) \quad (50)$$

The new equation is:

$$M = Y_{f_c}(M) \cdot X^t \cdot P \quad (51)$$

Regarding the solution, the momentum equation is not linear, due to the presence of  $M$  dependence in the  $Y_{f_c}$  matrix, and thus the two equations need to be solved simultaneously. The known vectors are  $M_{\text{ext}}$  and the incidence matrix  $X$ , while nodal pressures and flowrates distribution need to be identified.

#### 4.4.2 SIMPLE algorithm

To solve the mathematical problem, it is exploited an adaptation to networks of compressible fluids of the Semi-Implicit Method for Pressure-Linked Equations. The SIMPLE, invented by Patankar and Spalding in 1970s [30], is a widely used numerical procedure to solve the Navier–Stokes equations, and provides a robust approach for the calculation of pressures and velocities. Applied to this case study, it can be summarized in 5 steps:

- First, the exact solution of the unknown terms  $M$  and  $P$  can be written as the sum of an attempt value and a correction value:

$$M = M^* + M' \quad (52)$$

$$P = P^* + P' \quad (53)$$

- Second, a subtraction between the momentum equation with the exact solution and the momentum equation with the guessed solution is performed:

$$\begin{aligned} M &= Y_{fc}(M) \cdot X^t \cdot P \quad - \\ M^* &= Y_{fc}(M^*) \cdot X^t \cdot P^* \quad = \\ M - M^* &= Y_{fc}(M) \cdot X^t \cdot P - Y_{fc}(M^*) \cdot X^t \cdot P^* \end{aligned} \quad (54)$$

- Third, it is assumed that term  $Y_{fc}$  is weakly dependent on  $M$ , so that it can be stated:

$$Y_{fc}(M) \approx Y_{fc}(M^*) \quad (55)$$

Therefore, the mass flow rate correction equation is obtained:

$$M' = Y_{fc}(M) \cdot X^t \cdot P' \quad (56)$$

- Fourth, the mass flow rate balance equation is rewritten with the guessed and corrected terms:

$$X(M^* + M') = -M_{ext} \quad (57)$$

- Fifth, the term  $M'$  in the previous equation is substituted with its equivalent of the mass flow rate correction equation:

$$X \cdot Y_{fc} \cdot X^t \cdot P' = -X \cdot M^* - M_{ext} \quad (58)$$

Or, in a more compact form:

$$H \cdot P' = b \quad (59)$$

Finally,  $P'$  is derived:

$$P' = H \setminus b \quad (60)$$

The process of the algorithm is to start with attempts at pressure and flow values, i.e. to define the vectors  $P^*$  and  $M^*$ . However, the two guesses are not correlated, due to the non-linearity of the equation:

$$M^* = Y_{fc}(M) \cdot X^t \cdot P^* \quad (61)$$

Thus, an iteration is done to correlate them. Then the correction vectors  $P'$  and  $M'$  are calculated through eq. 60 and eq. 56. By summing the correction vectors with the guess vectors, updated guesses are derived for the successive iterative cycle:

$$P_{new}^* = P^* + P' \quad (62)$$

$$M_{new}^* = M^* + M' \quad (63)$$

This is repeated until a specified tolerance between the current guess and the new guess is reached.

The mathematical formulation is replicated in MATLAB, and input data relative to the network topology, gas demand and pipelines' attributes are needed.

The model consists of two network levels: transmission and high pressure. To apply the SIMPLE method, it is first used on the regional network and then on the national network. In the QGIS model, some lines are represented as reduction valves, which are used for the transition from the national network to the regional network that operates at reduced pressures according to Snam's network code [16].



The figure below shows an example of a valve in the QGIS representation of the network:



*Figure 4.9 – QGIS representation of reduction valves (in yellow)*

The SIMPLE is first applied to the green network, considering the gas source nodes as the exit nodes of the reduction valves. The pressure at the nodes exiting the valves is assumed and fixed at 24 bar for most nodes, and 33 bar for others. To proceed, the guessed pressures at the nodes (vector  $P^*$ ) and the gas demand at each node are given as input (vector  $M_{ext}$ ). For pipelines are provided the diameter  $D$ , length  $L$ , roughness  $R$ , and guessed mass flow rate (vector  $M^*$ ).

Since the objective of the fluid dynamic simulation is to find the transport capacities of the pipelines, in this case for the gas demand it is not considered the booked capacity at each redelivery point, but the transport capacity related to the latter.

From the Snam network code, the transport capacity of a redelivery point represents the daily flow of gas that can be redelivered, based on the technical checks carried out. It is identified on the basis of hydraulic verifications which are based on capacity requirement scenarios of the geographical area concerned and which derive from available historical data and any contacts with end customers (e.g. industrial users and Distribution companies) [16].

Considering the transport capacity instead of the booked capacity is useful to derive a maximum transportability of the pipelines, regardless of the actual gas demand.

The transport capacity at each node is converted from kWh/day into kg/s, by using a HHV equal to 10,92 kWh/Sm<sup>3</sup> and a gas density of 0,68 kg/Sm<sup>3</sup> [31]. The former is calculated through the mean of the higher heating values of each redelivery points in Piedmont, published by Snam [32].

The pipelines' roughness is assumed equal to 0,01 mm, while diameters and lengths are taken from the attributes list. The tables below resume the input data for a few nodes and pipelines of the high-pressure network:

*Table 4.8 – SIMPLE algorithm input data for high-pressure nodes*

<b>Node</b>	<b>Demand [kg/s]</b>	<b>p_guess [bar]</b>
Castellazzo Novarese	0,00	24
Intermezzo23	0,00	24
Busignetto	0,00	24
Alzate	0,00	24
Carlottina	0,00	24
Cascina Prati	0,00	24
Intermezzo13	0,00	24
Intermezzo14	0,00	24
.....		
Ornavasso	0,21	24
Omegna_4	1,32	24
Omegna_3	0,04	24
Mergozzo	0,10	24
Villadossola_2	0,40	24
Villadossola_1	0,30	24
Domodossola_2	1,14	24
Domodossola_1	0,10	24
Riduzione50	0,00	24
Intermezzo188	0,00	24
Intermezzo184	0,00	24
Intermezzo185	0,00	24

*Table 4.9 - SIMPLE algorithm input data for high-pressure pipelines*

<b>Node_in</b>	<b>Node_out</b>	<b>D [mm]</b>	<b>eps [mm]</b>	<b>L [m]</b>	<b>G_guess [kg/s]</b>
Castellazzo Novarese	Intermezzo23	660	0,01	15003,16	1,00
Intermezzo23	Peschiere	508	0,01	21847,24	1,00
Intermezzo23	Intermezzo21	660	0,01	5345,47	1,00
Busignetto	Mandria	660	0,01	5244,55	1,00
Castellazzo Novarese	Sologno	660	0,01	5152,65	1,00
Alzate	Sologno	305	0,01	1451,97	1,00
Carlottina	Cascina Prati	203	0,01	491,73	1,00
Cascina Prati	Baraggia	203	0,01	4480,90	1,00
.....					
Campone	Ornavasso	203	0,01	3299,12	0,21
Intermezzo124	Omegna_4	203	0,01	2160,28	1,32
Intermezzo124	Omegna_3	203	0,01	328,42	0,04
Intermezzo125	Isella	203	0,01	7249,35	1,00
Intermezzo125	Mergozzo	203	0,01	46,28	0,10
Riduzione44	Intermezzo130	305	0,01	556,61	1,00
Intermezzo130	Villadossola_2	203	0,01	239,39	0,40
Intermezzo130	Villadossola_1	203	0,01	204,30	0,30
Riduzione44	Intermezzo131	305	0,01	4993,31	1,00
Intermezzo131	Domodossola_2	203	0,01	1105,25	1,14
Intermezzo131	Domodossola_1	203	0,01	183,12	0,10

The same procedure is adopted for the transmission network. A pressure of 75 bar is assumed and fixed at the Passo Gries node, assuming the gas is supplied by this node only. The gas demand at the end nodes of the network, which are the start nodes of the valves, is evaluated by summing up the flowrates entering the exit nodes of the valves obtained from the previous simulation.

The tables below resume the input data for the nodes and a few pipelines of the transmission network:

*Table 4.10 - SIMPLE algorithm input data for transmission nodes*

<b>Node</b>	<b>Demand (kg/s)</b>	<b>p_guess (bar)</b>
Passo Gries	-605,85	75
Masera	0,69	75
Gravellona Toce	7,79	75
Gattico-Veruno	1,70	75
Margattino	35,10	75
Cascina Monferrona	4,69	75
Briona	41,11	75
Mortara	0,00	75
Gasperini	6,83	75
Castelceriolo	5,06	75
Smistamento	64,77	75
Intermezzo39	6,62	75
Neirole	125,45	75
Intermezzo61	4,23	75
Torrazzo	6,23	75
Moglia	0,70	75
Castello d'Agogna	3,02	75
Intermezzo20	15,31	75
Colazza	1,00	75
Mescia	3,34	75
Borgo Agnello	1,72	75
Olengo	9,07	75
Intermezzo3	10,28	75
Lucedio	31,66	75
Oviglio	27,83	75
Masio	0,50	75
Cerro Tanaro	2,89	75
Intermezzo60	0,01	75
Intermezzo40	0,54	75
Revigliasco d'Asti	21,35	75
Oviglia	0,18	75
Intermezzo129	1,93	75
Cortemaggiore	0,73	75
Poirino_1	153,61	75
Bizzarone	9,91	75

*Table 4.11 - SIMPLE algorithm input data for transmission pipelines*

Node_in	Node_out	D [mm]	eps [mm]	L [m]	G_guess [kg/s]
Passo Gries	Masera	1219	0,01	42299,50	605,85
Masera	Gravellona Toce	1219	0,01	34718,85	7,79
Gravellona Toce	Mescia	1219	0,01	26720,36	3,34
Gattico-Veruno	Cascina Monferrona	1219	0,01	12317,32	4,69
Margattino	Intermezzo3	864	0,01	2608,29	10,28
Cascina Monferrona	Briona	1219	0,01	8782,35	41,11
Briona	Castello d'Agogna	1219	0,01	37998,57	3,02
Mortara	Smistamento	762	0,01	48526,76	64,77
.....					
Lucedio	Neirole	1067	0,01	21115,10	125,45
Oviglio	Masio	559	0,01	7116,40	0,50
Masio	Cerro Tanaro	559	0,01	4260,69	2,89
Cerro Tanaro	Moglia	559	0,01	6818,87	0,70
Intermezzo60	Intermezzo61	559	0,01	1192,46	4,23
Intermezzo40	Oviglio	559	0,01	8921,51	27,83
Revigliasco d'Asti	Intermezzo60	559	0,01	22482,15	0,01
Oviglia	Poirino_1	660	0,01	7432,49	153,61
Intermezzo129	Colazza	864	0,01	47011,47	1,00

#### 4.4.3 Results of the fluid dynamic simulation

The main results are related to the mass flow rates in the pipelines and the absolute pressures at the nodes, as shown in the tables below.

*Table 4.12 – Results of fluid dynamic simulation, mass flowrates in pipelines*

Node_in	Node_out	D (")	G [kg/s]	rhom [kg/m <sup>3</sup> ]	Q [Sm <sup>3</sup> /s]	Capacity [MW]	Velocity [m/s]
Passo Gries	Masera	48	605,85	60,20	844,98	33232,50	8,62
Masera	Gravellona Toce	48	423,42	56,20	590,55	23225,88	6,45
Gravellona Toce	Mescia	48	415,63	54,12	579,68	22798,71	6,58
Gattico-Veruno	Cascina Monferrona	48	400,69	52,38	558,84	21978,94	6,55
Margattino	Intermezzo3	34	141,98	50,16	198,02	7788,13	4,83
Cascina Monferrona	Briona	48	396,00	51,71	552,31	21721,93	6,56
Briona	Castello d'Agogna	48	354,90	50,44	494,98	19467,15	6,03
Mortara	Smistamento	30	116,43	47,50	162,39	6386,61	5,38
.....							
Campone	Ornavasso	8	0,21	18,47	0,30	11,66	0,35
Intermezzo124	Omegna 4	8	1,32	18,18	1,84	72,49	2,24
Intermezzo124	Omegna 3	8	0,04	18,21	0,05	2,05	0,06
Intermezzo125	Isella	8	4,84	17,58	6,74	265,27	8,48
Intermezzo125	Mergozzo	8	0,10	18,46	0,14	5,40	0,16
Riduzione44	Intermezzo130	12	0,69	18,48	0,97	38,04	0,51
Intermezzo130	Villadossola 2	8	0,40	18,48	0,56	21,84	0,66
Intermezzo130	Villadossola 1	8	0,30	18,48	0,41	16,21	0,49
Riduzione44	Intermezzo131	12	1,24	18,47	1,73	68,03	0,92
Intermezzo131	Domodossola 2	8	1,14	18,46	1,59	62,58	1,91
Intermezzo131	Domodossola 1	8	0,10	18,47	0,14	5,45	0,17

Table 4.13 - Results of fluid dynamic simulation, absolute pressures at nodes

Type	Node_in	Node_out	P_in [bar_a]	P_out [bar_a]
Transmission	Passo Gries	Masera	76,000	70,036
Transmission	Masera	Gravellona Toce	70,036	67,498
Transmission	Gravellona Toce	Mescia	67,498	65,544
Transmission	Gattico-Veruno	Cascina Monferrona	65,068	64,204
Transmission	Margattino	Intermezzo3	62,273	62,132
Transmission	Cascina Monferrona	Briona	64,204	63,595
Transmission	Briona	Castello d'Agogna	63,595	61,429
Transmission	Mortara	Smistamento	61,026	57,478
.....				
High-Pressure	Campone	Ornavasso	24,994	24,991
High-Pressure	Intermezzo124	Omegna 4	24,652	24,595
High-Pressure	Intermezzo124	Omegna 3	24,652	24,652
High-Pressure	Intermezzo125	Isella	24,970	22,699
High-Pressure	Intermezzo125	Mergozzo	24,970	24,970
High-Pressure	Riduzione44	Intermezzo130	25,000	24,999
High-Pressure	Intermezzo130	Villadossola 2	24,999	24,999
High-Pressure	Intermezzo130	Villadossola 1	24,999	24,999
High-Pressure	Riduzione44	Intermezzo131	25,000	24,983
High-Pressure	Intermezzo131	Domodossola 2	24,983	24,961
High-Pressure	Intermezzo131	Domodossola 1	24,983	24,983

Through the mass flow rate and the average density of the gas in the pipe (obtained by considering the average pressure), the volumetric flow rate in m<sup>3</sup>/s can be derived. The velocity in the pipe is then calculated as follows:

$$v_{pipe} = Q_{pipe} \cdot \pi \cdot \frac{D^2}{4} \quad (64)$$

The pipeline's capacity in MW is calculated as in the following equation:

$$\gamma = \frac{\dot{m} \cdot 3600}{\rho_{stc}} \cdot HHV \quad (65)$$

where  $\rho_{stc}$  is the methane density in standard conditions (15°C, 1 atm) equal to 0,68 kg/Sm<sup>3</sup> [31], HHV is the higher heating value equal to 10,92 kWh/Sm<sup>3</sup> [32].

For each pipeline, it has been checked that the maximum speed of 25 m/s is not exceeded and that the pressure drops are not too high.

The graph below has been derived from the pipeline diameters and their respective capacities:

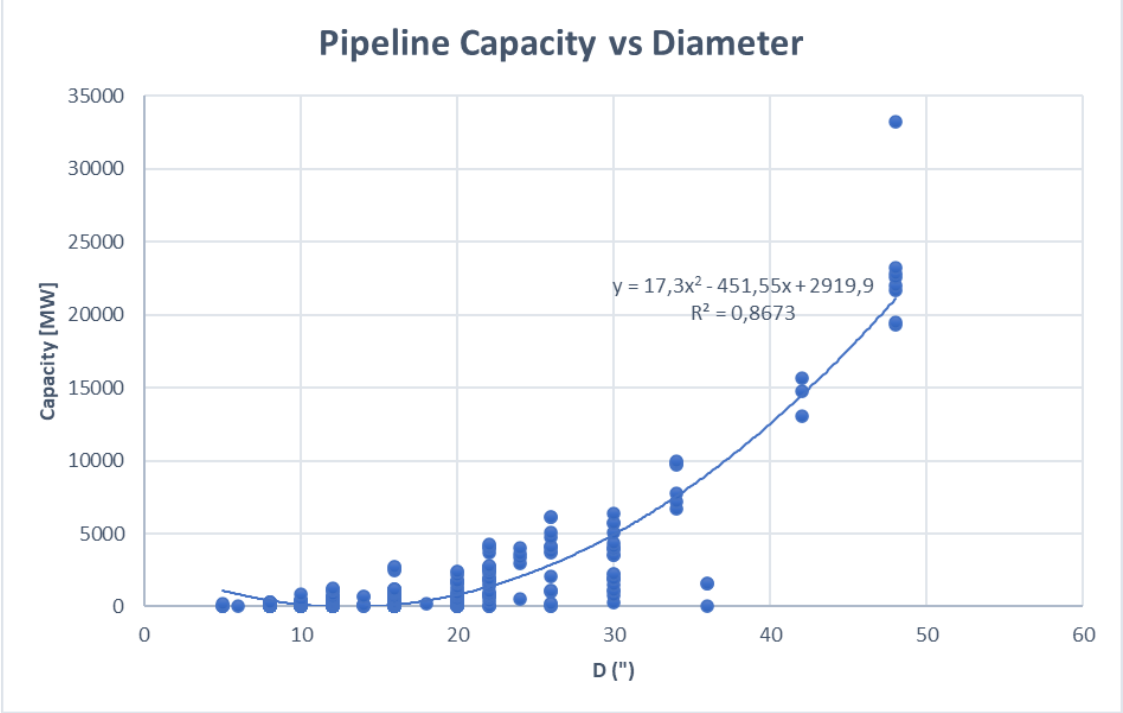
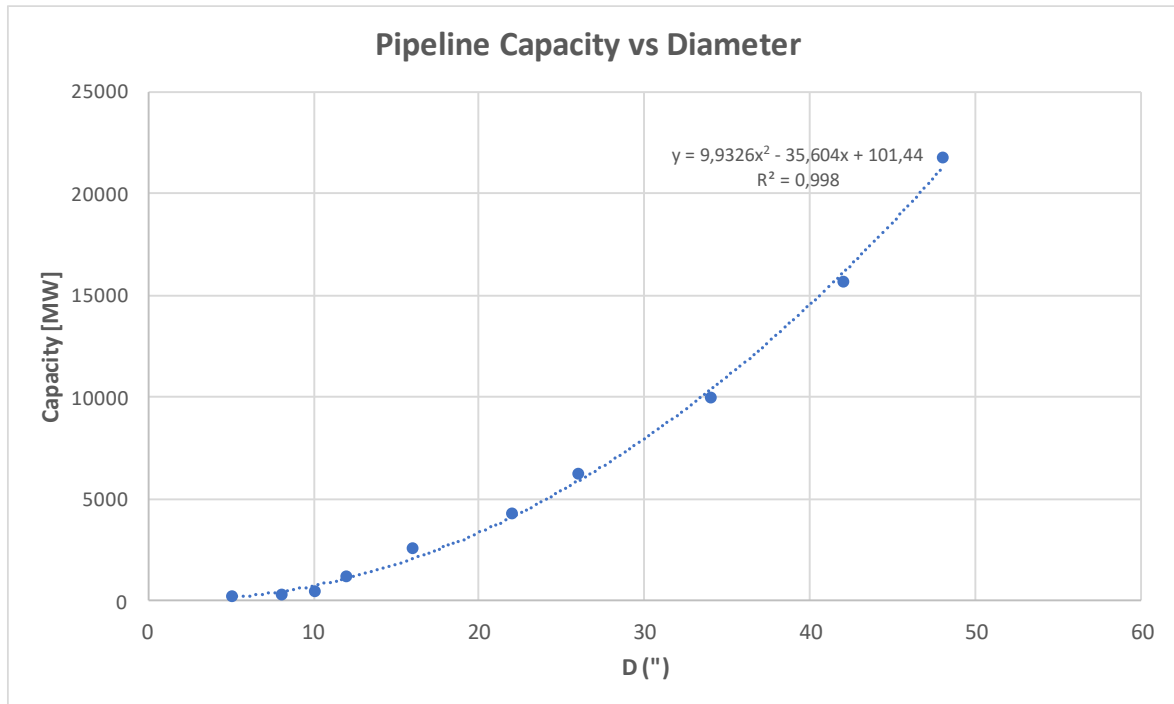


Figure 4.10 – Pipelines’ capacities per diameter

An increasing capacity trend can be seen, with increasing diameter, similar to a second-degree polynomial curve. However, to assume that the transportability of the pipe depends on the diameter alone, a single capacity must be assigned to each diameter. It is important to note that however the pressure drop, gas density, and length of the pipeline influences transportability too. The final correlation is constructed by selecting one of the highest capacities for each diameter and in such a way that the curve is more similar to a second-degree polynomial. For this reason, the highest capacity value of the 48" diameter (corresponding to the inlet pipe at Passo Gries) has been excluded, considering that the gas does not all come from this inlet point, as assumed in the fluid dynamic simulation instead.



*Figure 4.11 – Extrapolated correlation curve of capacities and diameters*

The table below shows the set of diameters of gas pipelines, and the assumed pipeline capacity:

*Table 4.14 – Values of capacity per pipeline diameter*

<b>CAPACITY [MW]</b>	<b>D(")</b>
172	5
245	6
452	8
739	10
1104	12
1550	14
2075	16
2679	18
3362	20
4126	22
4968	24
5890	26
7973	30
10373	34
11692	36
16127	42
21277	48

The capacity  $\gamma_{l,p,y}^{pre}$  for each pipeline until the year of decommissioning/refurbishment is set.



4.5 Year of decommissioning/refurbishment

The other input data required for the pipes are the year of installation and the service life. The year of construction has been estimated by averaging the year of commissioning of existing pipelines in Piedmont, taken from the list of pipelines published by MASE [17].

For the national network, the calculated average year of installation is 1990, while for the regional network is 1986. However, the main transmission pipelines are older than 1990 (e.g. the pipeline passing from Passo del Gries is already existing in 1975, as visible from Snam scheme [12]). To assign the year of construction to each pipe, an exact mapping of the network is necessary. Since it is not available, a distribution of years of construction ranging from the 1980s to the 1990s has been adopted, based on diameter size. It is reasonable to assume that the transmission backbone is made up of older pipes, while the regional network consists of newer pipelines with generally decreasing diameters. These pipelines are network extensions that have been developed from year to year, to dispatch gas across the whole region. The network configuration per year of construction is shown in the graph below:

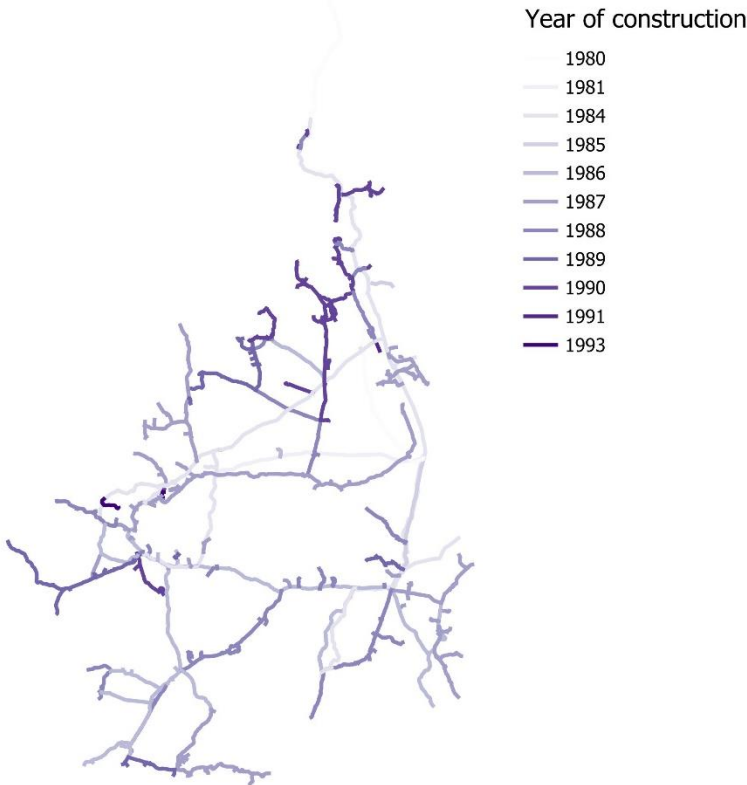


Figure 4.12 – Pipelines construction year distribution

A useful life of 50 years is assumed for the pipes, lower than the reference value of 60 years specified by ARERA<sup>14</sup> [33].

The parameter  $y_{l,p}^{inv}$  is determined by summing the useful life and the year of construction.

The technical parameters of the pipelines are provided as input data to the code:

*Table 4.15 – Pipelines’ technical parameters input data*

Start	End	Type	Capacity [MW]	Yr.-con.	Tec.-life
Passo Gries	Masera	Transmission	21277	1980	50
Masera	Gravellona Toce	Transmission	21277	1980	50
Gravellona Toce	Mescia	Transmission	21277	1980	50
Gattico-Veruno	Cascina Monferrona	Transmission	21277	1980	50
Margattino	Intermezzo3	Transmission	10373	1984	50
Cascina Monferrona	Briona	Transmission	21277	1980	50
Briona	Castello d'Agogna	Transmission	21277	1980	50
.....					
Intermezzo125	Isella	High-Pressure	452	1990	50
Intermezzo125	Mergozzo	High-Pressure	452	1990	50
Intermezzo129	Riduzione44	High-Pressure	1104	1988	50
Riduzione44	Intermezzo130	High-Pressure	1104	1988	50
Intermezzo130	Villadossola_2	High-Pressure	452	1990	50
Intermezzo130	Villadossola_1	High-Pressure	452	1990	50
Riduzione44	Intermezzo131	High-Pressure	1104	1988	50
Intermezzo131	Domodossola_2	High-Pressure	452	1990	50
Intermezzo131	Domodossola_1	High-Pressure	452	1990	50

#### 4.6 Unit investment and O&M costs

As regards the economic input data on unit investment costs for gas pipelines, the data provided by ACER have been taken and reprocessed. ACER is the European Union Agency for the Cooperation of Energy Regulators, and it represents an independent body to foster the integration and completion of the European Internal Energy Market for electricity and natural gas [34]. ACER published a report about UIC (Unit Investment Costs) of European energy infrastructure [35], which shows the average nominal unit investment costs for transmission pipelines from 2005 to 2014, broken down by diameter range:

---

<sup>14</sup>“Autorità di regolazione per energia reti e ambiente”, Italian authority for the regulation and control in the energy sector.

*Table 4.16 – Nominal Unit investment cost of transmission pipelines per year (average values, median) [35]*

Year	2005	2006	2007	2008	2009	2010	2011	2012	2013	2014
<b>Range 1 [&lt;16"]</b>										
Average of [€/Km]	224.188	347.546	302.115	613.826	503.408	446.575	525.754	622.525	617.838	642.001
Median of [€/Km]	244.766	279.494	324.956	656.667	398.839	448.437	478.845	519.152	680.005	618.431
<b>Range 2 [16"-27"]</b>										
Average of [€/Km]	450.172	586.611	653.752	730.959	664.286	576.261	594.774	642.054	625.873	744.800
Median of [€/Km]	455.696	493.115	689.039	728.387	648.101	502.636	589.935	576.562	542.842	652.115
<b>Range 3 [28"-35"]</b>										
Average of [€/Km]	377.512	1.179.046	1.092.603	956.769	1.000.469	1.061.858	1.052.414	797.939	875.506	847.190
Median of [€/Km]	377.512	1.250.272	1.091.808	987.148	1.027.610	959.156	901.379	565.827	875.506	679.679
<b>Range 4 [36"-47"]</b>										
Average of [€/Km]	-	-	1.227.631	1.129.720	1.125.227	1.200.970	2.075.282	1.306.233	1.912.028	1.415.715
Median of [€/Km]	-	-	1.215.966	977.124	1.043.446	896.821	2.209.299	1.456.409	1.912.028	1.415.715
<b>Range 5 [48"-57"]</b>										
Average of [€/Km]	1.617.808	2.125.003	2.159.664	2.316.646	2.559.148	2.546.308	2.319.164	2.139.961	2.251.163	2.089.522
Median of [€/Km]	1.617.808	2.115.536	2.159.664	2.357.337	2.559.148	2.858.767	2.307.104	2.147.260	2.217.173	2.089.522

These costs are expressed in €/km per diameters range. However, for the purpose of this study a unit investment cost expressed in €/MW/km is necessary.

The reference year for costs is 2014. The diameters have been converted into ranges of capacity, expressed in MW, according to the correlation found in the previous section. The average unit cost in €/MW/km per diameters range is found dividing the given value in Table 4.16 by the capacity corresponding to the mean diameter of the considered diameter range. The graph below shows a disparity in average unit cost between the smallest diameters (5-16 inches) and the largest diameters. Therefore, it is helpful to differentiate between two costs, one at the national level (transmission) and the other at the regional level (high-pressure).

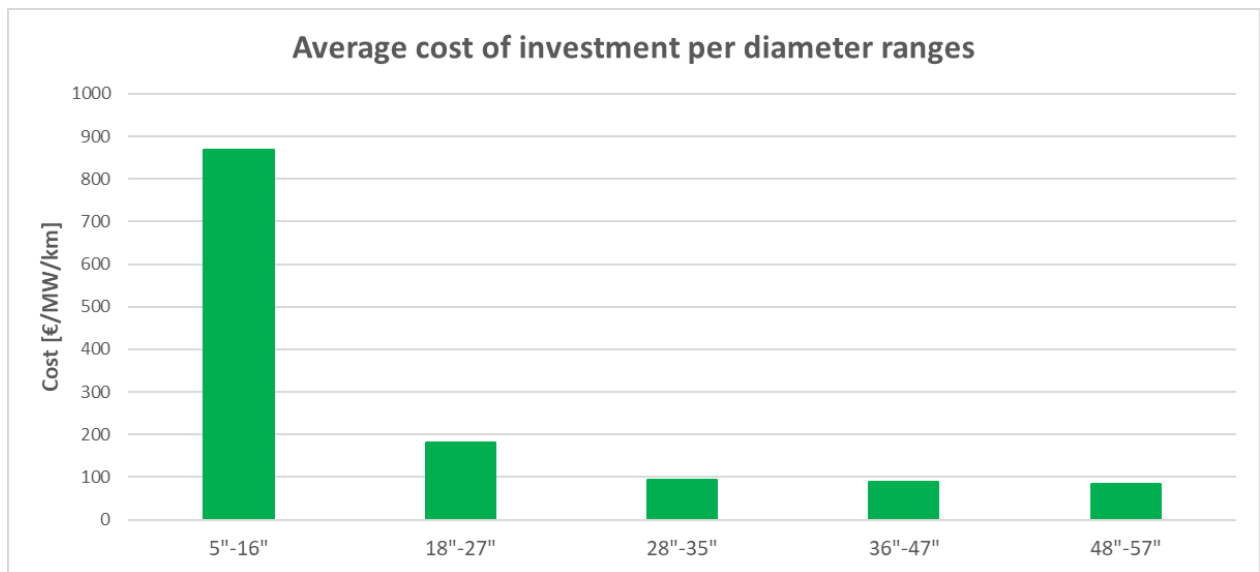


*Figure 4.13 – Average unit investment costs per diameter ranges*

The QGIS model shows that the green network has smaller diameters, while the red network has larger diameters, as per Snam network code too [16]. The number of pipes per diameter range and per network level, of the network modelled on QGIS, is shown in the table:

*Table 4.17 – Pipelines count per diameter range*

D (") range	Count transmission	Count high-pressure
5-16	0	482
18-27	17	76
28-35	9	18
36-47	4	2
48-57	8	0

The regional network is mainly composed of pipes with diameters ranging from 5 to 16 inches, while the national network has a more uniform distribution of diameters, with no pipes in the 5-16 inches range. Therefore, for the transmission network, the mean of the average unit costs of all diameter range except the first has been calculated. For the high-pressure network, the unit cost of the first diameter range has been considered. These costs are in line with the ones found in literature [36] [37].

Unit operation and maintenance costs have been assumed equal to 1,8% of the unit investment costs, for both network levels, excluding the cost of energy for the compressor [36].

Finally, the economic parameters relating to costs  $c_l^{inv}$  and  $c_l^{fix}$  are determined, and are given as input to the model:

*Table 4.18 – Input unit costs per network level*

<b>Name</b>	<b>Type</b>	<b>Costs</b>	<b>Comment</b>
Specific investment costs	Transmission	111	EUR/MW/km
Specific investment costs	High-Pressure	869	EUR/MW/km
Fixed costs	Transmission	2	EUR/MW/km
Fixed costs	High-Pressure	16	EUR/MW/km

## 5. Biomethane scenario input data

In view of the sustainability goals described in the introductory chapter, with the aim of decarbonising the gas sector, it has been considered a scenario in which all existing biogas power plants in Piedmont are converted to biomethane production plants, with the injection of the green gas into the regional and/or national gas grid. A further subdivision of the scenario is made. In one case, the certain connection of all biomethane production plants to the gas grid is considered, with the injection of all production. This is a realistic scenario, as the TSOs and DSOs of gas networks are required to connect biomethane plants that apply, if they meet safety (e.g., biomethane quality) and reliability constraints, as per the 64/2020/R/gas ARERA resolution [38].

In a second case, the TSO takes the decision to accept or not the connection of biomethane plants, per injection point. Furthermore, the TSO can decide on the amount of biomethane to be fed into the grid, within the limits of the plant's producibility. The purpose of this last scenario is to investigate the cost-effectiveness (as far as the gas infrastructure is concerned) in connecting biomethane plants.

The objective is still to minimize the overall investment and operational costs throughout the entire period. The additional input data, with respect to the base scenario, include:

- Updated network topology (nodes and pipelines),
- Annual plants' producibility,
- Year of connection for each plant,
- Investment and operation and maintenance costs,
- Year of connection decision (for the variable biomethane case only).

In the next section, there is a brief explanation of biomethane production and its possible uses.

## 5.1 What is biomethane?

Biomethane is a near-pure source of methane, which can be produced by the upgrading of raw biogas or through gasification of solid biomass and the subsequent methanation process [39]. Almost 90% of biomethane produced in the world is obtained by biogas, that is a gas obtained from the decomposition of organic materials. The residues are placed in an oxygen-free digester, where anaerobic digestion occurs. Thanks to bacteria action, the organic materials break down and release a blend of gases. The gases are mostly composed of methane (between 45 – 85 % in volume) and carbon dioxide (25 – 50% in volume), with small parts of undesired contaminants [40].

Biogas is then treated in an upgrading process, where CO<sub>2</sub> and trace gases are removed.

The general process of biomethane production from biogas is shown in the figure below:

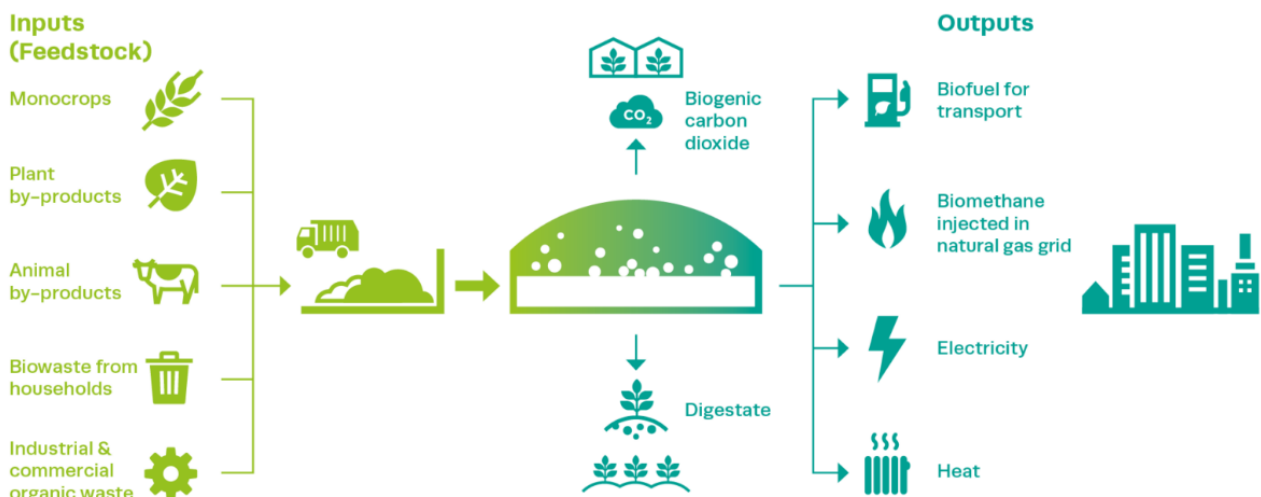


*Figure 5.1 – Schematic overview of inputs and outputs of the biogases production process [40]*

The final product is a methane rich renewable gas, which can be injected into gas network if the biomethane satisfies quality requirements.

The by-products of biogas purification are digestate, commonly used as fertilizer in agriculture, and carbon dioxide. The latter can be exploited in food industry, in greenhouses or even stored. The whole process finally results in a closed carbon loop [41].

## 5.2 Plants producibility

As reported in the introduction, the domestic production of biomethane in Italy will increase, in all scenarios analysed by Snam and Terna, as well as reported in the PNIEC 2023. For this reason, it is interesting to analyse how the injection of biomethane into the grid may change decisions on pipeline decommissioning and refurbishment by grid operators and thus be able to exploit the future new grid to transport renewable gases.

Concerning Piedmont region, the potential for biomethane production has been studied.

### 5.2.1 Database creation

The starting point is the analysis of the existing biogas production plants, assumed to be all upgradable to biomethane production sites.

To check how many biogas production plants exist in Piedmont, two different databases have been analysed:

- “*Atlaimpanti*”, developed by GSE<sup>15</sup>, it is an interactive geographical atlas that allows to consult the main data on the electricity and heat production plants that are incentivised by GSE and to check their location throughout Italy [42].
- “*Geoportale*” developed by Arpa<sup>16</sup> Piemonte, a portal which collects maps, texts, and graphics on environmental themes [43].

According to the first database, there are currently 235 plants of electricity production from biogas in Piedmont, accounting for a total electricity production capacity of 153 MW.

---

<sup>15</sup> “Gestore dei Servizi Energetici”, Italian Energy Service Operator.

<sup>16</sup> “Azienda Regionale per la Protezione Ambientale del Piemonte”, Regional Environmental Protection Agency of Piedmont



In the figure below are highlighted the locations of these plant:

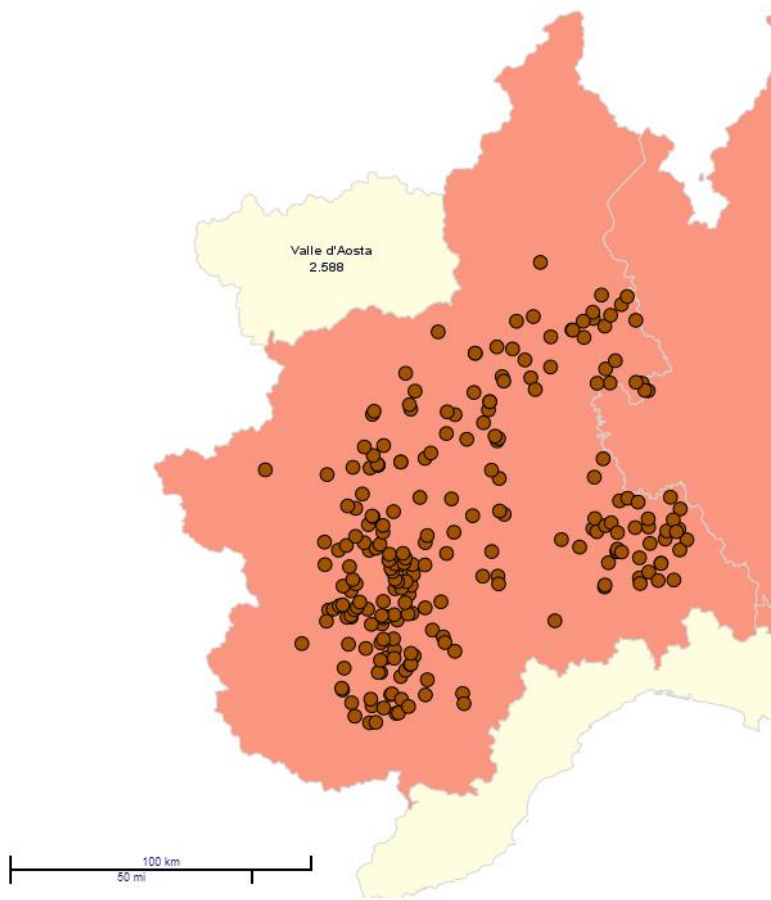


*Figure 5.2 – Locations of existing biogas plants in Piedmont, in Atlaimpanti [42]*

For each plant the exportable data are the nominal electrical power of the cogenerator, in kW, the municipality and the province. Meanwhile, the type of incentive and the address need to be manually extrapolated, as well as the geographical coordinates (latitude and longitude). In the figures below are summarized the characteristics of the plants, divided per capacity installed and province.

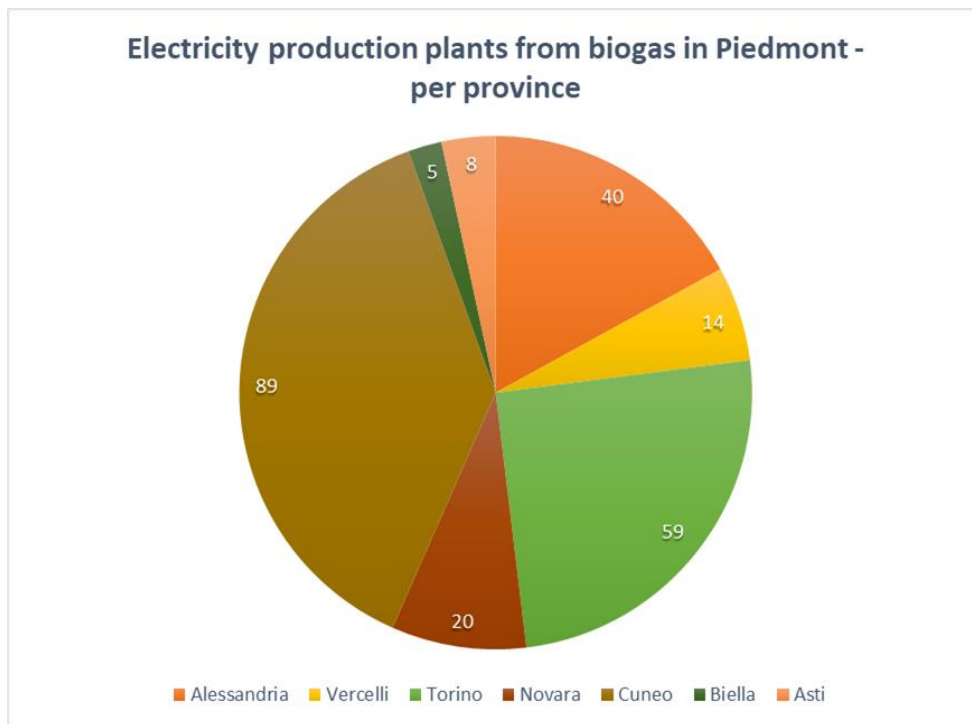


*Figure 5.3 – Biogas plants in Piedmont per province, GSE database*

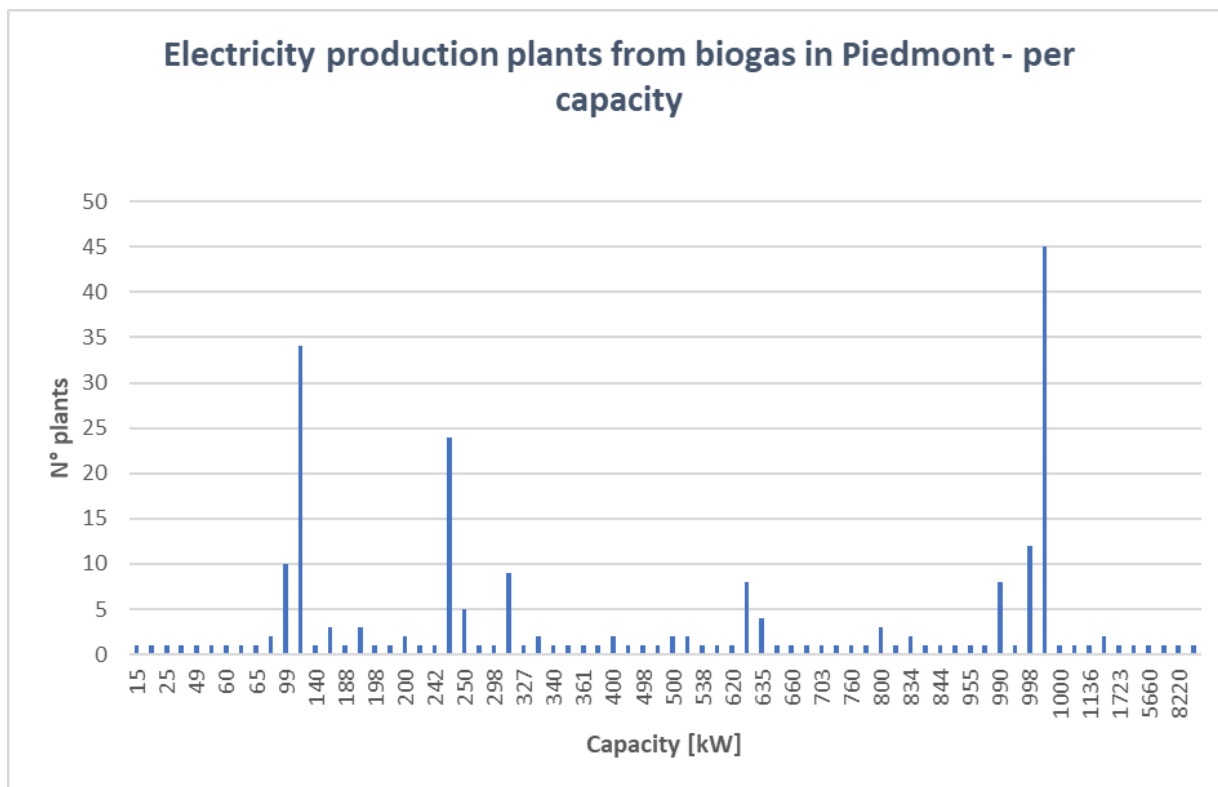


*Figure 5.4 – N° of biogas plants in Piedmont, per installed capacity, GSE database*

The second database analysed is that of Arpa Piemonte. From the geoportal it is possible to access the map showing the locations of anaerobic digestion plants producing biogas. The next figure shows the map on the geoportal. For each plant, more information is known compared to the ones provided by the GSE, such as:

- Company name,
- Year of commissioning of the plant, while the incentive type is not provided,
- Installed electric power [kW],
- Municipality,
- Address of the plant,
- Type of source in use (feedstock).

The main advantage of this geoportal is that the coordinates of the plant can be accessed via QGIS. So, it is useful to visualise the network model created with QGIS, together with the positions of the biogas plants. It is also possible to verify that the coordinates are more accurate than those manually extracted through Atlaimpianti.

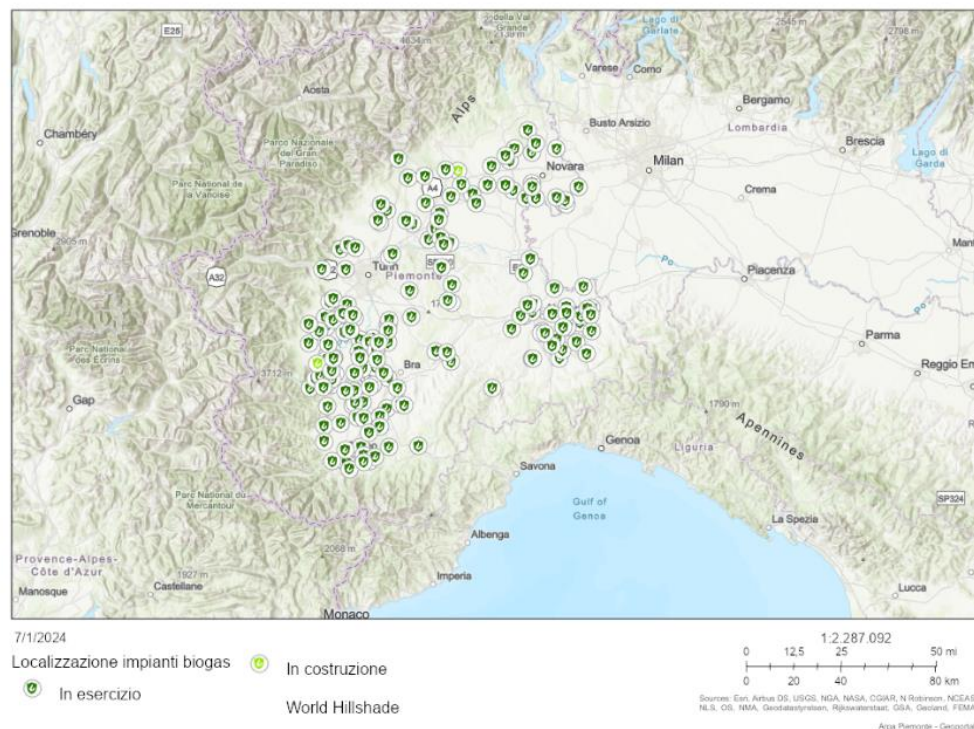


Figure 5.5 - Locations of existing biogas plants in Piedmont, in Arpa Piemonte geoportal [43]

The same analysis of installations by province and electrical capacity is carried out for the Arpa Piemonte database, as shown in the figures. The total number of biogas plants is 192, with a total installed capacity of 127 MW.

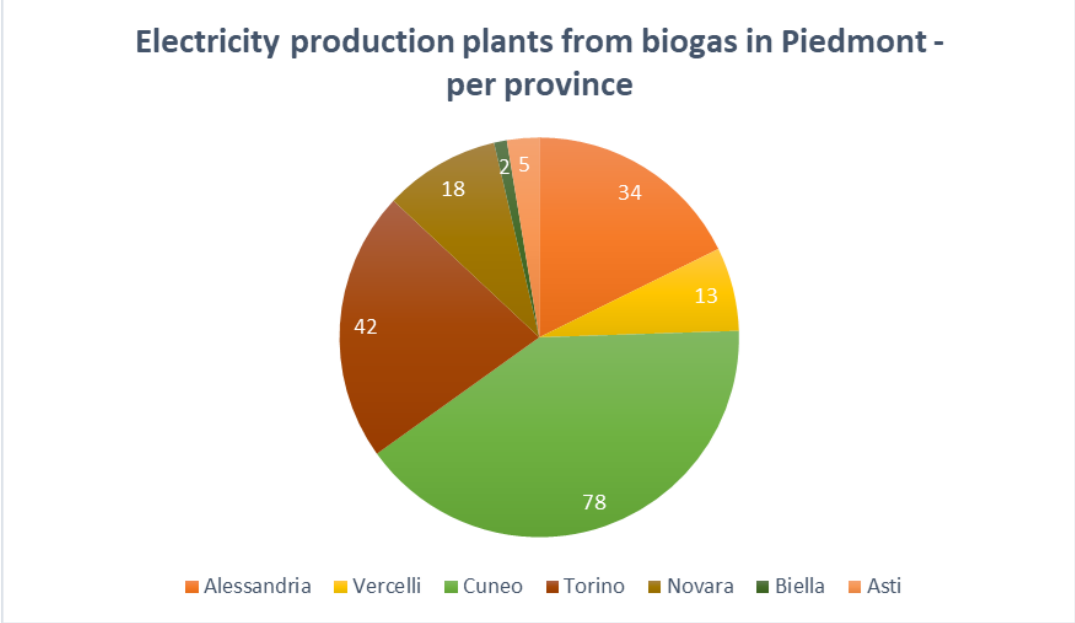


Figure 5.6 - Biogas plants in Piedmont per province, Arpa Piemonte database

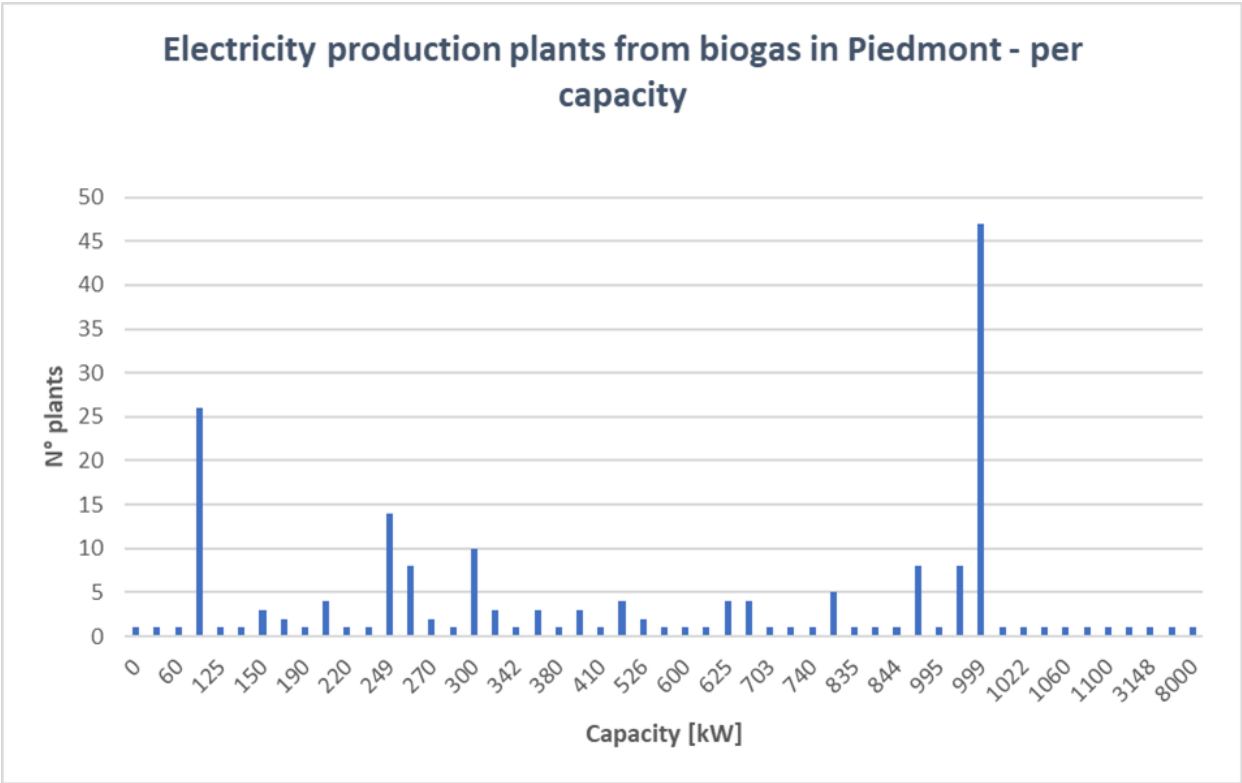


Figure 5.7 - N° of biogas plants in Piedmont, per installed capacity, Arpa Piemonte database

A comparison of the plants in the two databases has been carried out. In particular, the location addresses of the plants are compared for each municipality in the database. The addresses not always match perfectly, then Google Earth has been used to check whether the plant might be the same, having first checked that the installed capacity was similar. In the end, an exact match has been found for 141 installations.

Between the two databases, Arpa Piemonte has been chosen as reference database because it is more accurate in terms of addresses and matched with the provided geographical coordinates. Additionally, the map locations are imported into QGIS, by creating a WMS<sup>17</sup> layer and inserting a link available in the geoportal [43]. The created layer includes all the information listed above, which are available in the geoportal and can be accessed on QGIS from the attributes field.

However, it has been decided to extract useful data from the GSE and correct the Arpa Piemonte database. Specifically, for the 141 matching plants, the installed electrical power has been updated with the GSE data, and incentive information was added too. For the remaining 51 plants, the installed power has remained the same, while the type of incentive has been hypothesised.

In Italy, the different incentives accessed by biogas production plants are:

- CV<sup>18</sup> (Green certificates), with a duration of 15 years.
- FER<sup>19</sup> (Renewable Energy Sources), with a duration of 20 years.
- TO<sup>20</sup> (All-inclusive Tariff), with a duration of 15 years.

Each form of incentive has a specific duration and an expiry date [44]. Analysing the GSE database, plants with a commissioning year before 2013 typically have the TO as their incentive form. Conversely, from 2013 onwards, the FER form is more common. Therefore, for plants where the incentive is unknown, a TO or FER form is assumed, depending on the year of the plant's commissioning (before or after 2013). For those plants where no information about the commissioning year is available, it is assumed to be 2012, with a TO incentive type.

---

<sup>17</sup> Web Map Service

<sup>18</sup> “Certificati Verdi”

<sup>19</sup> “Fonti Energetiche Rinnovabile”

<sup>20</sup> “Tariffa Omnicomprensiva”

The following figure shows the number of installations by type of incentive, resulting from the database created:

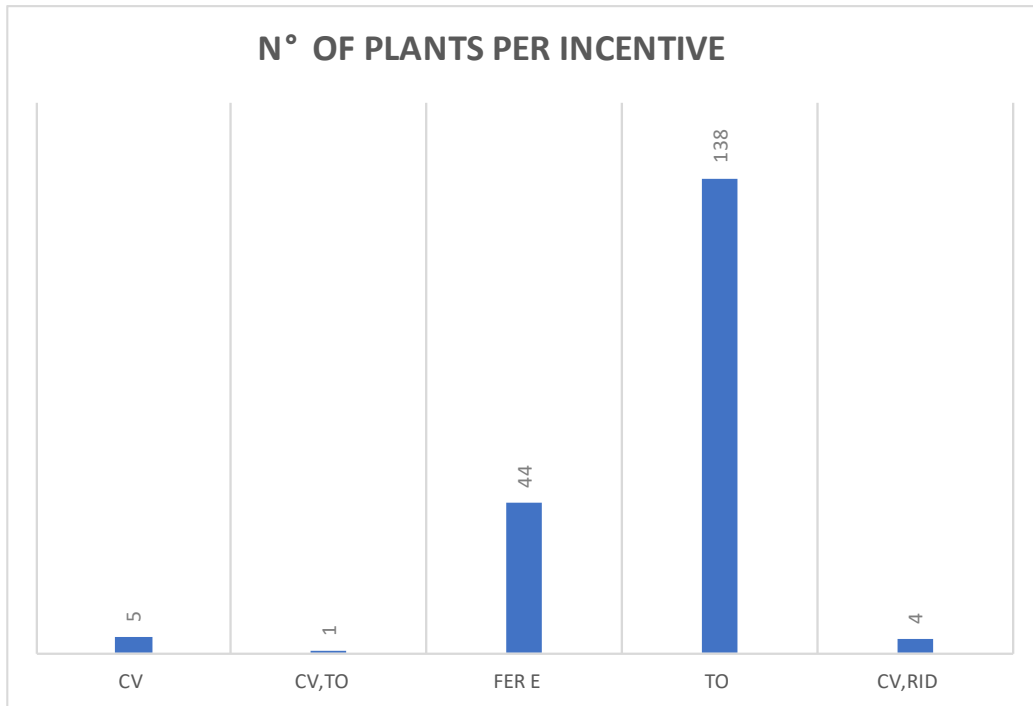


*Figure 5.8 – N° of biogas plants per incentive type*

The table below displays the relevant information of the mixed database, resulting from the intersection of the GSE and Arpa Piemonte databases. The mixed database counts 192 plants, 81,7% of those listed by the GSE, with a total installed electrical power of 127,5 MW, corresponding to 83,3% of the GSE's.

*Table 5.1 – Biogas plants database comparison*

Database	N° of plants	Capacity [MW]
GSE	235	153,1
Arpa Piemonte	192	126,6
Mixed	192	127,5

### 5.2.2 Biomethane producibility

The next step is to determine the producibility of biomethane for each plant. This involves deriving the hourly volumetric flow rate of biomethane produced, based on the nominal electrical output of the cogenerator. To achieve this, it is necessary to determine the electrical efficiency of the cogenerator, which will allow for the calculation of the volumetric flow rate of biogas. From this, it is possible to estimate the potential flow rate of biomethane exiting from an upgrading process.

As the database contains several cogenerator sizes, a size-dependent efficiency curve is necessary. The curve is manually built, using electrical efficiency values of cogenerators available on the market as a reference, of different sizes [45] [46] [47]. The curve obtained is shown in the graph below:

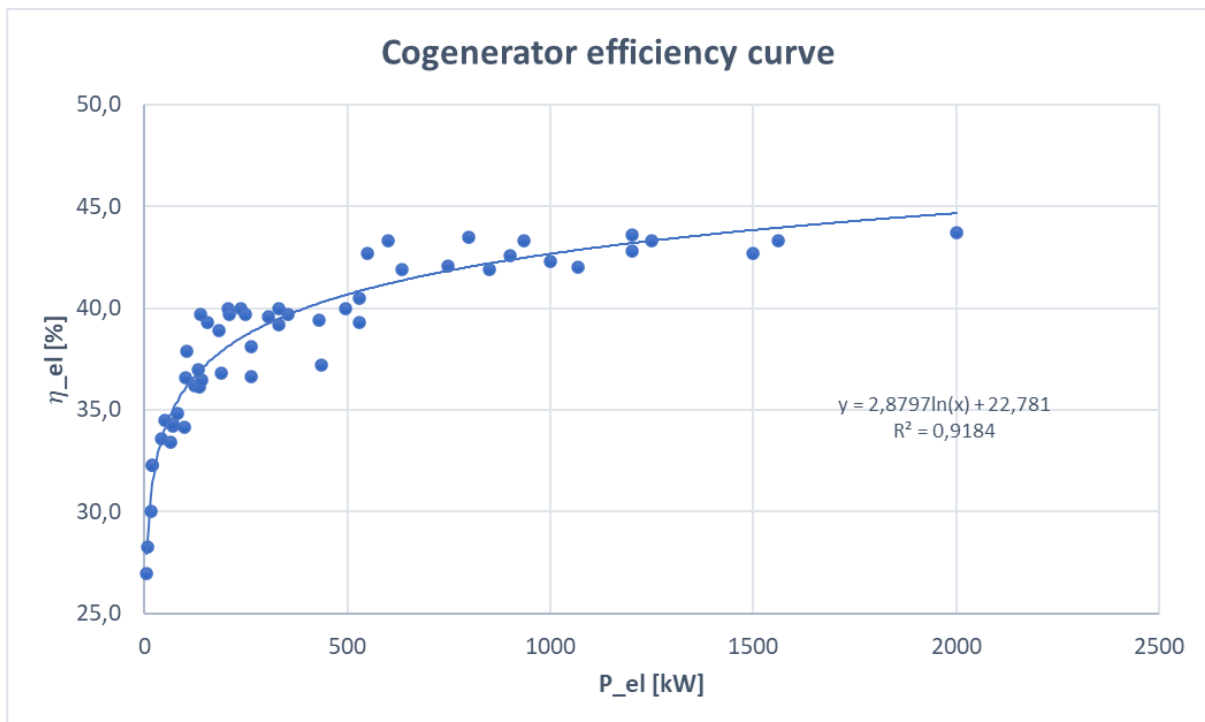


*Figure 5.9 – Electrical efficiency curve*

The biogas volumetric flowrate can be derived from the cogenerator's electrical efficiency equation:

$$\eta_{el} = \frac{P_{el}}{Q_{biogas} \cdot LHV_{biogas}} \quad (66)$$

Where  $Q$  is the volumetric flowrate [ $\text{Sm}^3/\text{h}$ ], LHV is the lower heating value [ $\text{kWh}/\text{Sm}^3$ ] and  $P_{el}$  is the installed electrical power. The capacity factor is assumed to be equal to 1. The LHV is calculated from the corresponding value of  $6,5 \text{ kWh}/\text{Nm}^3$  [48], and it is equal to  $6,16 \text{ kWh}/\text{Sm}^3$ .

Then the biomethane volumetric flowrate is determined:

$$Q_{biomethane} = Q_{biogas} \cdot x_{CH_4} \cdot \eta_{up} \quad (67)$$

Where  $x_{CH_4}$  represents the volume fraction of biomethane in biogas and  $\eta_{up}$  is the efficiency of the separation process in the upgrading (losses of methane). The former is assumed to be equal to 55% [48], while the efficiency of the upgrading is assumed to be 99,5% [49]. In terms of annual energy production, in  $\text{kWh}/\text{y}$ :

$$E_{biomethane} = Q_{biomethane} \cdot 8760 \cdot HHV_{CH_4} \quad (68)$$

For each plant, the potential production of biomethane is then calculated. The calculated total production of biomethane accounts for:

$$Q_{biomethane} = 26672,20 \left[ \frac{\text{Sm}^3}{\text{h}} \right]$$

with an estimated annual energy production of about:

$$E_{annual,bio} = 2,55 \left[ \frac{\text{TWh}}{\text{y}} \right]$$

or, in terms of annual volume of biomethane:

$$V_{annual,bio} = 233,34 \left[ \frac{\text{MSm}^3}{\text{y}} \right]$$

assuming a constant hourly volumetric flowrate throughout the year and a HHV equal to the one of methane,  $10,92 \text{ kWh}/\text{Sm}^3$  [32].

The producibility  $p_{b,n,y,l}^{bio}$  parameter is finally determined for each biomethane plant.



### 5.3 Updated network topology

Once the set of biomethane plants is defined and their producibility has been calculated, the network model in QGIS and the Python model are modified to allow biomethane to be fed into the grid. First, in QGIS, the connection points have been found using a tool that calculates the minimum distance of a point from a line. Nodes are added at the connection points of the plants, if not already existing (e.g. the connection point is at an end node of the network or at an existing intermediate node). As a result, the connection lines and connection points are derived for each biomethane plant, as shown in the figure below:

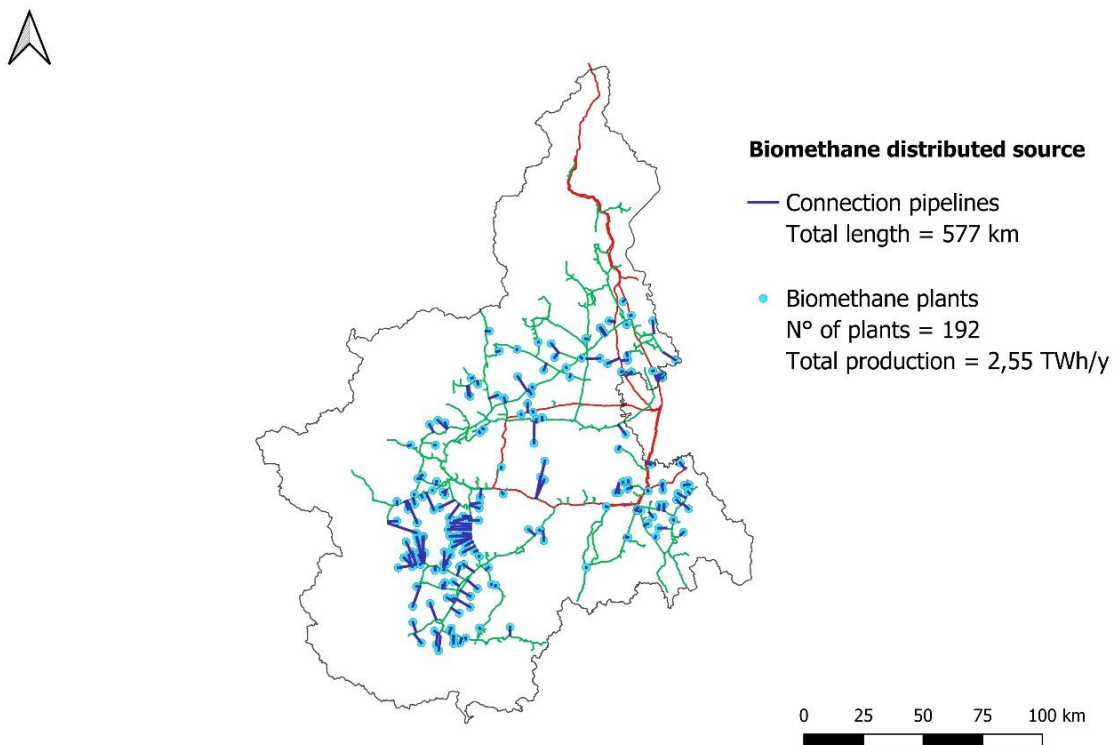


*Figure 5.10 - QGIS scheme of Piedmont's Gas Network, with biomethane connections*

The total length of connection pipelines is 577 km, with an average distance of the plants from the grid equal to 3 km.

The total number of nodes increased, as well as the number of pipelines, both for the transmission and the high-pressure networks. Of course, the total length hasn't changed, as the

new nodes have just caused the splitting of an existing pipeline into two or more parts. The blue lines (new connections) are not considered in the network topology.

The updated network is thus characterized by 760 pipelines (58 for the transmission network, 702 for the high-pressure network) and 724 nodes.

#### 5.4 Year of plants connection

To determine the maximum annual biomethane resource per node  $q_{n,y,l}^{bio}$ , the year of possible connection for all plants in the database is calculated. Before the year of connection, the available resource of the considered plant  $p_{b,n,y,l}^{bio}$  is set to zero. Once the plant is connected to the network, the biomethane source becomes available.

The year of connection is assumed to coincide with the year of expiry of the incentive which currently sustains the electrical production, assuming that the existing plants will undergo a revamping towards biomethane production. For each plant, the exact year is evaluated according to the incentive form and its duration, considering the year of commissioning of the plant. The graph below resumes the number of possible plants' connections for each year, due to the switch from electricity production by biogas to biomethane production and injection into the network:

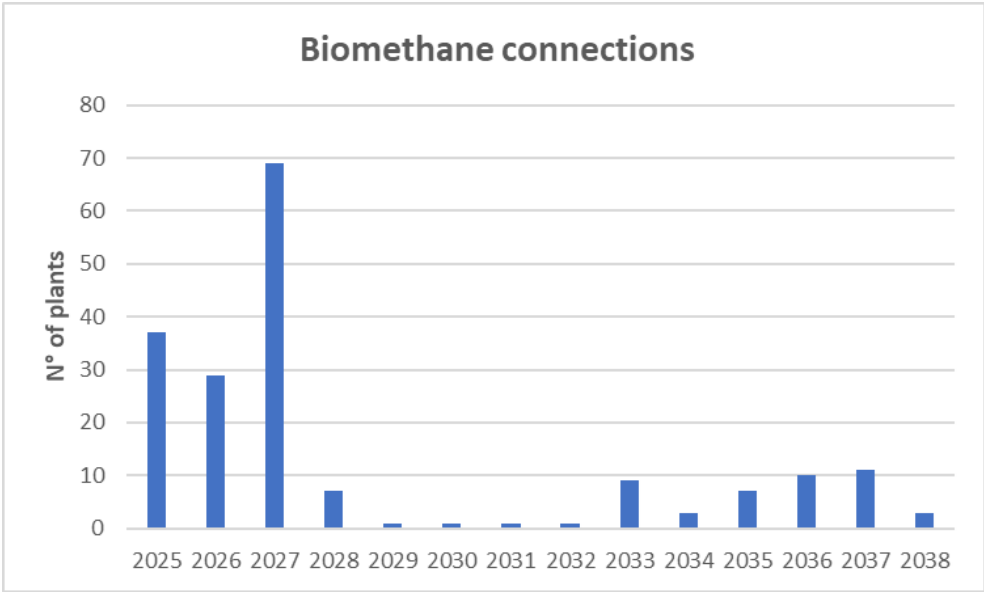


Figure 5.11 – N° of possible biomethane connections per year

It can be noticed that 2027 records the highest number of connections. This is due to the expiry of the TO incentive for those plant with 2012 as year of commissioning.

For each plant, the year of connection to the gas network  $y_{i,b}^{con}$  is finally determined.

## 5.5 Connection pipeline costs

To assess the connection costs for biomethane plants, the following assumptions have been made:

- A 5-inches pipeline with a capacity of 172 MW has been considered for all biomethane plants, resulting sufficient in transporting the production flow rates.
- The unit costs for investment and O&M are the same as in the base case.
- An 80%-20% costs split between the biomethane producer and the TSO is assumed for the connection, in line with the 64/2020/R/gas ARERA resolution [38].
- In case the plant is connected to an end node of the high-pressure network, no cost of connection is considered. It is assumed that in this case the producer would connect to the distribution network downstream the redelivery point, both for a probable closer proximity of the network, and to reduce connection costs by not needing to compress the gas to high pressures. Additionally, the possibility of a reverse flow of excess production (biomethane producibility higher than the gas demand) from the distribution network to the transporter's network is considered possible.

The table below resumes the input data provided to the code:

Table 5.2 – Biomethane connections input data

Plant id	Year	Distance [km]	Node	Type	Source [MWh/y]	Investment	Opex
82	2027	1,89	biometano126	High-Pressure	19871,49	56.441 €	5.080 €
80	2026	0,59	biometano124	High-Pressure	19704,52	17.720 €	1.595 €
81	2028	0,43	biometano16	Transmission	19871,49	12.819 €	1.154 €
108	2027	2,49	biometano135	High-Pressure	19871,49	74.301 €	6.687 €
111	2028	2,41	biometano17	Transmission	19871,49	71.929 €	6.474 €
135	2026	1,97	biometano134	High-Pressure	19871,49	58.791 €	5.291 €
15	2025	2,81	biometano40	High-Pressure	19852,95	83.948 €	7.555 €
154	2027	9,90	biometano98	High-Pressure	6495,62	295.514 €	26.596 €
.....							
3	2025	4,47	Cuneo_4	High-Pressure	16831,87	- €	- €
41	2027	7,61	biometano64	High-Pressure	10937,11	227.044 €	20.434 €
58	2026	12,07	biometano71	High-Pressure	5466,31	360.328 €	32.430 €
138	2036	9,83	biometano67	High-Pressure	6495,62	293.304 €	26.397 €
23	2027	0,53	biometano30	High-Pressure	19871,49	15.924 €	1.433 €
79	2025	3,26	Tortona_2	High-Pressure	19871,49	- €	- €
134	2027	5,14	biometano29	High-Pressure	21056,16	153.418 €	13.808 €
188	2037	6,57	biometano73	High-Pressure	2355,63	196.005 €	17.640 €
133	2027	1,16	biometano103	High-Pressure	19871,49	34.544 €	3.109 €

## 5.6 Year of connection decision

For the scenario with variable biomethane injection, it is necessary to define the year of the connection decision  $y_{l,b}^{dec,con}$  for each biomethane plant. Therefore, it is assumed that the year of the decision corresponds to the year of possible connection of the biomethane plant, which is the year in which the biogas incentive expires. In this scenario, this information act as a parameter to the code that unlocks the possibility to decide whether to connect or not each biomethane plant. The information provided to the code are resumed in the table below:

Table 5.3 – Year of connection decision per biomethane plant

Plant id	Year
82	2027
80	2026
81	2028
108	2027
111	2028
135	2026
.....	
58	2026
138	2036
23	2027
79	2025
134	2027
188	2037
133	2027

## 6. Results

This chapter presents the optimization results for all the scenarios analysed. After determining the input data, the network has been optimized. For the purpose, the solver Gurobi version 10.0.2, is used for the optimization by calling it up within the Python code. The optimization's primary outcomes are the total investment and operation and maintenance costs of the gas infrastructure from 2025 to 2050, the decision to replace or remove existing pipelines at the end of their useful life, the use of pipelines for gas distribution, and the gas source choice (biomethane, domestic production, imported, etc.).

For each scenario, i.e. the base scenario and the scenario with biomethane injection (fixed or variable), the 3 different demand evolutions presented in chapter 4 are considered.

### 6.1 Base scenario

The first grid optimization is performed for the scenario without biomethane injection into the grid, considering the different demand evolutions shown in Figure 4.3, Figure 4.4 and Figure 4.5.

For all the demand evolutions the objective function value is obtained:

*Table 6.1 – Objective function value per demand evolution scenario, base case*

<b>Scenario</b>	<b>TOTAL COSTS 2025-2050</b>
GA	1.235.719.566 €
DE	1.222.899.529 €
LT	1.324.015.708 €

The network configuration in 2050, in terms of diameter distribution, is shown below, per each demand scenario:

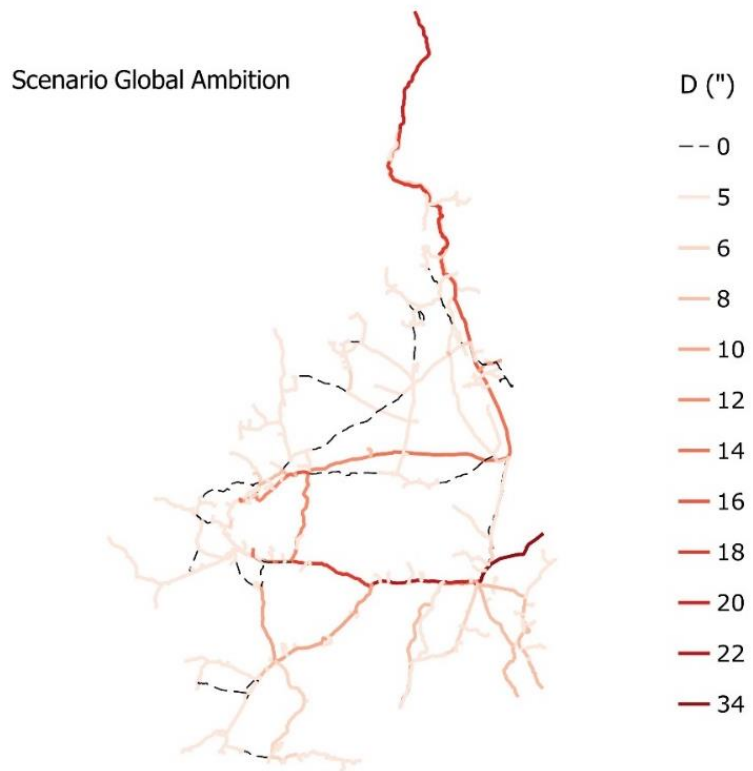


*Figure 6.1 – Network configuration in 2050, GA scenario, base case*

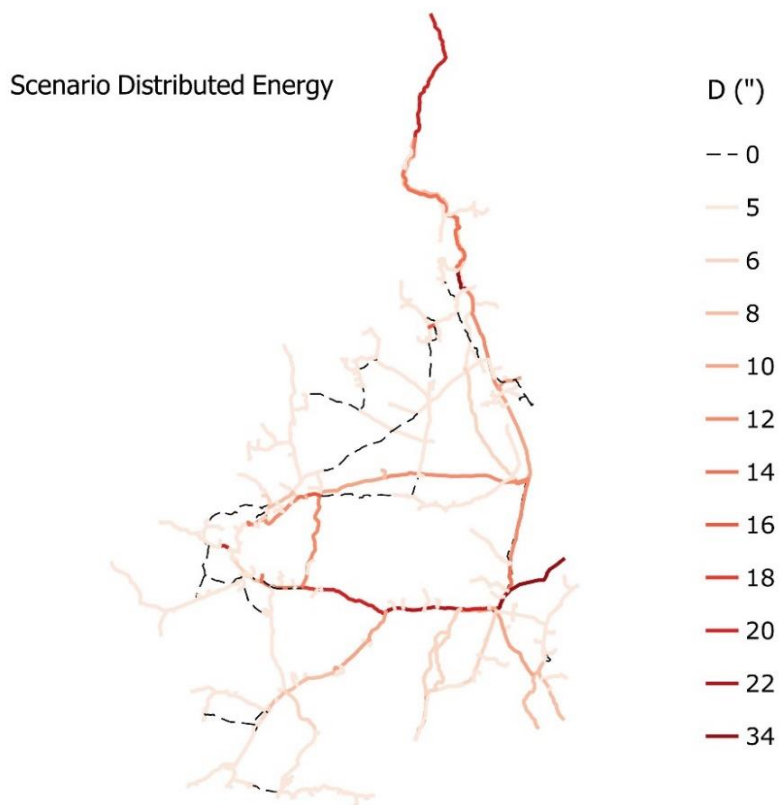


*Figure 6.2 - Network configuration in 2050, DE scenario, base case*

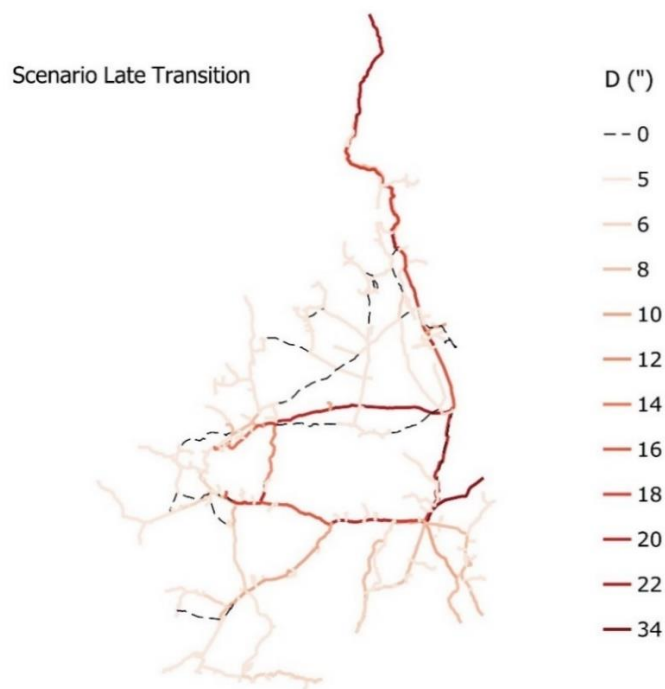


*Figure 6.3 - Network configuration in 2050, LT scenario, base case*

As shown in the legend, the hatched pipes are the decommissioned ones (zero diameter). The graph below reports the diameter distribution in 2050 per demand evolution scenario, compared to the initial diameter distribution in 2025:

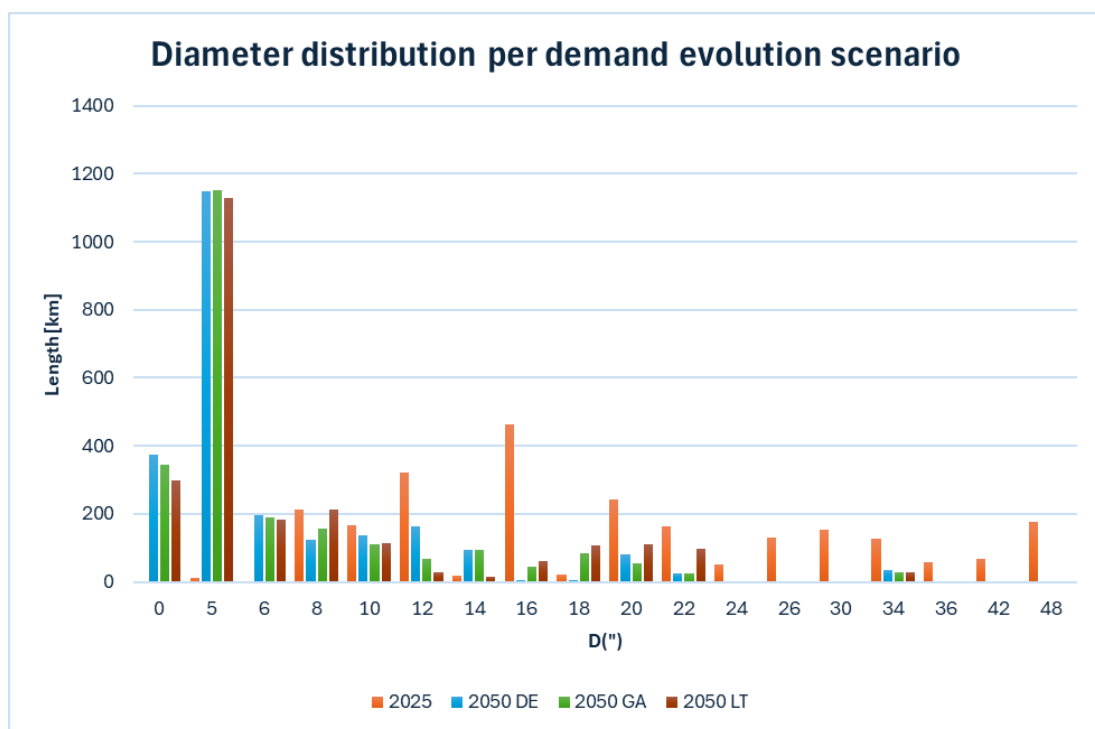


*Figure 6.4 – Diameter distribution per demand evolution scenario, base case*

The graph shows a shift towards smaller diameters in 2050 compared to 2025, for all demand evolution scenarios. This is mainly due to a decrease in gas demand and the initial pipeline capacities being sized based on transport capacities assigned to each redelivery point, rather than the actual gas demand. Specifically, most of the pipelines have a diameter of 5 inches. When comparing the scenarios, it is evident that the Distributed Energy scenario has the highest number of decommissioned kilometres, followed by the Global Ambition scenario and finally the Late Transition scenario. This is due to the varying evolution of gas demand for each scenario. For the same reason, the LT scenario is characterized by the highest number of kilometres of pipeline per diameter size over 14 inches.

As shown in the graph below, the Late Transition scenario still has a very high gas demand in 2050, approximately 64,3 TWh, which is significantly larger than the Global Ambition's 16,6 TWh or the Distributed Energy's 12,5 TWh.

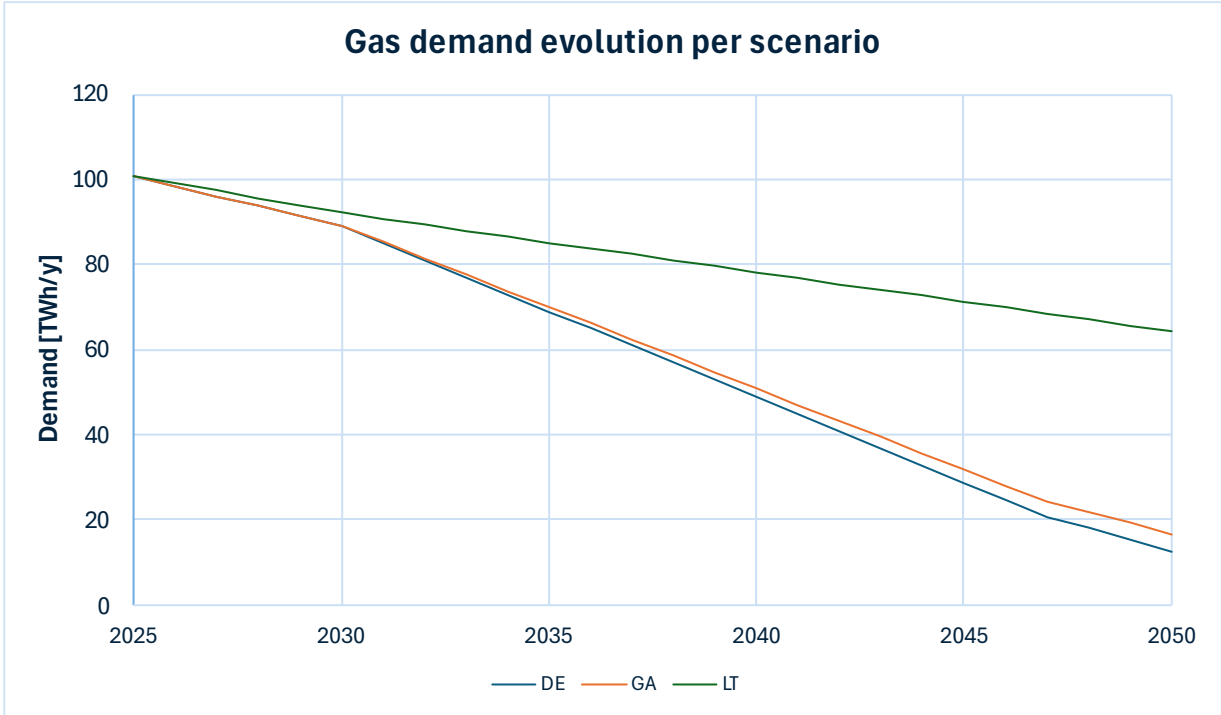


Figure 6.5 – Gas demand evolution per scenario

By having to meet more gas demand, it is not feasible to decommission some pipelines, such as end pipelines where gas demand is zero in the other scenarios, or some pipelines that create a loop in the network which are still needed. It can also be possible that, as example, decommissioning one pipeline and increasing the diameter of another is less cost-effective than



keeping both and with smaller diameters. This results in higher total costs for the LT scenario, as reported in Table 6.1.

In all scenarios, the gas resource in 2050 comes predominantly from the Cortemaggiore node, thus from the LNG resource in Panigaglia. This is because it is more convenient for the TSO to invest in a larger pipeline to receive gas from Panigaglia, rather than from Passo Gries. This is mainly because the pipeline coming from Cortemaggiore, stopping at the Piedmont border, is shorter than the one coming from Passo Gries. It also depends on where most of the demand is concentrated and the year in which the two pipelines are decommissioned. In this case, the bulk of Piedmont's demand could be met by the LNG resource from Panigaglia (fed through Cortemaggiore node), amounting to 54 TWh/y.

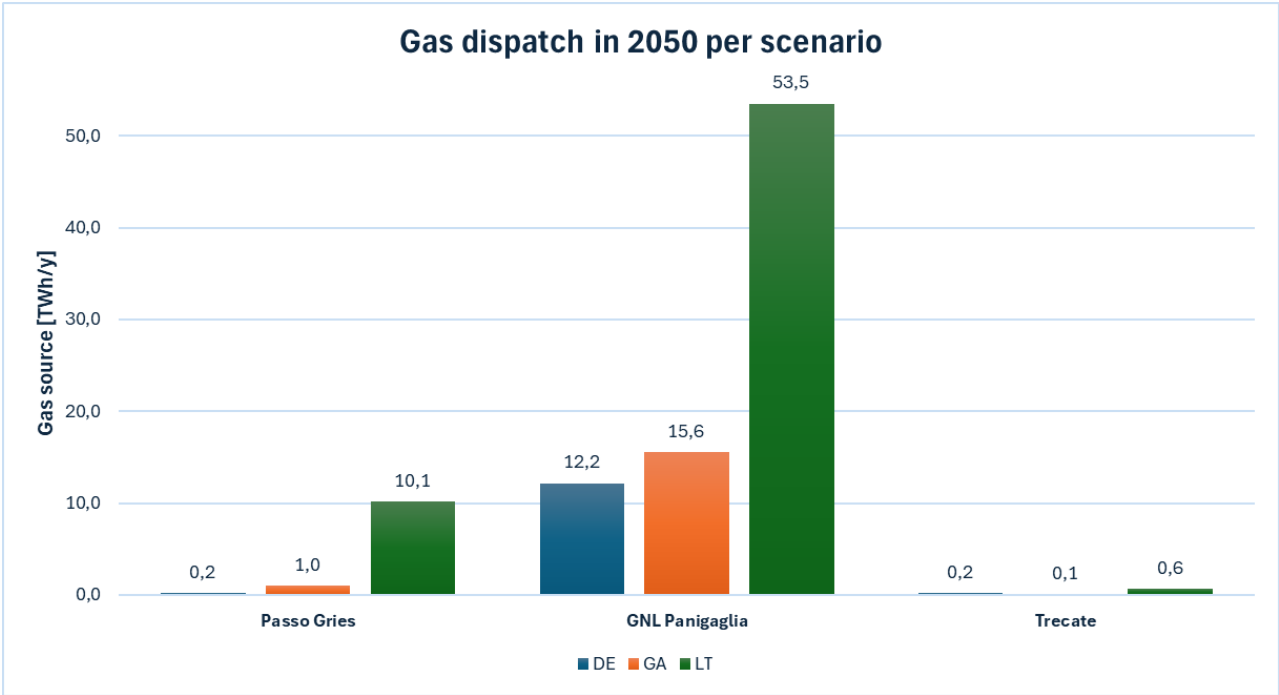


Figure 6.6 – Gas dispatch in 2050, per demand scenario, base case

6.2 Biomethane scenario

The second grid optimization is performed for the scenario with distributed biomethane injection into the grid, distinguishing between fixed and variable injection. In this scenario, the different demand evolutions are considered too.

6.2.1 Fixed biomethane injection

In the fixed injection scenario, all biomethane plants are connected to the grid and injects their producibility. Therefore, the investment for connecting the biomethane plants is not variable but fixed. Below are the network configurations in 2050 for all 3 scenarios with all biomethane plants connected.

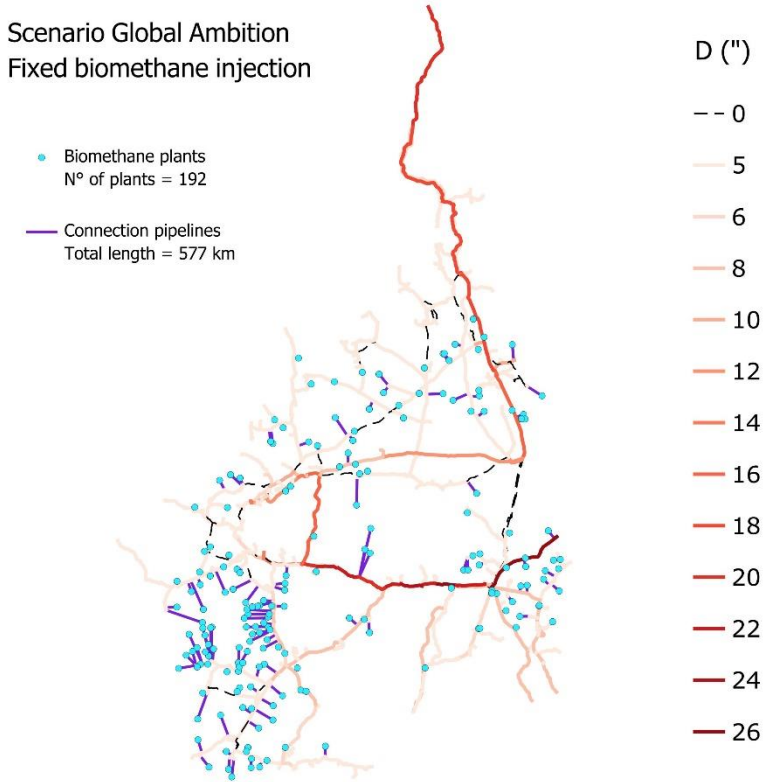


Figure 6.7 – Network configuration in 2050, GA scenario, fixed injection case

Scenario Distributed Energy  
Fixed biomethane injection

- Biomethane plants  
N° of plants = 192
- Connection pipelines  
Total length = 577 km

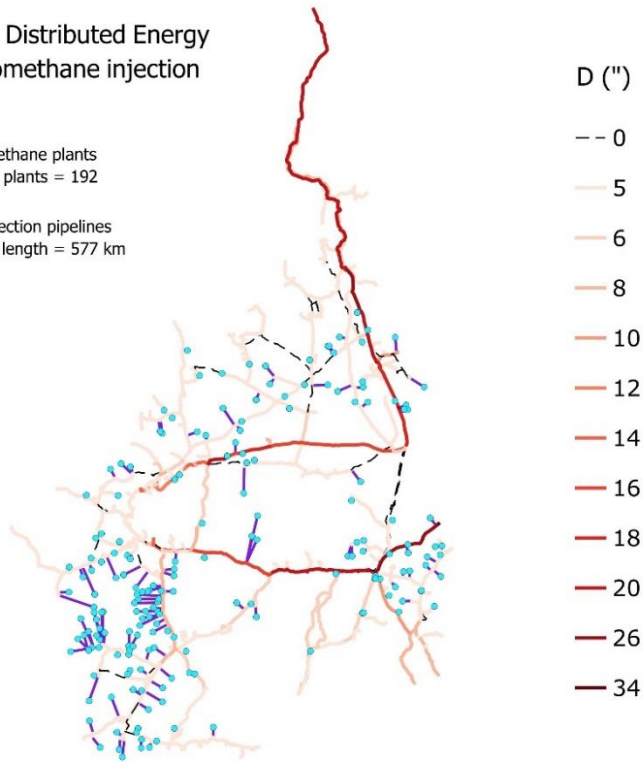


Figure 6.8 - Network configuration in 2050, DE scenario, fixed injection case

Scenario Late Transition  
Fixed biomethane injection

- Biomethane plants  
N° of plants = 192
- Connection pipelines  
Total length = 577 km

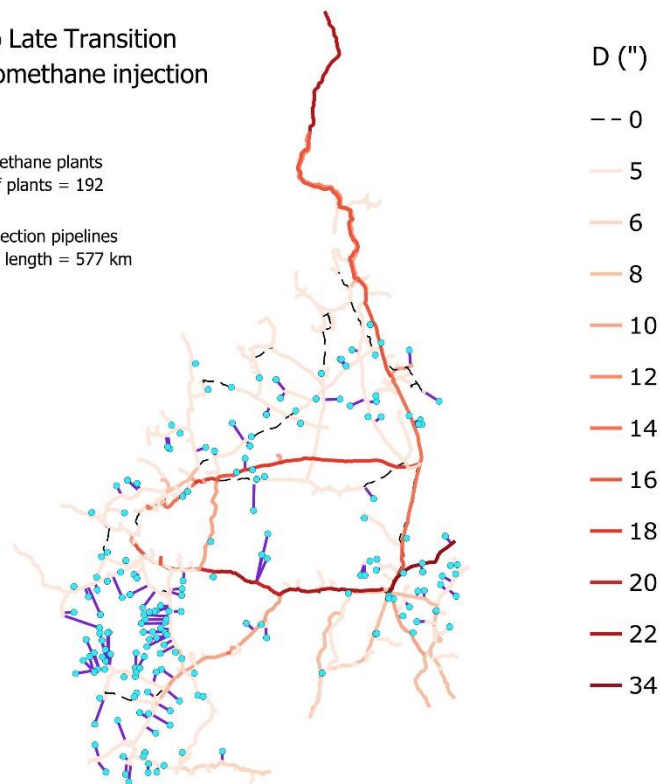


Figure 6.9 - Network configuration in 2050, LT scenario, fixed injection case

It is noticeable that the number of decommissioned lines is lower than in the base case, because otherwise part of the available biomethane resource would be excluded. In terms of costs, there is an increase in the objective function in all 3 demand scenarios compared to the base case. The increase in investment costs is due to the need to replace some pipelines instead of decommissioning them, and to the investment in plant connections. The objective function values are reported below:

*Table 6.2 - Objective function value per demand evolution scenario, fixed injection case*

Scenario	TOTAL COSTS 2025-2050
GA	1.269.368.176 €
DE	1.262.564.238 €
LT	1.349.354.585 €

A total of 192 biomethane plants have been connected over 161 injection points, with a total output of 2,55 TWh/year and 577 km of connection pipelines.

Below, the gas dispatch in 2050 is reported for all demand scenarios.

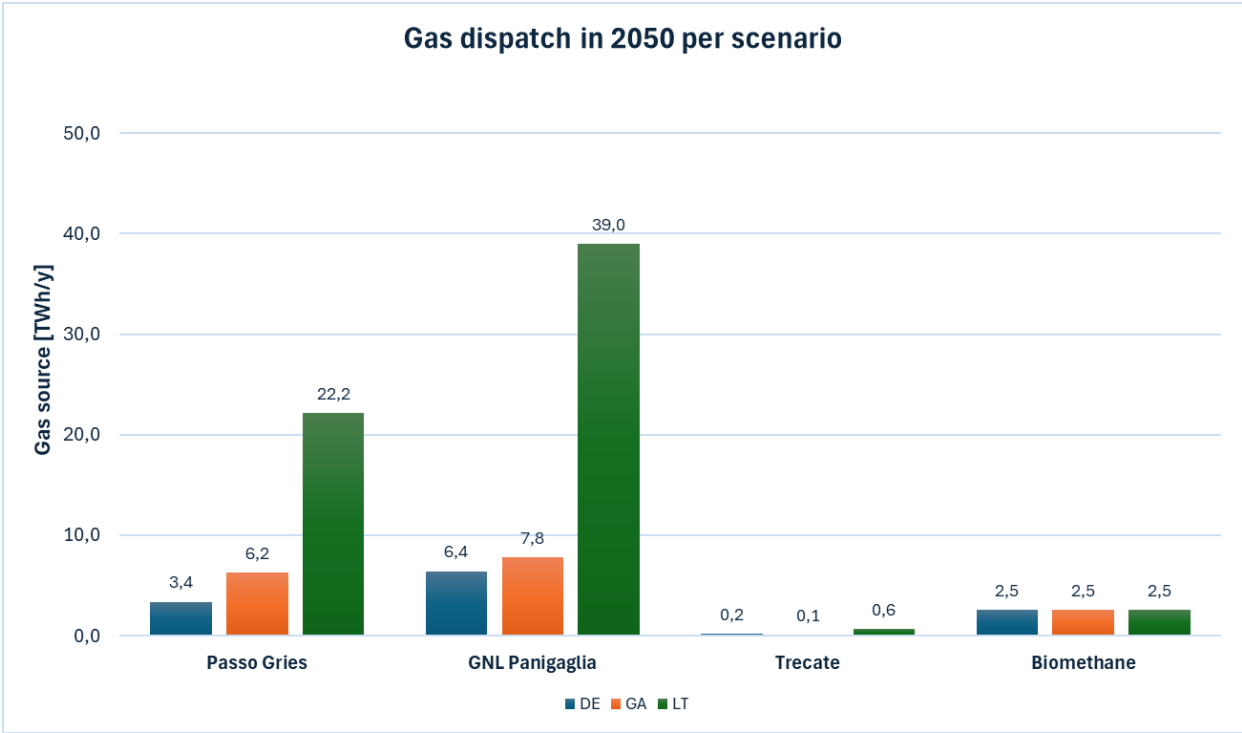


*Figure 6.10 – Gas dispatch in 2050, per demand scenario, fixed injection case*

In 2050, biomethane would cover a share of Piedmontese gas demand equal to:

- 20,42% in DE scenario,
- 15,32% in GA scenario,
- 3,96% in LT scenario.

### 6.2.2 Variable biomethane injection

For the variable biomethane scenario, the TSO can take the decision on the connection of individual biomethane plants in the year of the end of the biogas incentive. The purpose of this scenario is to see whether connecting part of the biomethane plants can be cost-effective compared to the base case. The values of the objective function are reported in the following table:

*Table 6.3 - Objective function value per demand evolution scenario, variable injection case*

Scenario	TOTAL COSTS 2025-2050
GA	1.213.399.989 €
DE	1.202.133.820 €
LT	1.313.399.639 €

The network configurations in 2050 for the 3 gas demand evolution scenarios are shown below.

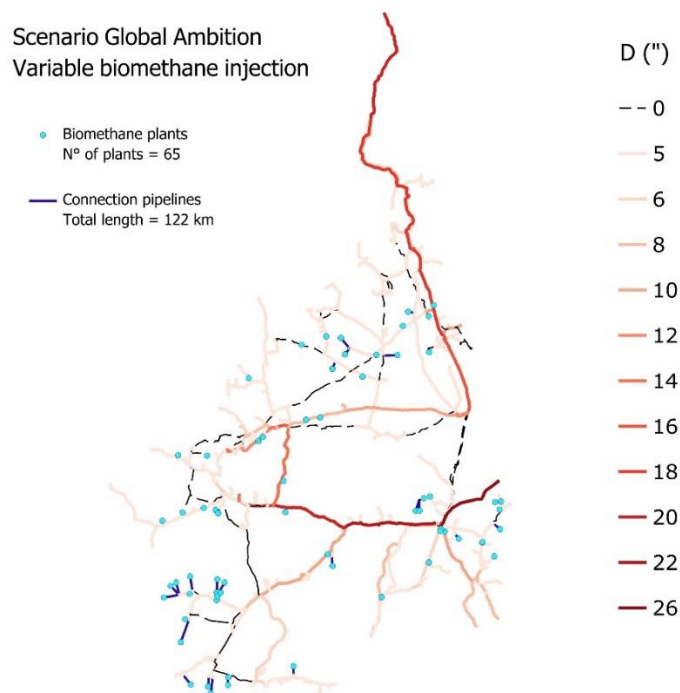


*Figure 6.11 – Network configuration in 2050, GA scenario, variable injection case*

Scenario Distributed Energy  
Variable biomethane injection

- Biomethane plants  
N° of plants = 55
- Connection pipelines  
Total length = 111 km

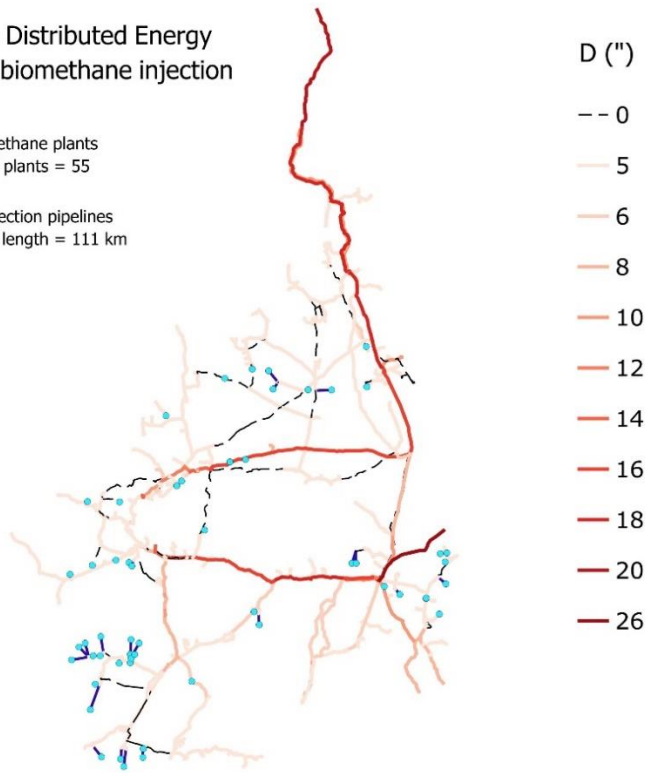


Figure 6.12 - Network configuration in 2050, DE scenario, variable injection case

Scenario Late Transition  
Variable biomethane injection

- Biomethane plants  
N° of plants = 41
- Connection pipelines  
Total length = 109 km

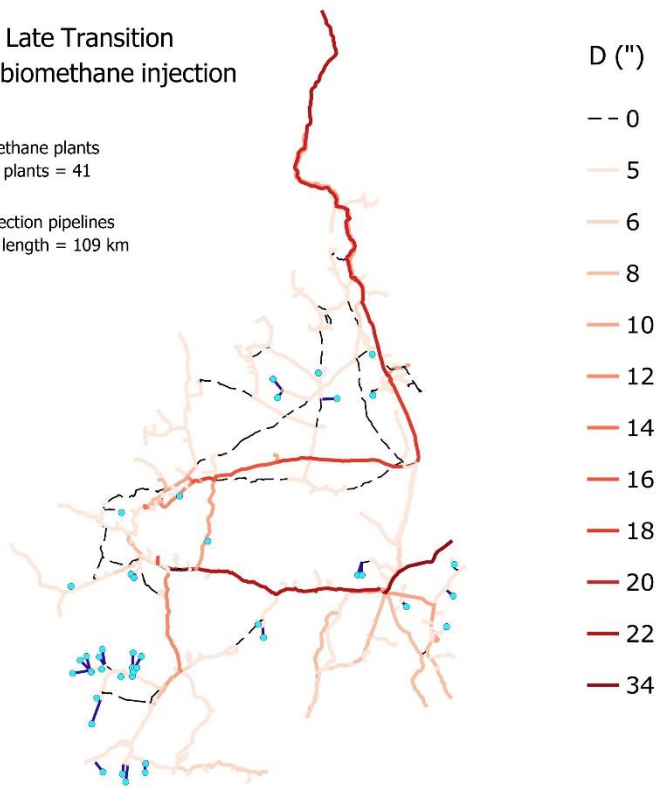


Figure 6.13 - Network configuration in 2050, LT scenario, variable injection case

In all scenarios not all biomethane plants have been connected, as shown in the table below:

*Table 6.4 – N° of plants connection per demand scenario, variable biomethane injection case*

	DE	GA	LT
<b>Injection points</b>	44	54	29
<b>Plants connected</b>	55	65	41
<b>Km of connection pipelines</b>	110,7	121,9	108,8
<b>Plants connected over total plants</b>	29%	34%	21%
<b>Sm3/h connected over total Sm3/h</b>	39%	46%	24%

Regarding the source of gas in 2050, biomethane would cover a share of gas demand equal to:

- 4,00 % in DE scenario,
- 2,40 % in GA scenario,
- 0,78 % in LT scenario.

Below, the gas dispatch in 2050 is reported for all demand scenarios.

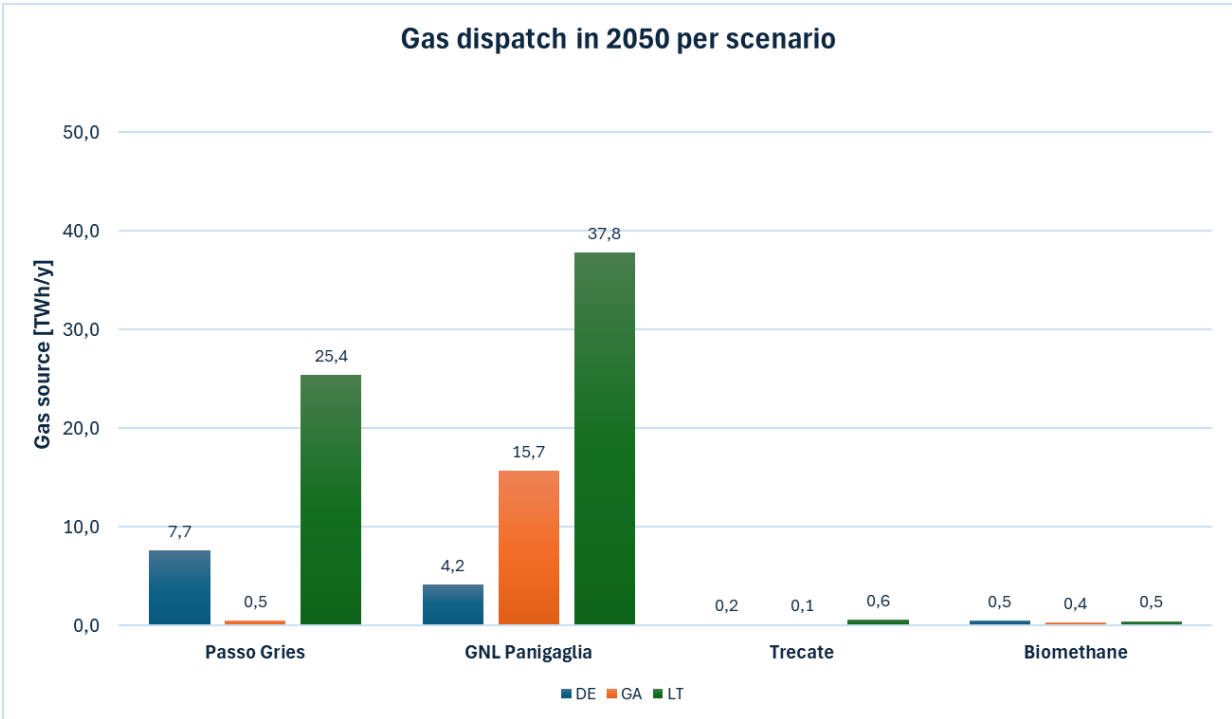


*Figure 6.14 - Gas dispatch in 2050, per demand scenario, variable injection case*

Thus, in the variable biomethane scenario, the amount of biomethane injected into the grid is greatly reduced. On the other hand, the amount of gas coming from outside the region is greater than in the fixed connection case. It is convenient for the TSO to connect only part of the plants,

especially those connected to the final network nodes (i.e. connected to the distribution network operated by the DSO), and then isolate parts of the network that would be fed exclusively with biomethane.

The GA scenario is characterized by the highest number of connections, due to the possibility of isolating additional parts of the network, where there is a lower demand compared with the other scenarios.

The graph below compares the evolution of biomethane injection into the grid for each scenario with the fixed injection case (same for all consumption scenarios).

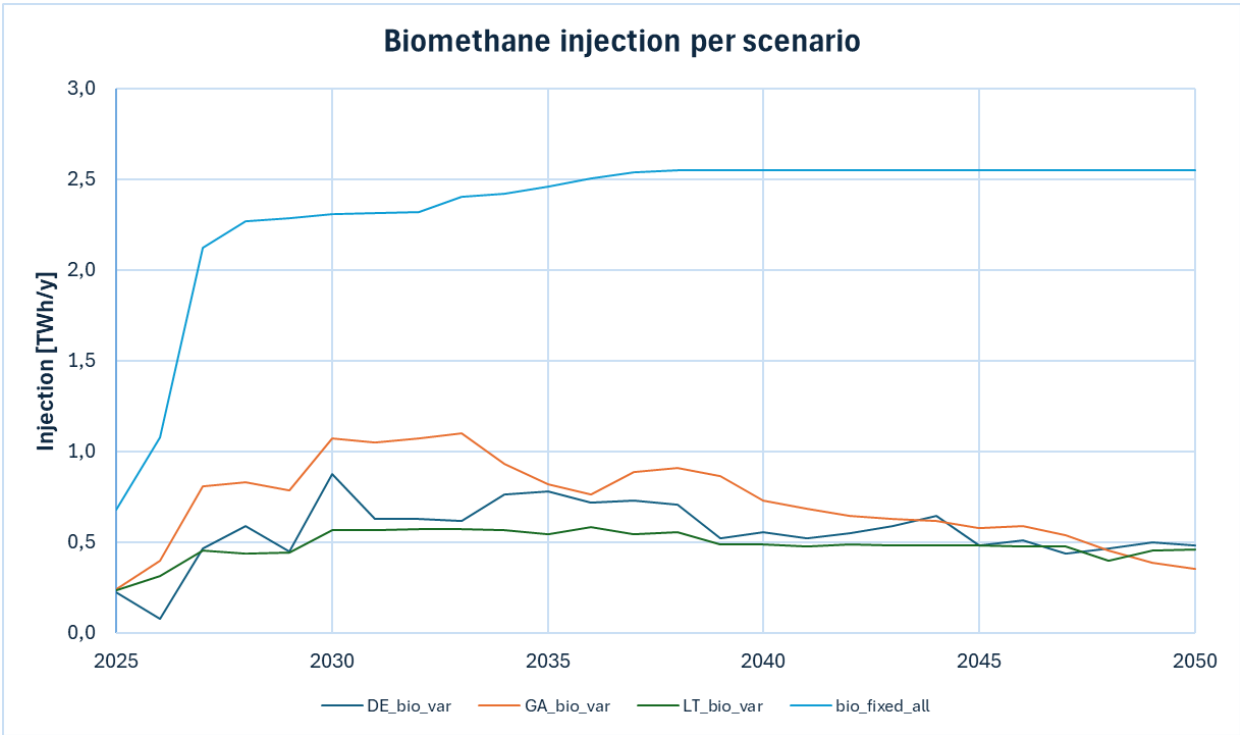


Figure 6.15 – Biomethane injection evolution 2025-2050, per scenario

As in the case of fixed injection, the biomethane resource shows an increasing trend and then stabilises from 2038 onwards, in line with the plant connections shown in Figure 5.11. In the variable injection scenarios, the distributed resource input is lower due to the smaller number of connections. Inputs do not follow a constant trend in recent years, due to the gradual decrease in demand at the nodes. This is because most plants are connected to isolated parts of the grid, so that the biomethane injection (which is variable and at the discretion of the TSO) follows demand exactly. Furthermore, in some scenarios there is an alternating decrease and increase in input. The first is probably due to the closure of some lines to which some plants are



connected, and which therefore stop feeding in for the rest of the analysis period. The second is related to the amount of biomethane injected by the plants connected to a central part of the grid, where the TSO decides monthly how much to withdraw, just satisfying the mass balance constraints. Both these circumstances highlight the rise of a critical condition: the possibility of curtailments of the injectable biomethane even for those plants that have been connected. This result is consistent to the optimization problem structure that focuses strictly to the costs of the gas network infrastructure and does not value the technical and economical inefficiencies due to curtailments.

To better illustrate the differences in network configuration between the baseline and the biomethane resource case, a graph of the diameter distributions for each case study and gas demand scenario is shown.

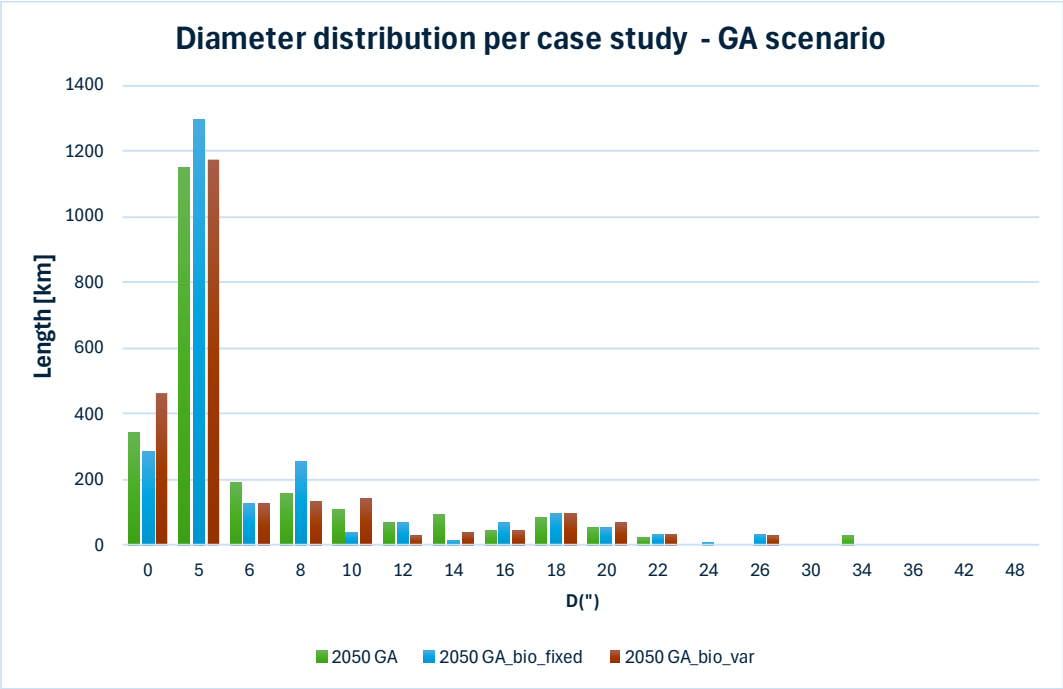


Figure 6.16 – Diameter distribution in 2050, per case study, GA scenario

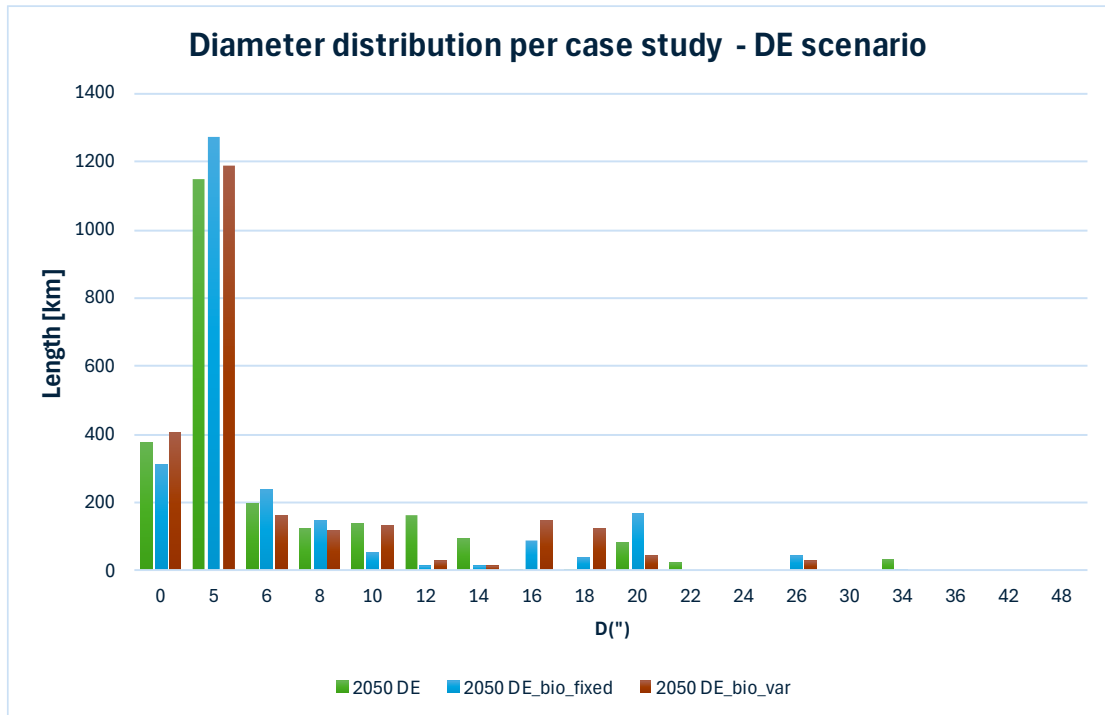


Figure 6.17 - Diameter distribution in 2050, per case study, DE scenario

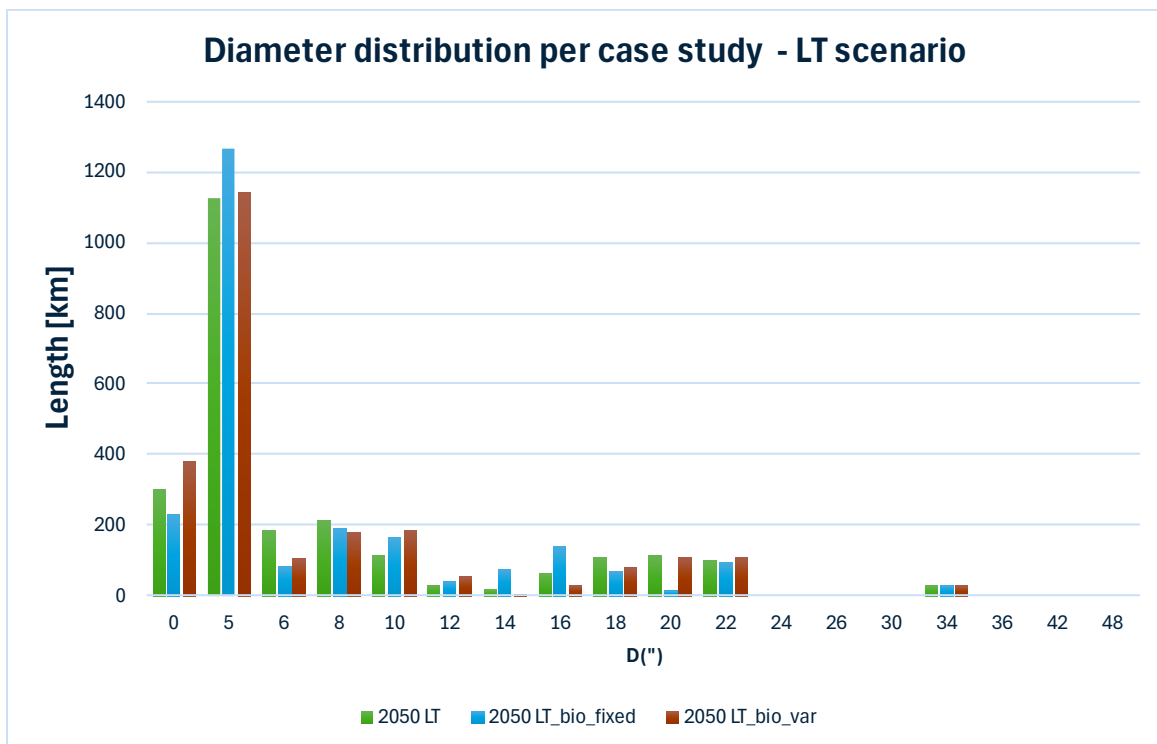


Figure 6.18 – Diameter distribution in 2050, per case study, LT scenario

For all scenarios, it appears that the variable biomethane resource case has the largest number of pipeline kilometres decommissioned, resulting in lower total gas infrastructure costs. However, it is worth highlighting that these lower infrastructure costs come along with a strong reduction of the amount of biomethane resource that is injectable into the infrastructure. In this case, the infrastructure purpose is still mainly as a distributor of fuel gas to demand centres, and so its development follows primarily the demand evolution.

### 6.3 Results comparison

In general, there is a shift in the distribution of diameters towards smaller values for all scenarios and all case studies. In the LT scenario, due to the high gas demand in 2050, there is a need for diameters up to 34 inches in all cases. In the GA and DE scenarios, the largest diameters are up to 26 inches for the cases with biomethane injection, as there is more availability of decentralised resources and a strongly reduced demand in 2050.

In the tables below the total costs for the period 2025-2050 and the biomethane volume injection in 2050, for all scenarios, are reported:

*Table 6.5 – Total costs for all scenarios, 2025-2050*

<b>TOTAL COSTS 2025-2050 [bn EUR]</b>			
<b>Case study</b>	<b>DE</b>	<b>GA</b>	<b>LT</b>
No_bio	1,223	1,236	1,324
Bio_fixed	1,263	1,270	1,349
Bio_var	1,202	1,213	1,313

*Table 6.6 – Total biomethane volume injection in 2050, for all scenarios*

<b>Total biomethane injection in 2050 [MSm3]</b>			
<b>Case study</b>	<b>DE</b>	<b>GA</b>	<b>LT</b>
No_bio	0	0	0
Bio_fixed	233,34	233,34	233,34
Bio_var	43,96	32,35	41,88

The LT scenario shows the highest total costs, due to the high gas consumption even until 2050. In all consumption developments, the scenario with fixed biomethane injection leads to higher costs. In contrast, the variable biomethane scenario is the cheapest. However, in terms of

volume of renewable gas injected, the variable case is strongly reduced compared to the fixed injection case, for all demand evolutions. Although the GA variable biomethane scenario allows more plants to be connected, as in Table 6.4, the amount of biomethane injected in 2050 is lower than in the other scenarios, resulting in a higher curtailment of the resource. This is because there is very limited demand in isolated grid zones fed only with biomethane.

## 7. Conclusions

This master's thesis presents an analysis of the most cost-effective decision regarding the gas infrastructure in Piedmont, with the possibility of injecting the distributed biomethane resource available in the region. The first chapter presents the European and national decarbonisation targets with a focus on the future of the natural gas system. European and national scenarios of the future energy system are published, to help TSOs in taking decisions on the energy infrastructure. In the national scenarios, the demand for natural gas is expected to decrease and the use of green gases such as biomethane is expected to increase. This is supported by the funding provided by the PNRR, which aims to achieve a national production of 2,3 billion cubic metres of biomethane by June 2026.

The Piedmont gas network is first built using GIS software, based on open-source data. Once the mathematical model is defined, including the definition of all parameters, variables, constraints and the objective function, the optimization has been carried out on Python. The definition of the mathematical model in Python is done using the Pyomo optimization language. Two main case studies have been analysed, a case where no biomethane is to be injected into the grid and a case where injection is planned. For each case study, 3 different demand evolution scenarios are considered, corresponding to the scenarios presented by the national gas and electricity TSOs.

For the biomethane injection case study, a distinction is made between fixed biomethane injection and variable biomethane injection. In the former, all biogas plants in Piedmont are converted to biomethane production and injected into the grid. In the latter case, the TSO decides on the connection of each plant, including the amount of biomethane to be injected into the grid. An optimization is performed for each case study and each demand scenario.

The results show that in all case studies and all demand scenarios, smaller pipelines will be needed in the future and some pipelines will be decommissioned. In the case study with fixed biomethane injection, the number of decommissioned pipelines will be smaller due to the forced connection of the plants, leading to higher infrastructure costs. However, the additional infrastructure costs are on average only 2% higher than in the case study without biomethane. In addition, biomethane would account for a significant share of future gas demand, up to 20% in scenarios consistent with the 2050 climate targets.

The variable biomethane case study has been analysed to see if connecting only part of the plants could lead to savings in infrastructure costs compared to the base case study. In fact, the

variable biomethane solution is the most cost-effective, as the TSO could isolate parts of the gas network that would be supplied exclusively with biomethane. On the other hand, the total injection of renewable gas into the Piedmont grid would decrease, as it would only cover 4% of the total demand of the region in 2050. In addition, it remains to be assessed whether part of the network could operate independently.

This study, using this approach, shows that to incorporate biomethane as much as possible, an infrastructure is needed that, although scaled down, still has its own complexity. The cheapest option follows the trend of demand, but also excludes the renewable resource.

The gas network is therefore destined to change its purpose: from a simple distributor of a resource to a collector. Whether this handling infrastructure is the cheapest (compared to e.g. LNG) needs to be assessed.

Variable injection of biomethane is therefore the most economical solution. However, if all plants were connected, this would lead to an increase in costs that would not be significant and would reach relevant proportions of injected green gas, in line with the decarbonization plans. In the future, a possible increase in producibility with the construction of new biomethane plants from scratch, in addition to the conversion of existing ones, could lead to a more significant use of the existing network in Piedmont, creating a distributed resource capable of satisfying most of the demand.

Possible future improvements to the model include the use of an accurate cartography of the network, to have a more accurate model of the network and an exact allocation of the redelivery points' demand. Implementing a fluid dynamic analysis in the optimization would also make the model more realistic but would require more computing power.

## 8. Bibliography

- [1] UNFCCC, “The Paris Agreement. What is the Paris Agreement?” Accessed: Sep. 04, 2023. [Online]. Available: <https://unfccc.int/process-and-meetings/the-paris-agreement>
- [2] Consiglio dell’Unione europea, “Green Deal europeo.” Accessed: Sep. 08, 2023. [Online]. Available: <https://unfccc.int/process-and-meetings/the-paris-agreement>
- [3] Consiglio dell’Unione europea, “Fit for 55.” Accessed: Sep. 08, 2023. [Online]. Available: <https://www.consilium.europa.eu/en/policies/green-deal/fit-for-55-the-eu-plan-for-a-green-transition/>
- [4] Consiglio dell’Unione europea, “Infografica - Spiegazione del piano REPowerEU.” Accessed: Dec. 02, 2023. [Online]. Available: <https://www.consilium.europa.eu/it/infographics/repowerEU/#:~:text=REPowerEU%20%C3%A8%20il%20piano%20dell,transizione%20verso%20l’energia%20pulita>
- [5] European Commission, “REPowerEU: Joint European Action for more affordable, secure and sustainable energy,” Mar. 2022. Accessed: Aug. 28, 2023. [Online]. Available: <https://eur-lex.europa.eu/legal-content/EN/TXT/?uri=COM%3A2022%3A108%3AFIN>
- [6] Entso-g and Entso-e, “TYNDP 2022 Scenario Report | Version. April 2022,” 2022. Accessed: Sep. 11, 2023. [Online]. Available: <https://2022.entsoe-tyndp-scenarios.eu/>
- [7] Snam and Terna, “Documento di Descrizione degli Scenari 2022.” Accessed: Sep. 13, 2023. [Online]. Available: <https://www.terna.it/it/sistema-elettrico/rete/piano-sviluppo-rete/scenari>
- [8] Governo Italiano | Presidenza del Consiglio dei Ministri and Commissione Europea, “Italia Domani, il Piano Nazionale di Ripresa e Resilienza.” Accessed: Dec. 10, 2023. [Online]. Available: <https://www.italiadomani.gov.it/content/sogei-ng/it/it/home.html>
- [9] IEA, “Italy Natural Gas Security Policy,” Part of Natural Gas Security Policy. Accessed: Sep. 24, 2023. [Online]. Available: <https://www.iea.org/articles/italy-natural-gas-security-policy>
- [10] Ministero dell’Ambiente e della Sicurezza Energetica, “PIANO NAZIONALE INTEGRATO PER L’ENERGIA E IL CLIMA,” Jun. 2023. Accessed: Dec. 10, 2023. [Online]. Available: [https://www.mase.gov.it/sites/default/files/PNIEC\\_2023.pdf](https://www.mase.gov.it/sites/default/files/PNIEC_2023.pdf)
- [11] Statista, “Imports and production of natural gas in Italy from 1st half 2021 to 1st half 2023, by country of origin, pipeline, and entry point.” Accessed: Oct. 04, 2023. [Online].

- Available: <https://www.statista.com/statistics/1325804/natural-gas-supply-in-italy-by-origin/>
- [12] Snam, “La rete di trasporto.” Accessed: Aug. 03, 2023. [Online]. Available: <https://www.snam.it/it/noi-snam/chi-siamo/le-nostre-infrastrutture/la-rete-di-trasporto.html>
- [13] Gestore Servizi Energetici, “PRODUZIONE DI BIOMETANO - DM 15/9/2022.” Accessed: Dec. 02, 2023. [Online]. Available: <https://www.gse.it/servizi-per-te/attuazione-misure-pnrr/produzione-di-biometano>
- [14] Snam, “Rete Snam rete gas e infrastrutture trasporto gas.” Accessed: Aug. 05, 2023. [Online]. Available: <https://www.snam.it/it/i-nostri-business/trasporto/servizi-online/la-rete/rete-gas-e-infrastrutture-trasporto-gas.html>
- [15] ACER, “The internal gas market in Europe: The role of transmission tariffs-European Union Agency Report on the application of reference price methodologies in Member States,” Apr. 2020. Accessed: Aug. 11, 2023. [Online]. Available: [https://www.acer.europa.eu/sites/default/files/documents/Official\\_documents/Acts\\_of\\_the\\_Agency/Publication/The%20internal%20gas%20market%20in%20Europe\\_The%20role%20of%20transmission%20tariffs.pdf](https://www.acer.europa.eu/sites/default/files/documents/Official_documents/Acts_of_the_Agency/Publication/The%20internal%20gas%20market%20in%20Europe_The%20role%20of%20transmission%20tariffs.pdf)
- [16] Snam, “CODICE DI RETE di Snam Rete Gas - Revisione LXXXV,” Nov. 2023. Accessed: Aug. 23, 2023. [Online]. Available: <https://www.snam.it/it/i-nostri-business/trasporto/codice-di-rete-tariffe-area-comitato-e-consultazioni/codice-di-rete.html>
- [17] Ministero dell’Ambiente e della Sicurezza Energetica, “Elenco completo dei gasdotti in esercizio e in progetto della rete di trasporto regionale al 1° gennaio 2023,” 2023. Accessed: Sep. 17, 2023. [Online]. Available: <https://www.mase.gov.it/node/16118>
- [18] M. L. Bynum *et al.*, *Optimization Modeling in Python Third Edition*. 2020. Accessed: Jul. 16, 2023. [Online]. Available: <https://www.osti.gov/biblio/1771935>
- [19] S. Zwickl-Bernhard, “Gas network decommissioning model (GND\_Mod).” Accessed: Aug. 08, 2023. [Online]. Available: [https://github.com/sebastianzwickl/GND\\_Mod](https://github.com/sebastianzwickl/GND_Mod)
- [20] S. Zwickl-Bernhard, A. Golab, T. Perger, and H. Auer, “Designing a model for the cost-optimal decommissioning and refurbishment investment decision for gas networks: Application on a real test bed in Austria until 2050,” *Energy Strategy Reviews*, vol. 49, p. 101138, 2023, doi: <https://doi.org/10.1016/j.esr.2023.101138>.



- [21] W. Kenton, “Declining Balance Method: What It Is, Depreciation Formula,” Apr. 2022, Accessed: Dec. 18, 2023. [Online]. Available: <https://www.investopedia.com/terms/d/decliningbalancemethod.asp#:~:text=The%20declining%20balance%20method%20is,during%20the%20asset’s%20later%20years>.
- [22] Snam, “Capacità di trasporto, Pressioni e Parametri Tariffari dei Punti di Riconsegna, situazione al 27/04/23 delle capacità disponibili per il conferimento annuale - Anno Termico 2022/2023,” 2023. Accessed: Aug. 24, 2023. [Online]. Available: [https://www.snam.it/it/trasporto/Processi\\_Online/Capacita/informazioni/capacita-trasporto/Capacita\\_trasporto/02\\_PdR/02a/02a\\_Elenco.html](https://www.snam.it/it/trasporto/Processi_Online/Capacita/informazioni/capacita-trasporto/Capacita_trasporto/02_PdR/02a/02a_Elenco.html)
- [23] Sorgenia, “Conferimento.” Accessed: Aug. 24, 2023. [Online]. Available: <https://www.sorgenia.it/guida-energia/conferimento>
- [24] Leonardo Berlen, “Quanto gas consumiamo ogni mese in Italia? Ecco perchè l’inverno è a forte rischio,” *Qualenergia*, Aug. 2022, Accessed: Oct. 18, 2023. [Online]. Available: <https://www.qualenergia.it/articoli/quanto-gas-consumiamo-ogni-mese-italia-perche-inverno-forte-rischio/>
- [25] Snam, “Capacità di trasporto nei Punti di ENTRATA e di USCITA interconnessi con la RETE NAZIONALE, situazione al 30/10/2023 - Anno Termico 2023/2024,” 2023. Accessed: Oct. 05, 2023. [Online]. Available: [https://www.snam.it/it/trasporto/Processi\\_Online/Capacita/informazioni/capacita-trasporto/Capacita\\_trasporto/01\\_Entrata\\_uscita/01a/01a\\_Elenco.html](https://www.snam.it/it/trasporto/Processi_Online/Capacita/informazioni/capacita-trasporto/Capacita_trasporto/01_Entrata_uscita/01a/01a_Elenco.html)
- [26] Energie Rete Gas, “Capacità di trasporto disponibile ai Punti di Riconsegna ad anno termico avviato, Anno Termico 2021-2022,” Sep. 2022. Accessed: Aug. 27, 2023. [Online]. Available: <https://www.italiaenergetica.com/at-20212022/>
- [27] Metanodotto Alpino S.R.L., “Capacità di trasporto disponibile ai Punti di Riconsegna Anno Termico 2021-2022,” Jul. 2022. Accessed: Sep. 06, 2023. [Online]. Available: <http://www.metanodottoalpino.com/asp/anni.asp?sezione=14>
- [28] Ministero dell’Ambiente e della Sicurezza Energetica, “Gas naturale: Consumi regionali.” Accessed: Oct. 22, 2023. [Online]. Available: <https://dgsaie.mise.gov.it/consumi-regionali-gas-naturale>
- [29] Marco Cavana, “Gas network modelling for a multi-gas system,” 2020. Accessed: Nov. 06, 2023. [Online]. Available: [https://pico.polito.it/discovery/openurl?institution=39PTO\\_INST&vid=39PTO\\_INST:VU&rft.date=2020-09-](https://pico.polito.it/discovery/openurl?institution=39PTO_INST&vid=39PTO_INST:VU&rft.date=2020-09-)

- 30&rft.space=1&rft.atitle=Gas%20network%20modelling%20for%20a%20multi-gas%20system
- [30] Wikipedia contributors, “SIMPLE algorithm,” Wikipedia, The Free Encyclopedia.
- [31] S.K.I. Schlegel & Kremer Industrieautomation GmbH, “Properties of Natural Gases, Acc. to AGA8-DC (1992), ISO 12213-2:2006, ISO20765-1.” Accessed: Oct. 12, 2023. [Online]. Available: <https://www.ski-gmbh.com/swa/calculation-natural-gas>
- [32] Snam, “Potere calorifico superiore convenzionale per impianti di distribuzione, riferito all’anno 2022,” Feb. 2023. Accessed: Oct. 12, 2023. [Online]. Available: [https://www.snam.it/it/trasporto/adempimenti-reporting-autorita/PCS\\_Convenzionale/](https://www.snam.it/it/trasporto/adempimenti-reporting-autorita/PCS_Convenzionale/)
- [33] ARERA, “Consultazione 30 luglio 2019 338/2019/R/gas - Orientamenti per la durata del periodo di regolazione e per la regolazione della qualità dei servizi di distribuzione e misura del gas nel quinto periodo di regolazione,” 2019. Accessed: Oct. 21, 2023. [Online]. Available: <https://www.arera.it/atti-e-provvedimenti/dettaglio/19/338-19>
- [34] ACER, “About ACER.” Accessed: Nov. 02, 2023. [Online]. Available: <https://www.acer.europa.eu/the-agency/about-acer>
- [35] ACER, “Report on unit investment cost indicators and corresponding reference values for electricity and gas infrastructure - Gas Infrastructure,” 2015. Accessed: Nov. 05, 2023. [Online]. Available: <https://www.acer.europa.eu/news-and-events/news/acer-publishes-report-unit-investment-costs-indicators-and-corresponding-reference-values-european-energy-infrastructure>
- [36] S. Zwickl-Bernhard *et al.*, “Modeling insights from the Austrian national gas grid under declining natural gas demand and increasing domestic renewable gas generation by 2040,” *Energy Reports*, vol. 11, pp. 1302–1317, 2024, doi: <https://doi.org/10.1016/j.egy.2023.12.064>.
- [37] G. Molnar, “Economics of Gas Transportation by Pipeline and LNG,” in *The Palgrave Handbook of International Energy Economics*, G. Hafner Manfred and Luciani, Ed., Cham: Springer International Publishing, 2022, pp. 23–57. doi: 10.1007/978-3-030-86884-0\_2.
- [38] ARERA, “Delibera 17 marzo 2020 64/2020/R/gas - Aggiornamento delle direttive per le connessioni di impianti di biometano alle reti del gas naturale,” Mar. 2020.
- [39] IEA, “Outlook for biogas and biomethane: Prospects for organic growth,” Paris, 2020. Accessed: Nov. 19, 2023. [Online]. Available: <https://www.iea.org/reports/outlook-for-biogas-and-biomethane-prospects-for-organic-growth>

- [40] European Biogas Association, “About Biogas and Biomethane,” 2023. Accessed: Nov. 25, 2023. [Online]. Available: <https://www.europeanbiogas.eu/about-biogas-and-biomethane/>
- [41] IEA, “CO2 storage resources and their development,” Paris, 2022. Accessed: Dec. 02, 2023. [Online]. Available: <https://www.iea.org/reports/co2-storage-resources-and-their-development>
- [42] GSE, “ATLAIMPIANTI.” Accessed: Nov. 17, 2023. [Online]. Available: [https://atla.gse.it/atlaimpianti/project/Atlaimpianti\\_Internet.html](https://atla.gse.it/atlaimpianti/project/Atlaimpianti_Internet.html)
- [43] Arpa Piemonte, “Geoportale di Arpa Piemonte - I dati ambientali a portata di mappa.” Accessed: Nov. 15, 2023. [Online]. Available: <https://geoportale.arpa.piemonte.it/app/public/>
- [44] GSE, “Rinnovabili elettriche - Gestione incentivi.” Accessed: Nov. 23, 2023. [Online]. Available: <https://www.gse.it/servizi-per-te/fonti-rinnovabili/gestione-incentivi/fer-elettriche>
- [45] MTM Energia, “Cogeneratori Biogas: Impianti di cogenerazione alimentati a biogas agricolo, depurazione e scarica.” Accessed: Nov. 28, 2023. [Online]. Available: <https://www.mtmenergia.com/it/>
- [46] Jenbacher, “COGENERATION / CHP Combined heat and power solutions.” Accessed: Nov. 30, 2023. [Online]. Available: <https://www.jenbacher.com/en/energy-solutions/applications/cogeneration-combined-heat-power>
- [47] Viessmann, “Cogeneratori ad elevata efficienza per produrre energia elettrica e termica.” Accessed: Nov. 28, 2023. [Online]. Available: <https://www.viessmann.it/it/prodotti/cogenerazione.html>
- [48] Owe JÖNSSON, Arthur WELLINGER, and Margareta PERSSON, “Biogas Upgrading to Vehicle Fuel Standards and Grid Injection,” 2006. [Online]. Available: [www.eia.doe.gov](http://www.eia.doe.gov)
- [49] Bright Renewables, “Biogas upgrading: PurePac.” Accessed: Dec. 02, 2023. [Online]. Available: <https://www.bright-renewables.com/solutions/renewable-gas/biogas-upgrading/>